

# Vacuum Vessels in Tension

EDRIC ROY MCKENZIE

Submitted in partial fulfilment of the requirements for the degree of Master of  
Science in the Department of Physics, University of Natal

Durban  
January 1999

## Preface

The work described in this thesis was carried out in the Laser Group, Physics Department, University of Natal, Durban, under the supervision of Professor M.M.Michaelis.

These studies represent the original work by the author and have not been submitted in any form to another University. Where use is made of the work of others it has been duly acknowledged in the text.

*EMelby*

*28 April 1999*

## Acknowledgements

I would sincerely like to thank my supervisor, Prof. Max Michaelis, for his enthusiasm, commitment, and steady stream of ideas.

Willem de Beer and all the workshop staff deserve a special mention for all their efforts with regard to the construction of numerous vacuum vessels. In particular, I am grateful to Willem for his patience and support, often going above and beyond the call of duty.

Richard Mace deserves a vote of thanks for his assistance with latex and for providing the template of this thesis.

Acknowledgements to the University of Natal for Graduate Assistance and to the FRD for their financial support.

I am grateful to all members of the laser group for their support and encouragement.

Finally, a special word of thanks to my parents.

## Abstract

Tensional Vacuum Vessels (TVV) are vessels constructed such that the walls are placed in tension rather than in compression as is the case with conventional vacuum vessels. TVVs have the advantage of being cost-effective, light weight in construction, and potentially portable. Tensional vessels have already been designed with regard to submarine applications. However, the use of this principle with regard to vacuum applications is believed to be novel. TVVs have two interlinked thin walled shells instead of the traditional single thick wall of conventional design. These shells are placed in tension by pressurising the intermediate space. This thesis outlines the theory of tensional vessels and describes the performance of a number of experimental chambers developed during this investigation.

The fundamental theory of the TVV is outlined and developed in more detail with regard to cylindrical vessels. These include vessels constructed from longitudinal and circumferential tubes. The basic theory for any TVV can be derived from the equilibrium condition. This states that the force due to the gauge pressure on the outer shell must be greater than or equal to the force due to the absolute pressure on the inner shell. If the inward force predominates implosion will occur. Materials science considerations are also taken into account. If the tension in the walls exceeds that required for yield, the vessel will deform. The use of novel tensile materials is also explored. TVVs are potentially inflatable and theory is developed with regard to the possibility of buoyant vessels.

The first experiments were based on earlier work performed at this institution with cylindrical TVVs constructed from longitudinal tubes. The tubes employed were soft drink cans which were sealed together with putty. The work described in this thesis outlines the development of larger versions and the instabilities which developed are noted. High vacuum experiments performed through the inclusion of a guard vessel are then described. This is followed by a further description of experiments performed with this basic tensional wall design in an attempt to gain a better understanding of its properties. These vessels were smaller and were gas pressurised in order to allow for increased flexibility with regard to pressure and volume variation. It is found that the compressional elements of such vessels cannot be ignored.

A series of cylindrical TVVs with the walls constructed from circumferential tubes is then described, including high vacuum experiments, also performed through the inclusion of a guard vessel. The initial experiments were small in scale and made use of small bicycle tyres as the TVV walls.

Larger vessels were then built, the walls being constructed from car tyres. These vessels are also inflatable and more stable than those constructed from longitudinal tubes. Also, the compressional elements do not play as great a role in these vessels.

A fully tensional cylindrical vessel is then described which includes tensional end plates. Experiments performed with large bowls as the end plates are outlined. The theory of the deformation of a circular plate is also given including finite element analysis.

Finally, a further novel vacuum vessel design is proposed. This is the spinning vacuum vessel. Proof of principle experiments are performed on a small scale vessel (a soft drink can with its interior reinforced with putty) which yields promising results.

# Contents

<b>1</b>	<b>Introduction</b>	<b>1</b>
1.1	Overview of Vacuum . . . . .	1
1.2	Alternative Vacuum Vessel designs . . . . .	4
1.2.1	Convoluted Vacuum tube . . . . .	4
1.2.2	Hialvac . . . . .	6
1.3	The principle of tensional vacuum vessels . . . . .	7
1.4	History of TVVs . . . . .	7
1.5	Early Experiments with Tubular TVV's . . . . .	9
1.6	Patents . . . . .	9
1.7	Tensional Submarines Applications . . . . .	11
1.8	Outline of thesis . . . . .	14
<b>2</b>	<b>Theory of the TVV</b>	<b>16</b>
2.1	The basic theory . . . . .	16
2.1.1	The Spherical TVV . . . . .	17
2.1.2	Cylindrical TVV's . . . . .	18
2.2	TVVs constructed from tubes . . . . .	22
2.2.1	Basic Theory . . . . .	23
2.2.2	Modifications to Basic Theory . . . . .	26
2.2.3	Instabilities in Tubular TVV's . . . . .	28
2.3	Cylindrical TVV's with Toroidal Walls . . . . .	29
2.4	Examination of materials science . . . . .	30
2.4.1	Tension in a Sphere . . . . .	30
2.4.2	Tension in a cylinder . . . . .	31
2.4.3	Tension in a Torus . . . . .	34
2.4.4	Specific Material Examples . . . . .	35
2.5	Inflatable Vacuum Vessels . . . . .	35
2.6	Conclusion . . . . .	44

<b>3</b>	<b>Low Vacuum Tubular TVV Experiments</b>	<b>45</b>
3.1	Aim of this Chapter . . . . .	45
3.2	TVV Dimensions . . . . .	46
3.3	Note about Plasma Instabilities . . . . .	47
3.4	General Experimental Outlay . . . . .	48
3.5	Presentation of Experimental Results . . . . .	50
3.6	Single Layer Experiments ( $m = 1$ ) . . . . .	50
3.6.1	Experiment 1 . . . . .	52
3.6.2	Experiment 2 . . . . .	53
3.7	Double Layered Experiment ( $m = 2$ ) . . . . .	56
3.8	Four Layered Experiment ( $m = 4$ ) . . . . .	57
3.9	Eight Layered Experiment ( $m = 8$ ) . . . . .	58
3.10	Tubular TVV for High Vacuum . . . . .	61
3.10.1	Experiment 1 . . . . .	62
3.10.2	Experiment 2 . . . . .	64
3.10.3	Experiment 3 . . . . .	66
3.11	Discussion and Conclusion . . . . .	67
<b>4</b>	<b>High Vacuum TVV Experiments</b>	<b>69</b>
4.1	General Experimental Outlay . . . . .	69
4.2	The first guard chamber . . . . .	73
4.2.1	Experiment 1 . . . . .	73
4.2.2	Experiment 2 . . . . .	76
4.2.3	Experiment 3 . . . . .	77
4.3	The Second Guard Chamber . . . . .	81
4.3.1	Experiment 1 . . . . .	81
4.3.2	Experiment 2 . . . . .	83
4.4	Conclusion . . . . .	84
<b>5</b>	<b>Further Tubular TVV Experiments</b>	<b>85</b>
5.1	Pressurisable Tubular TVV Experiments . . . . .	85
5.1.1	Experiment 1 . . . . .	86
5.1.2	Experiment 2 . . . . .	89
5.1.3	Experiment 3 . . . . .	91
5.2	Experiments with $p = 1 \text{ bar}$ . . . . .	94
5.2.1	Discussion and Conclusion . . . . .	96
<b>6</b>	<b>Cylindrical TVV's with Toroidal Walls</b>	<b>98</b>
6.1	Low Vacuum Experiments . . . . .	99
6.1.1	Experiment 1 . . . . .	99

6.1.2	Note on Plasma Sheaths . . . . .	100
6.1.3	Experiment 2 . . . . .	101
6.1.4	Experiment 3 . . . . .	103
6.1.5	Experiment 4 . . . . .	108
6.2	High Vacuum TTVV Experiment . . . . .	111
6.2.1	Further Experimentation . . . . .	113
6.3	Discussion and Conclusion . . . . .	114
<b>7</b>	<b>Fully Tensional Cylindrical TVV</b>	<b>115</b>
7.1	Theory . . . . .	115
7.2	Experimental . . . . .	118
7.2.1	Experiment 1 . . . . .	119
7.2.2	Experiment 2 . . . . .	119
7.3	Examination of a Deformed End Plate . . . . .	123
7.3.1	Theory of the Deformation of a Circular Plate . . . .	123
7.3.2	Finite Element Analysis of Deformed Plate . . . . .	127
7.4	Conclusion . . . . .	128
<b>8</b>	<b>The Spinning Vacuum Vessel</b>	<b>134</b>
8.1	Theory . . . . .	134
8.2	Experimental . . . . .	136
8.3	Conclusion . . . . .	141
<b>9</b>	<b>Conclusion</b>	<b>142</b>
<b>A</b>	<b>Structures in Compression</b>	<b>145</b>
A.1	Tubes in Compression . . . . .	145
<b>B</b>	<b>Simulation Programme for the Deformation of a Circular Plate</b>	<b>150</b>



# List of Figures

1.1	Convuluted Vacuum Vessel . . . . .	5
1.2	hialvac . . . . .	6
1.3	Two early TVV's . . . . .	8
1.4	The Rome Patent . . . . .	10
1.5	The Paris Patent . . . . .	11
1.6	The Milan Patent . . . . .	12
1.7	"Swedged" submersible design . . . . .	13
1.8	Tube stiffened submersible design . . . . .	13
2.1	Basic Structure of a TVV . . . . .	16
2.2	Diagram of a Cylindrical TVV . . . . .	18
2.3	Variation of $\Delta R$ with $P_{bar}$ for various $R_i$ values of Spherical TVV's According to Approximate Equation (2.5) . . . . .	19
2.4	Variation of $\Delta R$ with $P_{bar}$ for various $R_i$ values of Cylindrical TVV's According to Approximate Equation (2.10) . . . . .	20
2.5	Comparison of Spherical and Cylindrical TVV's with $R_i = 1$ Using Approximate Equations (2.5) and (2.10) . . . . .	20
2.6	TVV Data from fig(2.5) including comparisons with data obtained from the Exact Equations (2.3) and (2.8) . . . . .	21
2.7	Force experienced at the end plates of Cylindrical TVV's for various $R_i$ values . . . . .	23
2.8	Tubular TVV with appropriate terminology . . . . .	24
2.9	Forces Acting on an Individual Tube . . . . .	25
2.10	Tubular TVV Section with Equivalent Polygonal Structure Superimposed . . . . .	26
2.11	Basic diagram of a single layered torus after evacuation . . . . .	29
2.12	Forces Acting on a Sphere Under Internal Pressure . . . . .	30
2.13	Local Curvatures of a Spherical TVV Membrane . . . . .	31
2.14	Tension in a Cylinder Under Uniform Internal Pressure . . . . .	32

2.15	Tension in the Walls of a Cylindrical TVV (End Plate not shown) . . . . .	33
2.16	Diagram of a Torus under internal Pressure . . . . .	34
2.17	Yield Pressures of Structural Steel . . . . .	37
2.18	Yield Pressures of Aluminium Alloy (1100-H14) . . . . .	37
2.19	Yield Pressures of Cold-rolled Brass . . . . .	38
2.20	Yield Pressures of Nylon . . . . .	38
2.21	Yield Pressures of Rigid PVC . . . . .	39
2.22	Yield Pressures of Silicon . . . . .	39
2.23	Yield Pressures of Silicon Carbide . . . . .	40
2.24	He Pressurised Spherical TVV with Aluminium Alloy Walls .	42
2.25	He Pressurised Spherical TVV with Structural Steel Walls . .	43
2.26	He Pressurised Spherical TVV with Silicon Carbide Walls . .	43
3.1	Plasma Column alongside Sausage and Kink Instabilities . . .	48
3.2	Plasma Column alongside Flute(Interchange) Instability . . .	49
3.3	General Apparatus . . . . .	50
3.4	Edwards High Vacuum rotary pump . . . . .	51
3.5	Mechanical Vacuum Gauge . . . . .	51
3.6	Tubular TVV( $m = 1$ ) with Sand-filled Bowl as Interior Support	52
3.7	Tubular TVV with Supporting Columns . . . . .	54
3.8	Four layer Tubular TVV . . . . .	57
3.9	Sausage Instability in TVV Wall . . . . .	59
3.10	Diagram Showing Support Structure for Eight Layer TVV . .	60
3.11	Original Compressional Vacuum Vessel . . . . .	62
3.12	Rotary pump with connection to main chamber . . . . .	63
3.13	Proposed Tubular TVV Wall for High Vacuum Experiments .	64
3.14	Implosion photographs with Columns shifted to the opposite side of the chamber . . . . .	65
3.15	Shift in TVV . . . . .	65
3.16	Internal view of rim stabilised TVV . . . . .	67
4.1	External Plumbing Arrangement . . . . .	71
4.2	Valve connecting inner chamber with mechanical gauge . . .	72
4.3	The First Guard Vessel . . . . .	74
4.4	Guard Vessel within TVV structure . . . . .	75
4.5	Connection of Ionisation Gauge to Guard Vessel . . . . .	78
4.6	Wires passing through TVV wall . . . . .	79
4.7	Pirani and Ionisation Gauge Heads . . . . .	80
4.8	Second Guard Vessel placed over Diffusion Pump . . . . .	81

4.9	Ionisation Gauge connected externally to TVV . . . . .	82
4.10	Ionisation Gauge with direct link to Internal Vessel . . . . .	83
5.1	First Pressurisable Tubular TVV ( $n = 6$ ) . . . . .	87
5.2	TVV walls for $n = 10$ vessel . . . . .	89
5.3	$n = 12$ Vessel Painted to Prevent Rust . . . . .	92
5.4	Vacuum and Pressure Apparatus . . . . .	93
6.1	Rupture of inner tube . . . . .	102
6.2	Clamping arrangement for car tyre . . . . .	104
6.3	Internal structure of double layered TTVV . . . . .	105
6.4	TTVV with ( $m = 2$ ) before evacuation . . . . .	106
6.5	TTVV with ( $m = 2$ ) after evacuation . . . . .	107
6.6	$m = 4$ TTVV before evacuation . . . . .	109
6.7	$m = 4$ TTVV after evacuation . . . . .	110
6.8	Guard Vessel used in High Vacuum Toroidal Experiments . .	111
6.9	Guard Vessel within $m = 4$ TTVV . . . . .	112
7.1	Dome Under External Pressure . . . . .	116
7.2	Simulated Dome Inverted Against Pressure . . . . .	117
7.3	Tensional Stresses on a the Membrane of a Dome Under In- ternal Pressure . . . . .	118
7.4	Side View of TVV with Sausage Instability . . . . .	120
7.5	Tensional End Plate . . . . .	121
7.6	Diagram of TVV with Tensional End Plate . . . . .	122
7.7	Bowl with Stabilising Rim Attached . . . . .	123
7.8	Deformed TVV End Plate . . . . .	124
7.9	Bending of a Circular Plate Due to Uniform Pressure . . . . .	125
7.10	Stresses of a Circular Plate Bending due to Uniform Pressure	126
7.11	3-D Plot of Plate before Deformation . . . . .	129
7.12	3-D Plot of Plate after Deformation . . . . .	130
7.13	Plot of VonMises Stress on Plate . . . . .	131
7.14	Plot of Total Displacement . . . . .	132
7.15	Side View of Displacement: Scale = 2%, 5% and 10% respec- tively . . . . .	133
8.1	Graph of Required Rotational Frequencies of SVV's Con- structed from Aluminium Alloy(1100-H14) with Regard to Varying Parameters . . . . .	136

8.2	Graph of Required Rotational Frequencies of SVV's Constructed from Structural Steel with Regard to Varying Parameters . . . . .	137
8.3	Graph of Required Rotational Frequencies of SVV's Constructed from Phosphor Bronze (Spring Temper) with Regard to Varying Parameters . . . . .	137
8.4	Modified Can with Bearing . . . . .	139
8.5	Modified Can Attached to Lathe with Vacuum Hose . . . . .	140
A.1	Standard Thick Walled Tube: $I_1 = t^3/12$ , $V_1 = \pi(2R + t)t$ . .	146
A.2	Thinner Walled Tube with Ring Stiffeners: $I_2 = \frac{5}{6}th^2$ , $V_2 = 4\pi Rt$ for $T = t$ and $l = h$ . . . . .	147
A.3	Thin Walled Tube with Rectangular Profile: $I_3 = (t/3l)(h^3 + 3h^2l)$ , $V_3 = 2\pi R(l + h)t/l$ . . . . .	147
A.4	Thin Walled Tube with Semicircular Profile: $I_4 = \pi/4tr^2$ , $V_4 = \pi^2(R + r)t$ . . . . .	148
A.5	Thin Walled Tube with Triangular Profile: $I_5 = h^2Lt/3l$ , $V_5 = 2\pi(R + h)Lt/l$ . . . . .	148
A.6	Thin Walled Tube with Corrugated Profile . . . . .	149

# List of Tables

1.1	Overview of Vacuum Categories . . . . .	2
1.2	Pumps and Gauges associated with Vacuums . . . . .	3
2.1	Yield Strengths of Various Materials . . . . .	36

# Chapter 1

## Introduction

### 1.1 Overview of Vacuum

Vacuum occupies a significant place in modern science today. Vacuum is required in many laboratories for a wide variety of practical applications. This is also true for both industry as well as educational institutions at the tertiary and sometimes secondary level.

Examples of fields of research to which vacuum is indispensable include plasma physics, electron microscopy as well as high energy particle physics which require long vacuum tubes for the accelerators. In all of the above applications, collisions with air molecules make operation at atmospheric pressure impossible. Other examples include research into nuclear fusion and gravity wave detectors which require very large vacuum systems which will be described in more detail later. Moore, Davis and Coplan give a number of vacuum applications[1]. These include the removal of air through evacuation as a necessary first step in the creation of a new gaseous environment. This may be to ensure that a chemical reaction or surface is not contaminated. Also included is spectrometry. Vacuum is required in mass spectrometry where collisions with air molecules must be reduced to a minimum. Far-IR and far-UV spectrometers require a vacuum as these frequencies are absorbed by air and therefore cannot propagate over any significant distance in this medium. Further examples given include vacuum dehydration and freeze-drying. One could also mention the laying down of thin films (for instance microcircuitry), optical coating and electron beam welding which is required for the welding of single crystal fan blades in jet engines. This is by no means an exhaustive commentary on the uses of vacuum technology but does give some idea of the place occupied by vacuum in the scientific

and engineering disciplines.

Perfect vacuums do not exist<sup>1</sup>. All vacuum vessels retain certain trace gases after the system has been pumped down and so the quality varies. The quality measure is the pressure exerted by these residuals. Pressure is defined as the force per unit area which can be represented in mathematical form as the simple equation:

$$P = \frac{F}{A} \quad (1.1)$$

The unit for pressure measurement is therefore the Newton per square metre ( $Nm^{-2}$ ) otherwise known as the Pascal ( $Pa$ ). In vacuum research, pressure is often measured in terms of millimeters of mercury ( $mm\ Hg$ ). The standard unit for this method of measurement is the *Torr* where  $1\ Torr = 1\ mm\ Hg$ . Atmospheric pressure is  $760\ Torr$ . The unit most frequently used is the *bar*, where  $1\ bar$  is the equivalent of one atmosphere of pressure.

Table 1.1: Overview of Vacuum Categories

Pressure range ( <i>Torr</i> )	Type of Vacuum	Mean free path ( <i>cm</i> )	Number of molecules per $cm^3$
$10^2 - 10^{-2}$	Rough or fore vacuum	$\approx 10^{-5} - 10^{-1}$	$\approx 10^{19} - 10^{15}$
$1 - 10^{-4}$	Intermediate or booster vacuum	$\approx 10^{-2} - 10^1$	$\approx 10^{16} - 10^{13}$
$10^{-2} - 10^{-6}$	High vacuum	1 <i>cm</i> to larger than vac. vessel	$\approx 10^{14} - 10^{10}$
Less than $10^{-8}$	Ultrahigh vacuum	Much larger than vac. vessel	less than $10^{10}$

Tables 1.1 and 1.2 have been adapted from a volume edited by G.L. Weissler and R.W. Carlson [2]. These give the basic vacuum classification and the equipment required when working with each category.

This thesis will employ the units of *Torr* to represent pressure values in the intermediate and high vacuum ranges. Values in the ultrahigh range were beyond the scope of the experimental work outlined in this thesis. The

---

<sup>1</sup>This statement may be disputed by researchers involved with particle and antiparticle trapping. The vacuum vessels in these experiments effectively contain only the particles injected into the system. At very low temperatures ( $\approx 0K$ ), the pressure may also be considered as non-existent.

Table 1.2: Pumps and Gauges associated with Vacuums

Pressure range ( <i>Torr</i> )	Type of pump	Type of pressure gauge	Principal residual gases
$10^2 - 10^{-2}$	Mech. oil-sealed, steam-ejector, or sorption pumps	Liq.-filled U-tube manometer, membrane compression (spiral) gauge	Air, $H_2O$ , $CO_2$
$1 - 10^{-4}$	Oil-ejector or oil booster pumps	Thermo couple or alphanatron gauges	As above as well as pump oils, hydrocarbons, and $H_2$
$10^{-2} - 10^{-6}$	Oil or $Hg$ diffusion pumps	Ordinary ionisation gauge	Pump oils, hydrocarbons
Less than $10^{-8}$	Ion, $Ti$ -getter, cryo-, or turbomolecular pumps	Bayard-Alpert type ion gauge	$H_2$ and $CO$ , $He$ , and other rare gases

experiments performed could be divided into two broad categories. The first operated in the rough or fore vacuum range and were aimed at testing mechanical strength and stability. The second operated in the intermediate and high vacuum ranges to illustrate that useful vacuums could be obtained.

When operating in the rough vacuum range, it was found to be more convenient to use the *bar* pressure unit. The Pascal unit is only used when it is necessary to make actual calculations of the forces acting upon a vessel.

The fluctuations of these forces due to pressure fluctuations within the vacuum vessel itself in the intermediate and high vacuum ranges can be considered negligible. This means that all vacuum vessels are essentially vessels required to withstand the force due to atmospheric pressure and subsequent theory will be developed with this in mind. This means that every square metre cross-sectional area of a vacuum vessel will be subject to a force equivalent to ten *tons* of mass under one gravity. From the



mathematical definition of pressure given in Equation (1.1) it is obvious that the larger the vacuum vessel, the larger the forces involved. Any vessel of any significant size will therefore have to meet the requirement of having high mechanical strength.

Vacuum chambers are generally built from metals due to the need for high mechanical strength. Other materials such as glass can also be used effectively but there is the danger of implosion from glass vessels because although glass is one of the strongest materials known under compression, the mechanical strength is greatly reduced in situations where tensile strain is introduced. This is not unlikely due to its low impact strength. For this reason these vessels are generally confined to a few litres in size [3]. Faults or imperfections in glass also cause failure. This means that any vacuum vessel of any substantial size is likely to be made from metal.

Vacuum vessels are currently costly items <sup>2</sup> and this certainly presents a problem in developing countries, particularly in institutes of higher learning. In industry as well, for those processes that require large vacuum vessels, there may well be a preference for chambers requiring less or cheaper material. This is shown in alternative vacuum vessel designs which are outlined in the next section.

## 1.2 Alternative Vacuum Vessel designs

The need for cheaper alternative designs is demonstrated through research into such vessels. This can be illustrated through two such developments. The first is a thin walled corrugated vessel, designed for the long vacuum systems necessary for gravitational wave detectors. The other is known as hialvac which is a glazed high alumina cement vacuum chamber.

### 1.2.1 Convolute Vacuum tube

The convolute vacuum tube is an idea developed by J.R.J.Bennett [9] and represents a saving both in cost and weight. This design has been proposed for use in the joint German-British interferometric gravitational wave detector, GEO [7, 8, 9]. The detector requires two vacuum tubes 3 *km* in length and 1,5 *m* in diameter. The GEO600 in Hannover uses two 600 *m* long convolute tubes which are 600 *mm* in diameter.

A standard vacuum tube corresponding to these dimensions would be extremely expensive due to the amount of material required. This is due to

---

<sup>2</sup>The 1994 value was 20\$ /litre.

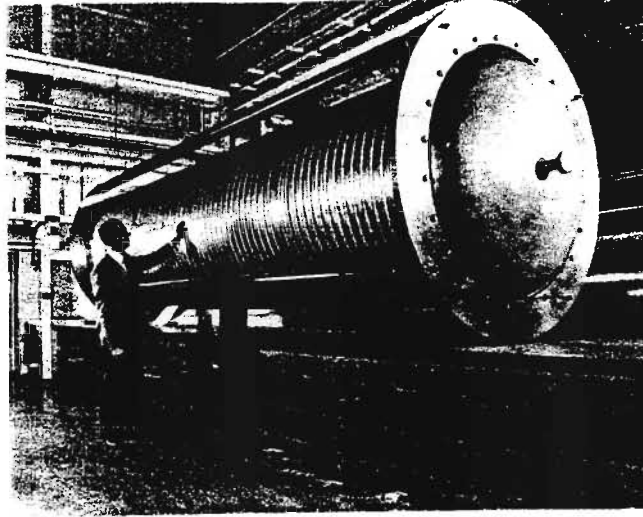


Figure 1.1: Convoluted Vacuum Vessel

the fact that a standard plain tube derives its strength from the thickness of its walls. However, this can be reduced through the addition of stiffening rings at regular intervals. The convoluted vacuum vessel is essentially a corrugated wall design employing this principal. The corrugations behave as stiffening rings.

The convoluted vessel can be manufactured for one fifth of the cost of a plain tube vessel [7]. The wall thickness required is  $0,91\text{ mm}$  as opposed to the wall thickness of a regular vessel which is required to be  $13\text{ mm}$  in thickness. In terms of material this represents a large saving,  $200\text{ tonnes}$  as opposed to  $2700\text{ tonnes}$  for the plain tube. At  $\text{£}2000\text{ tonne}^{-1}$  the plain tube would cost  $\text{£}5.4\text{M}$ . The convoluted design costs only  $\text{£}0.5\text{M}$ .

A  $5\text{ m}$  long convoluted tube prototype with  $0,91\text{ mm}$  wall thickness has been tested. Separated into  $1\text{ m}$  sections, these were then welded together at  $12\text{ mm}$  thick rings, each  $50\text{ mm}$  long. Dished end plates, each  $6\text{ mm}$  thick were welded to the end. This vessel operated in the high vacuum region.

This thesis aims to explore thin walled vacuum vessels. Bennett [7] has highlighted some of the advantages of thin walls in addition to the cost and material savings. Handling, cutting, bending and welding are easier with thin walls. Transportation of smaller loads is more convenient. Also, a thin wall has a relatively high electrical resistance and hence can be heated by

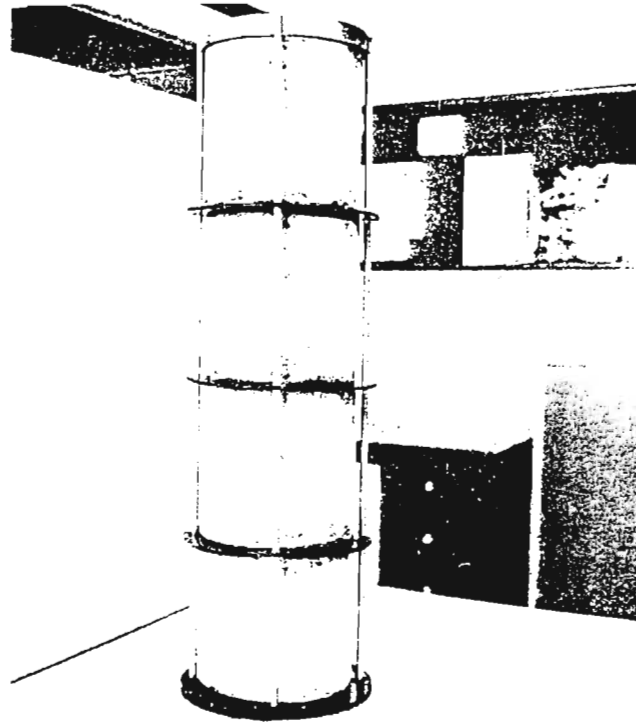


Figure 1.2: hialvac

passing an electrical current through it. This can be done in order to achieve low outgassing rates. A thicker walled vessel would require a larger current to obtain the same results. A thin walled vessel can also be self aligning.

### 1.2.2 Hialvac

The hialvac system was developed by M.M.Michaelis [4]. The vessel can be pumped down to  $10^{-6}$  torr. Further research by Michaelis and Poole [5] showed that the material is suited to high vacuum use. An  $11\text{ cm}^2$  sample was tested for its outgassing properties with a quadrupole mass spectrometer. The rate of outgassing was so low that it could not be detected.

There is some uncertainty as to whether or not hialvac could be used for large chambers, but certainly smaller chambers can be linked together. This method of vessel design represents a cost saving over traditional vacuum designs. However, a disadvantage of such a vessel is that it most certainly does not represent a saving in terms of mass and therefore tends to be bulky.

### 1.3 The principle of tensional vacuum vessels

The tensional vacuum vessel (TVV) is the subject of this thesis. TVV's are different from standard vacuum vessels in that the walls are placed in tension as opposed to regular vacuum vessels which have the walls in compression. A regular vacuum vessel will have to withstand the compressional forces due to atmospheric pressure. The TVV has two thin walls linked together with the intermediate layer pressurised to place the walls in tension.

Metals, the material of most large vessels, do have a propensity to buckle under compression due to instabilities and current designs (vessels in compression) fail to utilise the high tensile strength of these materials. The TVV allows one to take advantage of this property whilst saving a great deal in terms of the amount of material used and also allows the use of novel materials with high tensile strengths. The TVV could be developed not only to produce lightweight chambers but also chambers that can be folded away when not in use thus saving space. In addition TVV's have the advantages of thin walled vessels listed in the previous section. Added to these is the fact that if tensional end plates are used, then a fully inflatable TVV is possible. If the intermediate layer of a TVV is pressurised with lighter than air gases it is also possible to create a lighter than air vessel provided that the vessel is sufficiently large.

### 1.4 History of TVVs

Preliminary work on TVVs was performed in our department by Prof. M.M.Michaelis and A. Forbes [6]. The idea of the TVV was not at any stage believed to be totally novel and further research has indeed revealed three patents which were based on the same principle. These will be discussed later but it is worth mentioning that none of these patents explicitly mention vacuum work as they all concern the submarine applications of the tensional principle.

There were two early experiments set up, one to illustrate the principle and the other designed to gain more experience working with tensional structures. The first experiment simply consisted of two transparent plastic containers, a smaller one within a larger one linked together by nylon wire. This apparatus was connected to two vacuum cleaners, one being connected to the inner container, the other to the intermediate layer. These were then set on suck and blow respectively. Tensional dimples could be seen to form at the connection points of the nylon at the outer surface. If the pressure in

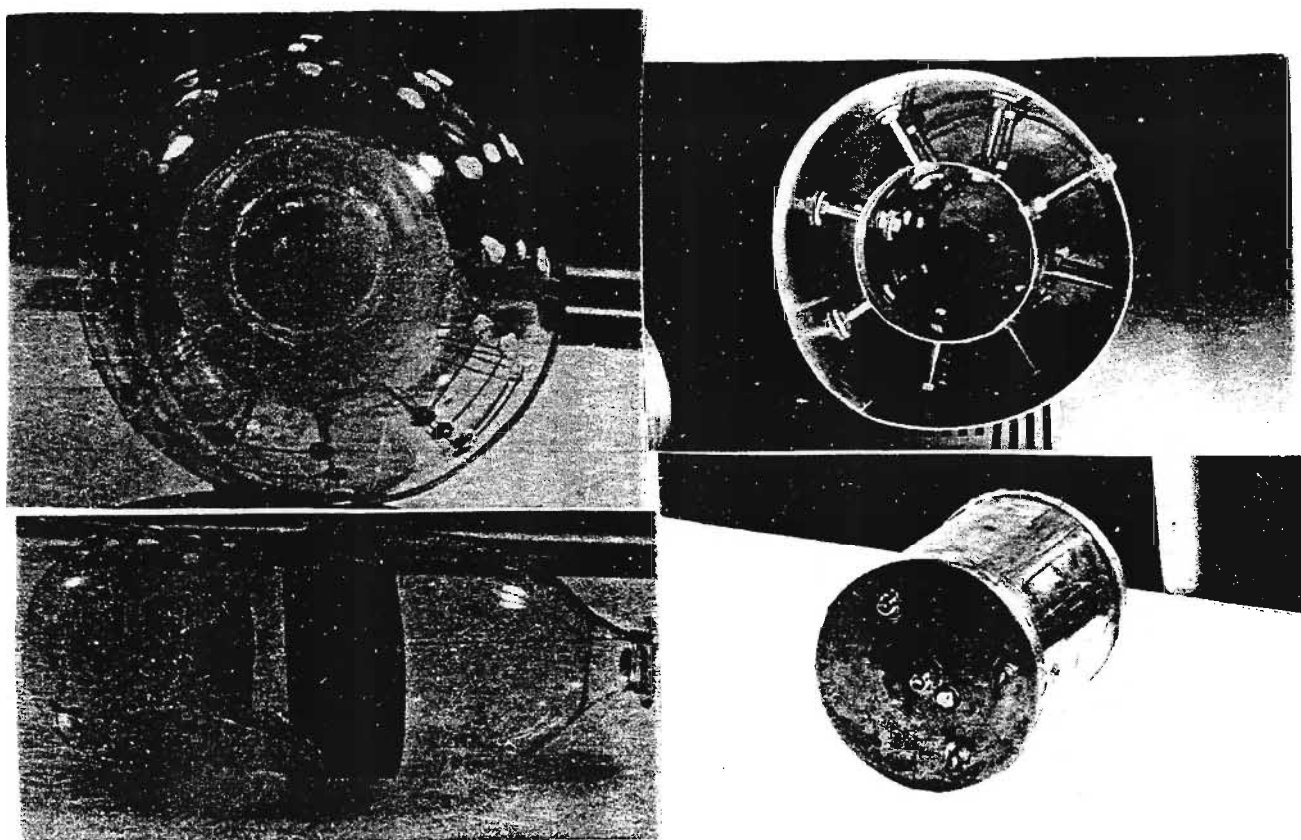


Figure 1.3: Two early TVV's

the intermediate layer was reduced the chambers would begin to implode. Even slight pressure on the outer container would cause the inner chamber to begin to collapse.

The second experiment was a more serious experiment aimed at producing a more useful result. The plastic containers were replaced with  $0.2\text{ mm}$  thick brass sheets. These were rolled into cylinders each  $17\text{ cm}$  long, the inner cylinder being half the radius of the outer cylinder (the previous experiment had a similar arrangement) which measured  $6\text{ cm}$ . These were connected by sixteen studs each  $3\text{ mm}$  thick which were soldered at each end. This arrangement was capped and glued at each end with  $1\text{ cm}$  thick aluminium plates. One of these was fitted with two ports for a  $4\text{ mm}$  vacuum hose as well as a pressure hose. The first version imploded due to the fact that the early theory predicted a lower pressure for the intermediate layer than was actually required. The later version worked well although only at a higher intermediate pressure than predicted. This apparatus was designed purely for structural purposes and was not intended to produce a high vacuum.

These early experiments were subject to a number of technical difficulties: wire welding problems, high material stress at wire welds, and there were problems with air leaks if the studding and washer method was cho-

sen. The design principle of the TVV allows one to replace the double wall connected by struts with tubes arranged in a concentric ring and interconnected. This is effectively the same design and utilises the same tensional principle. For purposes of easier construction of the early TVVs it was found to be convenient to construct the next series of chambers using a jacket of liquid filled tubes. The easiest method was to build a concentric ring of soft drink cans sealed together with putty.

## 1.5 Early Experiments with Tubular TVV's

The first experiments conducted with tubular TVV's were performed by Andrew Forbes of the UND Laser Group and are discussed in his doctoral thesis. Several small scale vessels were constructed in the manner described above. The first vessel had a wall consisting of a single layer of six cans arranged in a concentric circle and sealed at each end by 1 *cm* thick aluminium plates. This chamber could support a low vacuum. In order to further test its structural capabilities, the chamber was modified such that it could be lowered into a water bath and tested at various depths. A low vacuum could be maintained at depths of between 2 and 3 metres. Tests were not conducted at further depth due to the limitations imposed by the length of vacuum hose and pool depth.

A larger version of this vessel was constructed using twenty cans. This was a double layer design with ten cans in each layer. A further layer of ten cans was later added to create a larger chamber. Each of these vessels could maintain a low vacuum but instabilities manifested in that the cans clearly showed signs of movement. The vessels "breathed" and a small assymetry in the initial alignment resulted in implosion. Also inward curvatures were noted in the vertical alignment. This showed that instability increased with an increase in the number of vertical layers.

## 1.6 Patents

As has already been mentioned, there are three patents regarding designs incorporating the tensional principle which have been proposed for marine technology. All of these avoid being specific about marine applications and as such could apply to the TVV.

The first of these is the "Rome patent" of Marcella de Cesaris and family [11]. This describes a structure with rigid walls but having cavities filled with compressible fluid under high pressure. These walls have the same properties

as those of purely solid construction but are considerably lighter than the conventional structures. No specific mention of vacuum applications is made.

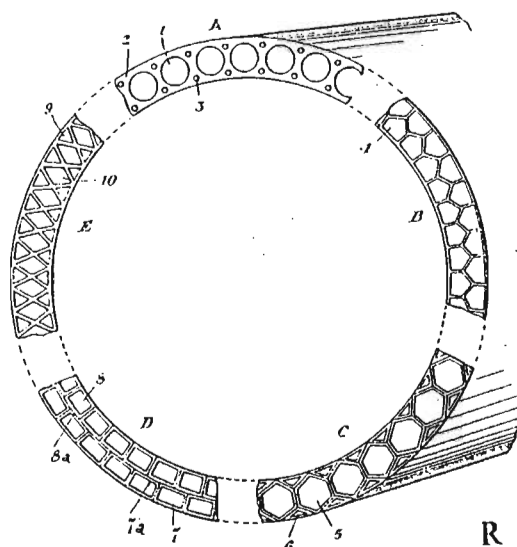


Figure 1.4: The Rome Patent

The second is the "Paris patent" by André Grihangne and Guy Delamare [12] is more detailed than the "Rome patent". Some of these ideas include walls purely in tension, the savings in terms of weight and amount of material, fold away structures, and the use of non metals. No specific mention is made of vacuum applications although there are claims made for a reservoir or duct under a lower pressure than its surroundings. The patent is concerned with marine applications and petro-chemical ducting. Basic calculations of intermediate pressures required to put the walls into tension are made.

The final patent is the "Milan patent" by Sub Sea Oil Services [13] and concerns the use of underwater hulls or tanks with "toric components" pressurised with the aid of "compressed substances".

Up until this point various military and civilian bodies have failed to find any use for this technology regarding marine applications. However,

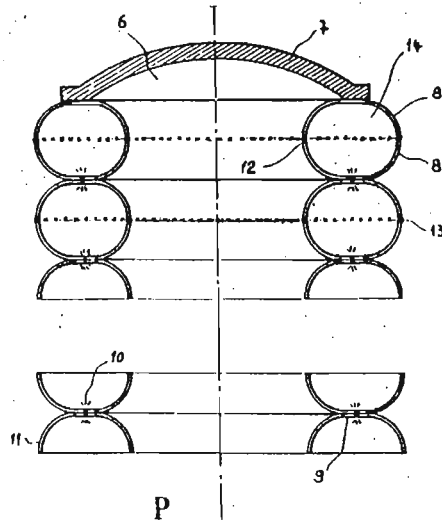


Figure 1.5: The Paris Patent

a tensional submarine design could very easily be converted to a TVV by reducing the required strength and thickness of the walls.

## 1.7 Tensional Submarines Applications

The correlation between submarines and vacuum vessels is obvious. Both are required to withstand a significant external pressure. The internal pressure of such vessels is negligible by comparison. Submarines have to withstand an extra ton per square metre for every metre descended. This requires considerable mechanical strength and these vessels are usually constructed as cylinders for hydrodynamic reasons. A spherical shape would be ideal due to the fact that this shape provides maximum resistance. Submarines usually have thin walled hulls with ring stiffeners.

C.F.T.Ross has outlined possible alternative pressure hull designs [14, 15]. Submersibles have been designed that are spherical in shape but are



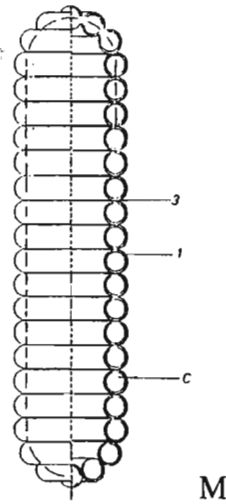


Figure 1.6: The Milan Patent

surrounded by a cylindrical casing which encloses a water jacket. Ross proposes to use such a water to enclosed a "swedged" vessel. This is essentially a corrugated design. This can be strengthened with ring-stiffeners. These can come in the form of pressurised tubes placed in an initial state of tension. F.J.Harris suggested in a private communication with Ross [14, 15] that the vessel be stiffened with longitudinal tubes. Ross suggested that circumferential tube stiffeners be employed.

A deepwater submarine, the CEE-22, employing a toroidal hull design, has been developed independently by Sub Sea Oil Services. This design enables the storage of ample oxygen and is rated for depths of 650 *m*. The vessel can carry up to twenty men under atmospheric or hyperbaric conditions in the event of a subsea rescue although its main use is for underwater jobs that require extended periods of time.[16]

This hints at the tensional designs explored in this thesis where longitudinal tubes were employed as well as pressurised toroids. Ross has also suggested the use of tensional ends. Submarines usually employ dome shaped

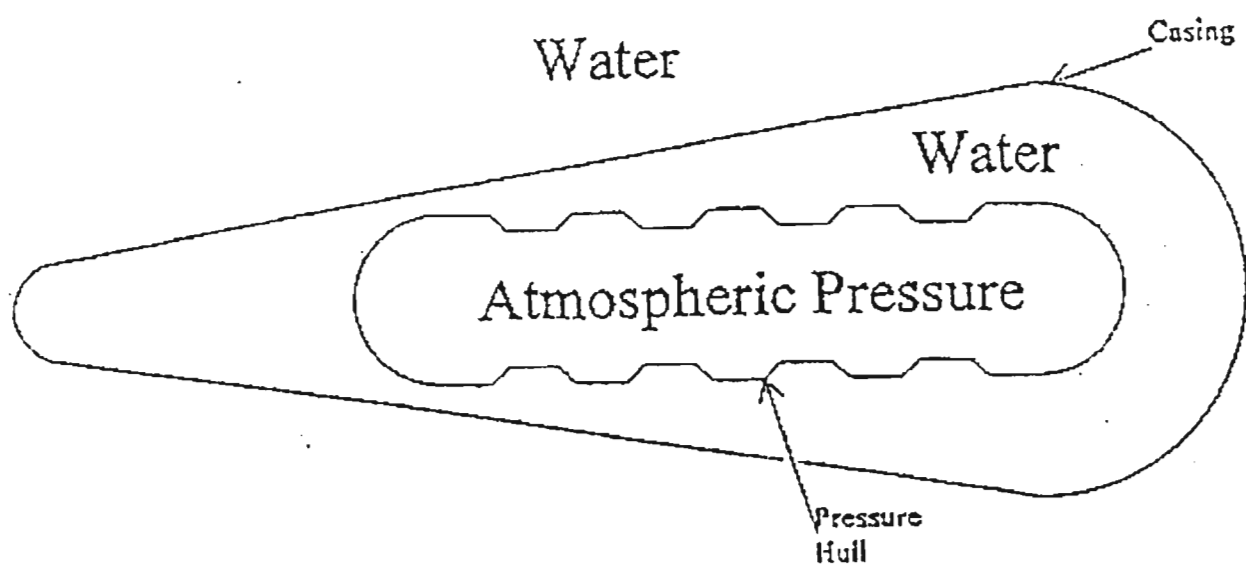


Figure 1.7: "Swedged" submersible design

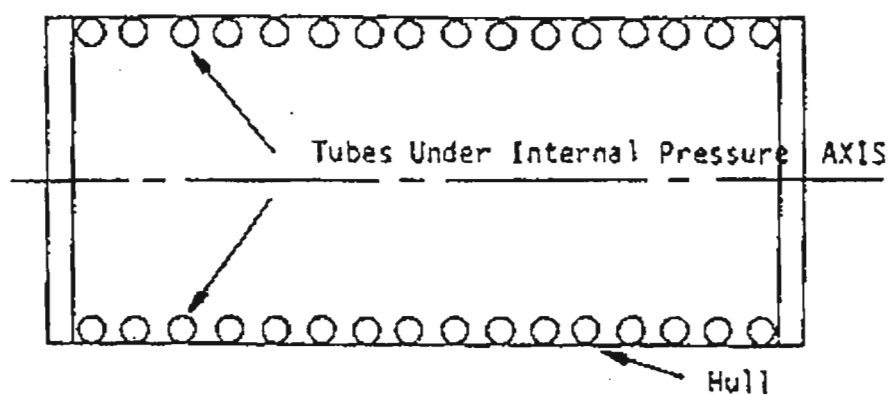


Figure 1.8: Tube stiffened submersible design

ends. If these are inverted, placing the ends in tension, a material saving of fifty percent and probably more is obtained as outlined in Chapter 7.

## 1.8 Outline of thesis

An overview of the uses for vacuum and the types of vacuum have been given in this chapter to illustrate the need for cheaper and lighter vessels. Examples of research into such vessels has been given and this has provided a context for the theme of this thesis, research into tensional vacuum vessels. This chapter has served to outline the tensional principle with regards to designing vessels required to withstand compressive forces. Some history has been given and it has been found that although the principle is not entirely new, very little work has been done with regards to vacuum applications. Research into tensional submersibles has been conducted but there are no patents regarding TVV's. The rest of this thesis is devoted to providing the theory of TVV's. In addition several chapters describe in some detail experiments that were performed in order to illustrate that TVV's could provide a high vacuum.

Chapter Two outlines the theory behind the TVV's. The basic theory is given for spherical and cylindrical designs. The theory behind cylindrical TVV's constructed from longitudinal tubes (tubular TVV's) and tori (toroidal wall TVV's) is also examined. Some discussion about material science limitations is also given in addition to novel concepts such as the buoyant chamber.

Chapter Three examines low vacuum tubular TVV experiments. These followed on from earlier experiments which proved the viability of the TVV principle. These demonstrate that TVV's can be scaled up in size and show the viability of a high vacuum TVV through the addition of a guard vessel.

Chapter Four outlines the high vacuum experiments which demonstrate conclusively that the tensional principle is practical with regards to vacuum applications.

Chapter Five describes further tubular TVV experiments which illustrate that these vessels can operate at much lower intermediate wall pressurisation than those required by the basic TVV theory developed in Chapter Two. This could be due to the compressional components such ring stiffeners present in the tubes.

Chapter Six examines experiments performed with cylindrical TVV's with walls constructed from toroidal tubes. These Toroidal Wall TVV's (TTVV's) are found to be inflatable and high vacuum experiments are con-

ducted successfully.

Chapter Seven outlines experiments performed with tubular TVV's which are equipped with tensional end plates. Theory behind the buckling of domes is given and the advantage of placing a dome in tension is discussed. The fully tensional cylindrical TVV concept is examined and finite element analysis is performed in order to simulate the deformation of a circular end plate.

Chapter Eight outlines a novel concept, the Spinning Vacuum Vessel (SVV). This does not necessarily require the walls to be in tension and therefore represents a slight digression from the main topic of this thesis. However, this vessel does allow the use of thinner walls and novel materials. The basic theory is outlined and a description of a small scale experiment is given.

Chapter Nine is the conclusion and provides a summary of the results obtained during the course of this research.

## Chapter 2

# Theory of the TVV

### 2.1 The basic theory

Much of the theory of the TVV has been worked out by M.M.Michaelis and A. Forbes of the Plasma Physics Research Institute, University of Natal in Durban.[6]

As outlined earlier, the TVV consists of two thin walled shells, an inner shell and an outer shell, which are linked together by struts. The intermediate layer is pressurised placing the shells in tension. Figure (2.1) is a basic diagram of the TVV structure.

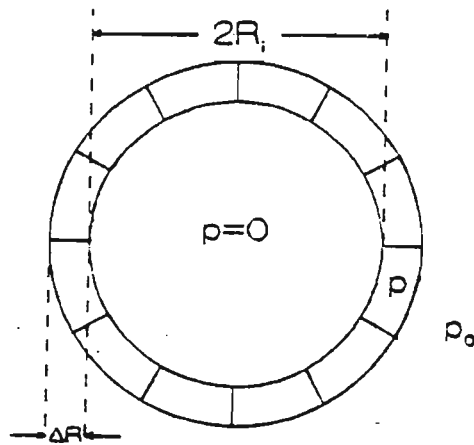


Figure 2.1: Basic Structure of a TVV

For the chamber to be stable<sup>1</sup>, the inward forces on the struts,  $F_i$ , must cancel the outward forces,  $F_o$ . If the inward forces predominate, the chamber will implode, if the outward forces predominate, the chamber will explode. The condition for equilibrium is therefore:

$$\sum F_i = \sum F_o \quad (2.1)$$

The pressure in the intermediate layer will be referred to as  $p$ , and atmospheric pressure will be referred to as  $p_0$ . The radius of the inner wall will be referred to as  $R_i$  whilst the radius of the outer wall will be referred to as  $R_o$ .

### 2.1.1 The Spherical TVV

The spherical TVV is the simplest configuration of a tensional vessel and is therefore useful in the development of basic TVV theory. Using the symbols defined above, equation (2.1) becomes, in the spherical case:

$$4\pi(p - p_0)R_o^2 = 4\pi p R_i^2 \quad (2.2)$$

This is the equilibrium condition. The force on the outer wall due to the gauge pressure must be greater than or equal to the force on the inner wall due to the absolute pressure in order to ensure that the forces on the struts are in equilibrium. After simplifying 2.2, the following is obtained:

$$R_o = R_i \sqrt{\frac{p}{p - p_0}} \quad (2.3)$$

If it is assumed that  $p \gg p_0$ , then (2.3) may be approximated to:

$$R_o = R_i \left( 1 + \frac{p_0}{2p} \right) \quad (2.4)$$

If  $\Delta R$  is defined such that  $\Delta R = R_o - R_i$ , then from (2.4) it can be seen that:

$$\frac{\Delta R}{R_i} = \frac{p_0}{2p} = \frac{1}{2p_{bar}} \quad (2.5)$$

If equation (2.3) is examined using the assumption that  $p \gg p_0$ , then one can see that  $\frac{p}{p - p_0} \rightarrow 1$  and therefore that  $R_i \rightarrow R_o$ . This means that for large  $p$ , (2.5) will tend to become:

$$\frac{\Delta R}{R_o} = \frac{p_0}{2p} = \frac{1}{2p_{bar}} \quad (2.6)$$

This illustrates a logical principle. The greater the pressure in the intermediate layer, the smaller will be the required  $\Delta R$ .

---

<sup>1</sup>The fundamental theory assumes that the TVV has no rigidity of its own

### 2.1.2 Cylindrical TVV's

The above equations describe the most basic TVV. A more common configuration is likely to be a cylinder with the side walls in tension as illustrated in figure (2.2).

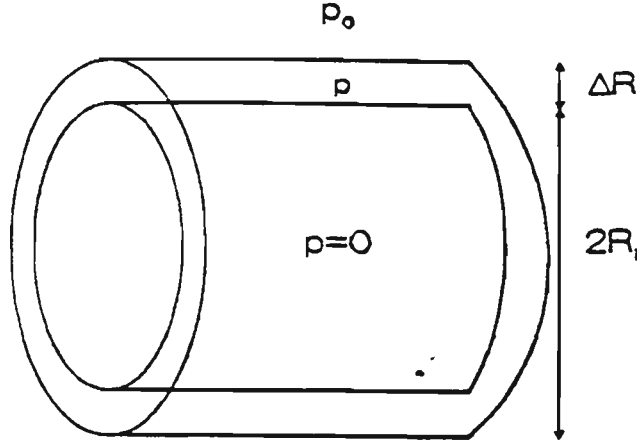


Figure 2.2: Diagram of a Cylindrical TVV

The forces at the cylinder sides of length  $l$  can be calculated in the same manner as applied in the spherical case. Equation (2.1) now becomes:

$$(p - p_0)2\pi R_o l = 2\pi p R_i l \quad (2.7)$$

This can then be simplified to:

$$R_o = R_i \left( \frac{p}{p - p_0} \right) \quad (2.8)$$

If once again it is assumed that  $p \gg p_0$  then (2.8) can be approximated to:

$$R_o = R_i (1 + p_0/p) \quad (2.9)$$

Using the standard definition of  $\Delta R$ , according to (2.9), this now becomes:

$$\frac{\Delta R}{R_i} = \frac{p_0}{p} = \frac{1}{p_{bar}} \quad (2.10)$$

A straightforward algebraic manipulation of the variables in (2.8) gives

$$\frac{\Delta R}{R_o} = \frac{p_0}{p} = \frac{1}{p_{bar}} \quad (2.11)$$

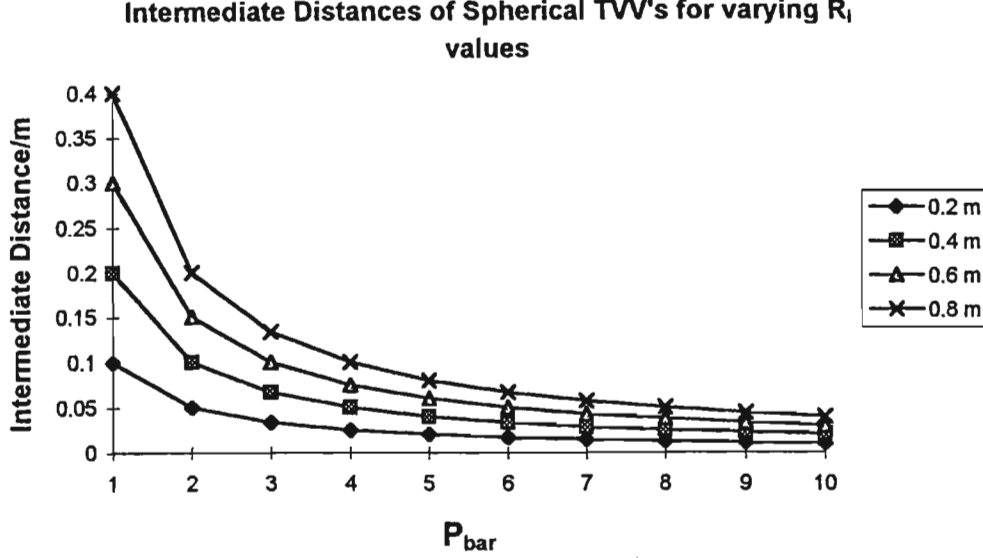


Figure 2.3: Variation of  $\Delta R$  with  $P_{bar}$  for various  $R_i$  values of Spherical TVV's According to Approximate Equation (2.5)

Equations (2.5) and (2.10) show that for greater values of  $p$ , smaller volumes of the intermediate space are required, as in the spherical case. This means that a TVV with a large inner chamber does not necessarily require a bulky double walled structure. Further confirmation is obtained through the derivation of equation (2.11).

Equations (2.5) and (2.10) are illustrated graphically with figures (2.3), (2.4) and (2.5) which show how  $\Delta R$  varies with  $p$  for various values of  $R_i$ .

All of these graphs are asymptotic in nature. This illustrates that variation in  $\Delta R$  is small when  $p$  is large. Both the spherical and cylindrical case are examined graphically in figure (2.6) in order to determine the accuracy of the approximations made for  $p \gg p_0$ .  $\Delta R$  is plotted both for the approximate expressions, (2.5) and (2.10), and for the exact expressions (2.3) and (2.8). The figure shows that in the spherical case, the values are almost identical for values greater than 6 *bar*. The discrepancy only becomes serious for values that are less than 2 to 3 *bar*. This means that the approximation is quite realistic for most spherical TVV's. The situation is a little more serious in the case of cylindrical TVV's where the values are almost identical for  $p$  values greater than 9 *bar*. The discrepancy becomes noticeable for  $p$  values that are less than 3 to 4 *bar*. This has to be taken



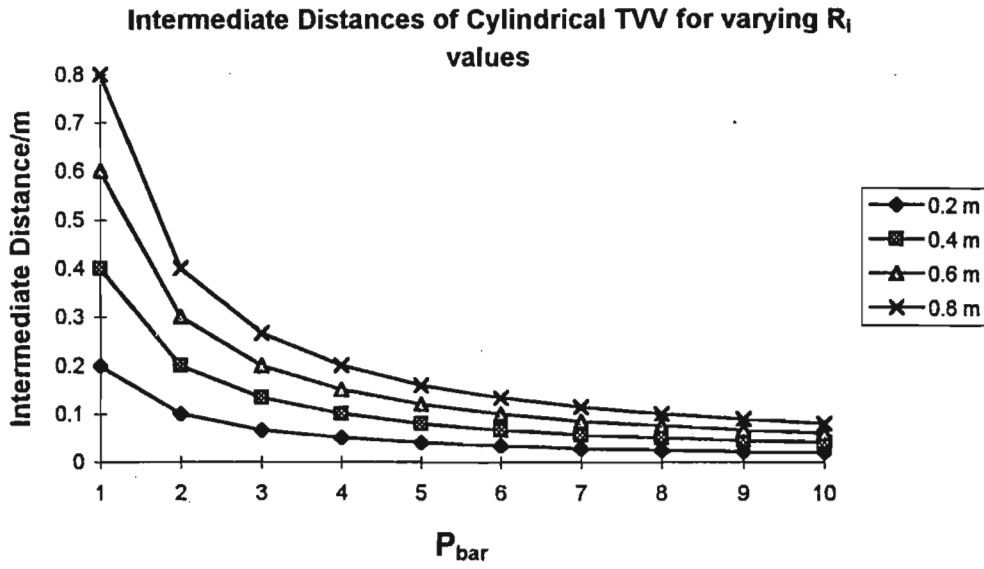


Figure 2.4: Variation of  $\Delta R$  with  $P_{bar}$  for various  $R_i$  values of Cylindrical TVV's According to Approximate Equation (2.10)

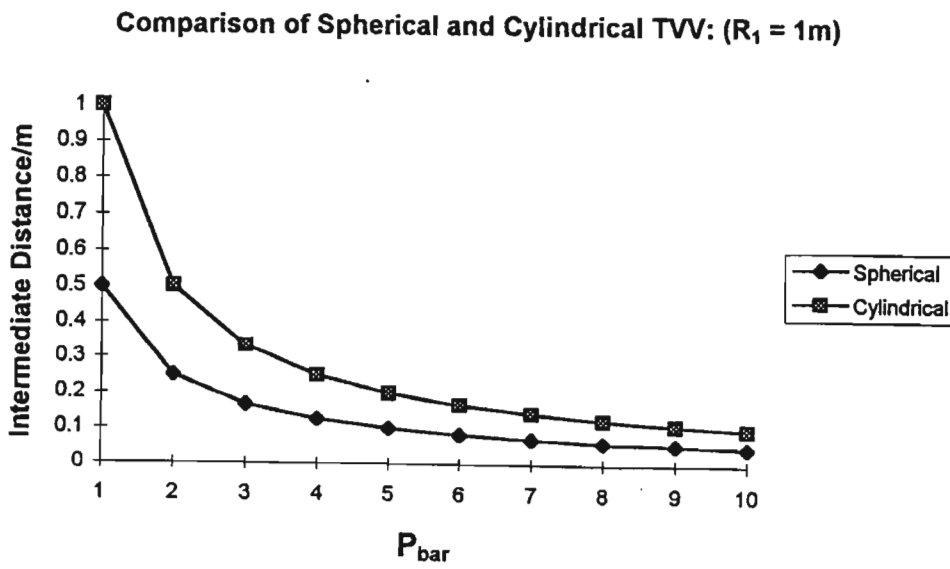


Figure 2.5: Comparison of Spherical and Cylindrical TVV's with  $R_i = 1$  Using Approximate Equations (2.5) and (2.10)

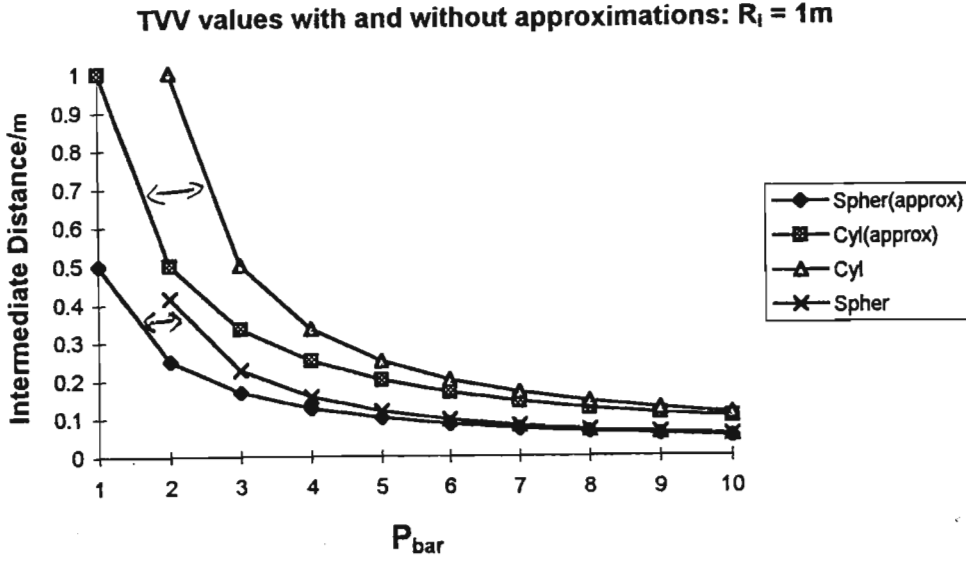


Figure 2.6: TVV Data from fig(2.5) including comparisons with data obtained from the Exact Equations (2.3) and (2.8)

into account as most TVV's are likely to be cylindrical in nature and will possibly operate with these  $p$  values. This is due to the fact that a designer will have to balance the desire to reduce the pressure in the walls with the desire to reduce the vessel bulk.

In the case of the cylindrical design, the forces due to the end plates also have to be taken into account. These forces are due to the intermediate pressure acting outwards and the atmospheric pressure acting inwards. The net force,  $F_{\text{end}}$ , may be given by the following equation:

$$F_{\text{end}} = (\pi R_o^2 - \pi R_i^2)(p - p_0) - \pi R_i^2 p_0 \quad (2.12)$$

where  $F_{\text{end}}$  is defined to be positive if the net force is outwards. This can be simplified to give:

$$F_{\text{end}} = \pi [R_o^2(p - p_0) - R_i^2 p] \quad (2.13)$$

We can manipulate equation (2.8) in order to obtain an expression for  $R_i^2$ :

$$R_i^2 = \frac{R_o^2(p - p_0)^2}{p^2} \quad (2.14)$$

It should be noted that this is an exact expression for cylindrical TVV's, no approximations are involved. Substituting we obtain:

$$F_{end} = \pi R_o^2 \left[ p - p_0 - \frac{(p - p_0)^2}{p} \right] \quad (2.15)$$

which can be simplified to give:

$$F_{end} = \pi R_o^2 \left( p_0 - \frac{p_0^2}{p} \right) \quad (2.16)$$

This expression can be further factorised to give the general equation:

$$F_{end} = \pi R_o^2 p_0 (1 - p_0/p) \quad (2.17)$$

This is an important result as (2.17) shows that as long as the intermediate pressure is greater than that of atmospheric pressure, which is necessarily the case, the net force will always be outwards. There will always be a tension in the vessel along its length. The corrugated vessel developed by Bennett[7] requires supports at both ends in order to resist the force in the end plates. The TVV has the advantage in that it is stable against these end forces. There is no need of further support.

This equation can be expressed in terms of  $R_i$ . If equation (2.8) is used to provide a substitute expression for  $R_o$ , we obtain:

$$F_{end} = \pi p_0 \left( \frac{R_i^2}{1 - p_0/p} \right) \quad (2.18)$$

This is illustrated graphically in figure(2.7).

All of the graphs in this figure are asymptotic in nature. The overall variation of the end forces for a particular  $R_i$  value is small and for values greater than 4 *bar* tends to be negligible. This is the case for the overall variation of smaller vessels. The values obtained for large  $p$  do not converge for different  $R_i$  values and therefore the larger the vessel, the greater will be the end force regardless of  $\Delta R$ . However, for large  $p$ , a further increase in this pressure will not effect the overall forces on the end plates of a particular vessel, assuming that the walls are in equilibrium.

## 2.2 TVVs constructed from tubes

As mentioned earlier, a variation of the conventional TVV, which has a double wall connected by struts, is a TVV with a wall consisting of longitudinal

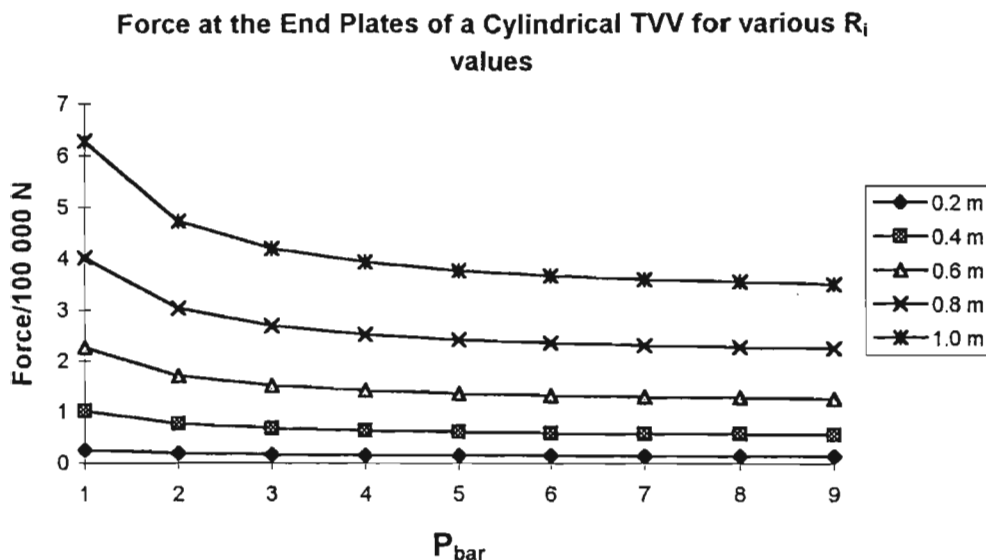


Figure 2.7: Force experienced at the end plates of Cylindrical TVV's for various  $R_i$  values

tubes. The pressure can be provided by a solid, but a fluid is far more convenient as this allows for pressure variation. This concept obviously applies to the cylindrical TVV in general. During the course of experimental work it was found that tubular TVV's were the simplest and most cost effective chambers in terms of construction.

### 2.2.1 Basic Theory

Further calculations have been done by Michaelis and Forbes regarding the above TVV model [17]. This model assumes that the primary forces holding the cans together is friction. The following theory is therefore idealistic.

If one takes the TVV to be  $m$  tube layers and  $n$  tubes in each layer, we can develop the following theory. Each tube has a height,  $l$ , and a radius,  $R_t$ . The vessel is represented by figure (2.8). This notation will be adopted throughout the remainder of this thesis. The evacuated volume is worked out to be:

$$V = \frac{ml}{\pi} [R_t(n - \pi)]^2 \quad (2.19)$$

where the approximation has been made that  $2nR_t = 2\pi R_i$ .  $R_i$  is the internal radius of the chamber which is defined to be the distance from the

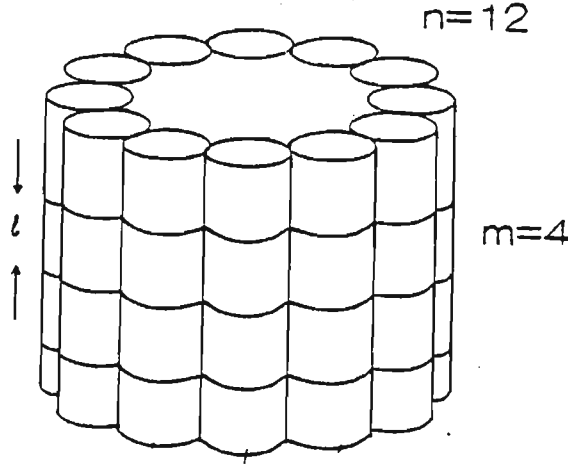


Figure 2.8: Tubular TVV with appropriate terminology

central axis of the vessel to the innermost part of the tubes. The surface area of the end plates exposed to the vacuum,  $S_e$ , is therefore:

$$S_e = \frac{1}{\pi} [R_t(n - \pi)]^2 \quad (2.20)$$

This is useful for finding  $F_a$  exerted on these plates. If  $n \gg \pi$  then the following approximations can be made:  $S_e = \pi R_t^2$  and  $V = ml\pi R_t^2$ . This is not to say that the chamber can be scaled up arbitrarily in terms of size as there are other factors involved which impose constraints on the values of  $m$  and  $n$ . A better approximation may be  $2nR_t = 2\pi R_o$ . However,  $\Delta R$  is typically small compared with  $R_i$  for these vessels as the  $R_t/R_i$  must be relatively small assuming little distortion of the tubes. This would necessarily be true for liquid jackets due to their incompressible nature. The initial approximation may therefore be considered valid, particularly for vessels with large  $n$ .

The force acting vertically upon each can,  $F_{a_n}$  is therefore:

$$F_{a_n} = \frac{p_0}{n\pi} [R_t(n - \pi)]^2 \quad (2.21)$$

Figure (2.9) is a diagram which shows the forces acting on a tube due to the atmosphere and the neighbouring tubes.

If the force acting upon a single tube due to the atmospheric pressure is labelled  $F_a$ , then this force is well described by the simple equation,  $F_a = 2p_0lR_t$ . From the diagram, it can be shown that the component of the force

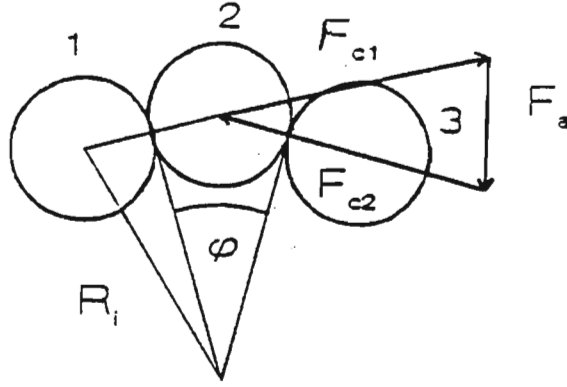


Figure 2.9: Forces Acting on an Individual Tube

due to the action of a neighbouring tube,  $F_t$  (indicated by  $F_{c1}$  and  $F_{c2}$  in fig (2.9)), is:

$$F_t = \frac{F_a}{\sin \phi} \quad (2.22)$$

It can also be seen from the diagram that  $\phi$  is the angle subtended by each tube at the central axis of the TVV. This means that  $\phi = 2\pi/n$  and so, if  $n$  is large, one can make the following approximation:

$$F_t \approx \frac{nF_a}{2\pi} \quad (2.23)$$

Each tube will have a certain area of contact with the neighbouring tubes<sup>2</sup> and if one defines  $d$  as the width of the area of contact with an adjacent tube then one can obtain:

$$F_t = pld = \frac{nF_a}{2\pi} = \frac{n}{2\pi} p_0 2l R_t \quad (2.24)$$

In terms of  $d$  this means that:

$$d = \frac{n}{\pi} \frac{p_0}{p} R_t = R_i \frac{p_0}{p} \quad (2.25)$$

This is the same as  $\Delta R$  for the case of non-tubular cylindrical TVVs for  $p \gg p_0$ . However, as stated above  $\Delta R$  is small for these vessels and therefore

---

<sup>2</sup>This theory assumes that there is some deformation of the cans when the vessel is subjected to atmospheric pressure

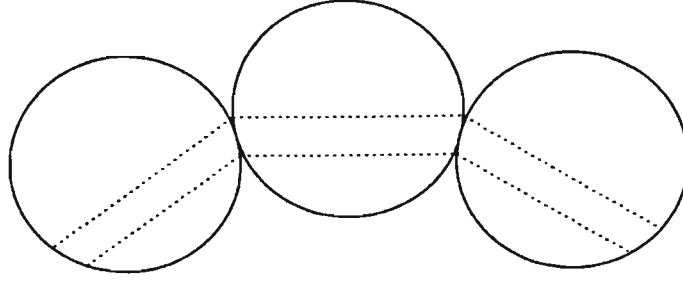


Figure 2.10: Tubular TVV Section with Equivalent Polygonal Structure Superimposed

$R_i \rightarrow R_o$ . This means that if one assumes that the relationship is the same then  $d$  is indeed equal to  $\Delta R$ .

The same result can be derived if the outer and inner walls of the tubes are replaced with flat plates joining the contact lines. This is illustrated below

### 2.2.2 Modifications to Basic Theory

Equation (2.25) can be used to establish an upper bound for  $n$ . If the pressure at which the tubes begin to rupture is called  $p_{max}$  then the following upper bound can be established:

$$n_{max} = \frac{\pi d p_{max}}{R_t p} \quad (2.26)$$

From a geometrical point of view it appears that at high pressures the contact area with neighbouring tubes may be expressed as the ratio:  $d/R_t = 1/3$ . Looking at equation (2.26),  $n_{max}$  is approximately equal to  $p_{max}$  expressed in bars. This would appear to place strict limitations on the number of tubes used at lower pressures. A large  $n$  value will require very high pressures.

The above equations are not very useful for the purpose of establishing an upper bound. In order to obtain this, the frictional forces have to be taken into account, friction by assumption being the primary forces holding the tubes together. If a tube does get pulled into the evacuated area, the

furthest that it could move before losing the frictional contact with the adjacent tubes, would be to the point that all three tubes were in a straight line. The contact force on a tube due to the adjacent frictional forces is  $p_0 R_i l$ . In order to balance air pressure, the following equation must hold:

$$\mu_t p_0 R_i l \geq F_a = 2p_0 R_t l \quad (2.27)$$

where  $\mu_t$  is the frictional coefficient. Due to the fact that  $R_i/R_t = n/\pi$ , equation (2.27) can be expressed in the following way:

$$n \geq \frac{2\pi}{\mu_t} \quad (2.28)$$

This creates some difficulty with regards to the use of metal tubes (these were the type used in experiments with TVVs of this type) due to the fact that metals have a typical metal on metal frictional coefficient of around 0.2. This means that for typical metals, TVVs of this type would require at least 30 tubes. This poses a problem in that practical TVVs would require fewer tubes than this and so it appears that  $n_{min} > n_{max}$ . However, the above equations do not take the effects of the end plates into account. The end plates also produce frictional forces which provide further stability against the atmospheric pressure. If this frictional force is termed  $F_{fr}$ , then one can obtain the following:

$$F_{fr} = 2\mu_e \frac{p_0 \pi R_i^2}{n} \quad (2.29)$$

where  $\mu_e$  is the frictional coefficient due to the end plates.

When  $F_{fr}$  is taken into account, equation (2.27) is modified to become the following:

$$2p_0 R_t l \leq \mu_t R_i l p_0 + \mu_e \frac{2p_0 \pi R_i^2}{nm} \quad (2.30)$$

where  $F_{fr}$  is distributed evenly amongst  $n$  tubes. This equation can be used to derive a new value of  $n_{min}$ :

$$n_{min} = \frac{2\pi l}{\mu_t l + 2\mu_e R_i/m} \quad (2.31)$$

If  $\mu_e$  is made to be reasonably large then the problem discussed above can be made to disappear.

A large  $\mu_e$  will tend to counteract  $F_a$ . This means that the earlier equations have to be modified taking this into account. If the modified  $F_a$  is replaced with the term  $F_i$  referring to the net inwards force we can derive the following:

$$F_i = F_a - F_{fr} \quad (2.32)$$



Substituting for  $F_a$  and  $F_{fr}$  we obtain:

$$F_i = 2R_i l p_0 - \frac{\mu_e 2\pi R_i^2 p_0}{n} \quad (2.33)$$

This can be simplified to:

$$F_i = 2p_0 \left( R_i l - \frac{\mu_e \pi R_i^2}{n} \right) \quad (2.34)$$

If equation (2.23) is now modified, the following is obtained:

$$F_i = p l d = \frac{n F_i}{2\pi} = \frac{n p_0}{\pi} \left( R_i l - \frac{\mu_e \pi R_i^2}{n} \right) \quad (2.35)$$

If  $d$  is equated with  $\Delta R$  then we find after some manipulation:

$$\Delta R = \frac{R_i}{p_{bar}} \left( 1 - \frac{\mu_e R_i}{l} \right) \quad (2.36)$$

This modified equation shows that for large  $\mu_e$ , the value of  $p$  and  $\Delta R$  can remain much smaller than predicted by the earlier theory. The above equation applies to a single layer ( $m = 1$ ) vessel. The  $l$  term should be modified to  $ml$  for multi-layer vessels. The assumption has been made that the tubes are stacked such that the vertical contact surfaces interlock and therefore have no effect on  $F_{fr}$ .

### 2.2.3 Instabilities in Tubular TVV's

The walls of a tubular TVV should contract when subjected to  $F_a$ . This should be expected to create instabilities as the tubes are unlikely to contract evenly. Small misalignments should be expected which are amplified when subjected to an external force. This is particularly serious for a vessel with large  $n$ .

Such a vessel will have small  $\phi$ . A misalignment,  $\Delta\phi/\phi$ , can be large and because  $F_t = F_a/\phi$  is substantially larger than  $F_a$ , the resulting imbalance  $2F_c\Delta\phi$  can be of the same order as  $F_a$  itself.

This amplification of initial geometric misalignments is a most likely cause of implosion and therefore precautionary measures will have to be taken. This will be in the form of circular rims placed internally to maintain symmetry. These will not be intended to behave as ring stiffeners.

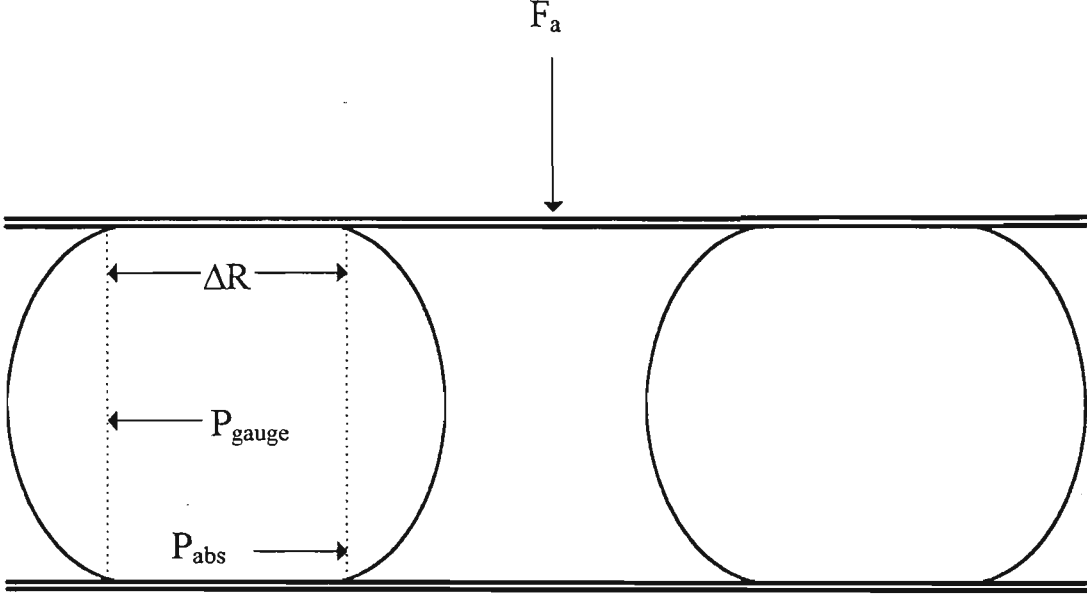


Figure 2.11: Basic diagram of a single layered torus after evacuation

### 2.3 Cylindrical TVV's with Toroidal Walls

The alternative to longitudinal tubes is the use of toroidal tubes placed in tension through pressurisation. It must be stated that these tubes are not necessarily perfect tori, but it is useful to refer to them as such, particularly with regard to developing theory which will describe the stress in the walls.

One can see from figure (2.11) that the cross-sectional area across which the intermediate pressure acts is the same as for a perfect cylinder and therefore the theory is identical in many respects to that developed earlier. The force of atmospheric pressure at the TVV ends will create a contact area equivalent to  $\Delta R$ . The basic TVV theory for cylinders demonstrates that there should always be a tension parallel to the axis of symmetry which acts in the outward direction.

To avoid confusion with vacuum vessels which are toroidal in shape, this design is labelled, the toroidal wall TVV (TTVV).

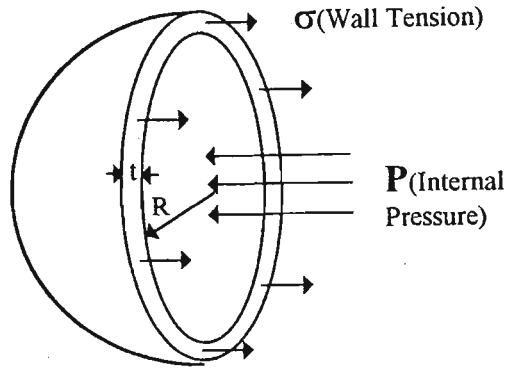


Figure 2.12: Forces Acting on a Sphere Under Internal Pressure

## 2.4 Examination of materials science

The theory given above is useful for deriving equilibrium conditions. However, it is oversimplified in that it does not allow one to calculate the actual rupture pressure of the TVV walls given a particular material. In order to do this one has to take into account the actual wall material and thickness.

### 2.4.1 Tension in a Sphere

Theory is first developed for the most basic TVV design, the spherical vessel. In the case of a thin walled sphere under uniform internal pressure, the tension in the walls has to balance the internal pressure as illustrated by figure (2.12). In order for this to be true, the following must hold:

$$4\pi R^2 \Delta p = 2\pi R t \sigma \quad (2.37)$$

where  $\sigma$  is the tension in the material and  $t$  is the thickness.  $R$  is the radius of curvature and  $\Delta p$  is the pressure difference across the membrane. This

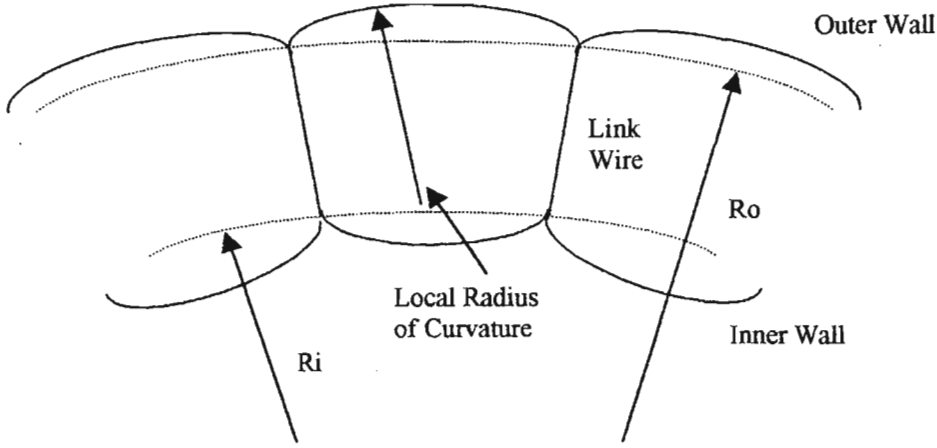


Figure 2.13: Local Curvatures of a Spherical TVV Membrane

can be simplified to give the well known expression:

$$\sigma = \frac{\Delta p R}{2t} \quad (2.38)$$

The tension in the material is directly proportional to the radius of curvature which means that smaller values of  $R$  are desirable. However, this is not to say that the vessel itself will have to be smaller. Figure (2.13) gives a more realistic view of a cross-section of the TVV walls. They are not smooth, but rather consist of a number of local curvatures. The value of  $R$  in each case is reduced thereby reducing  $\sigma$ . The value of such a local curvature can be of the order of  $2\Delta R$  and therefore if one considers a vessel with  $R_i = 2\text{ m}$  pressurised to  $10\text{ bar}$ , this value will be of the order of  $20\text{ cm}$ . A designer will therefore have to balance the desire to reduce  $R$  with the desire to reduce the number of struts. It is probable that the material between the local curvatures will be under greater stress, particularly at the points where the struts connect to the walls, and will therefore have to be reinforced.

#### 2.4.2 Tension in a cylinder

Tension in a cylinder under uniform internal pressure is characterised by acting parallel to the axis of symmetry as well as perpendicular to it. This is illustrated by figure (2.14).

The tension along the axis of symmetry is defined as  $\sigma_x$ . The perpendicular stress, also known as the hoop stress, is defined as  $\sigma_y$ . The value of  $\sigma_x$  can be obtained from equation (2.38) as it is apparent from the figure that

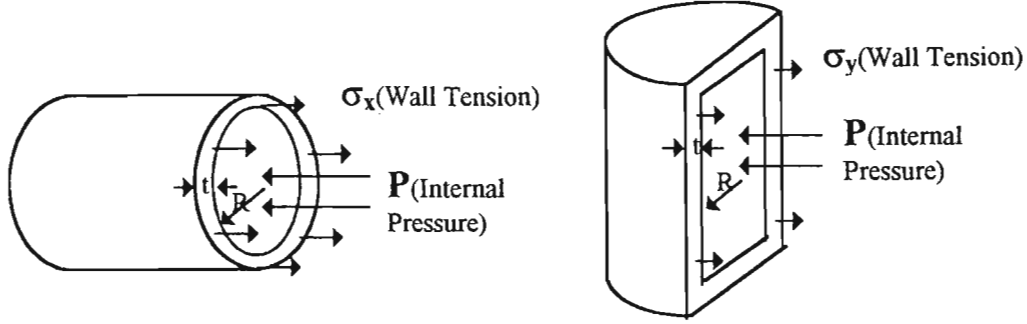


Figure 2.14: Tension in a Cylinder Under Uniform Internal Pressure

the calculation of  $\sigma_x$  is identical to that of a sphere under uniform internal pressure.

The calculation of the hoop stress is slightly different. Examination of figure (2.14) reveals that:

$$2Rl\Delta p = 2lt\sigma_y \quad (2.39)$$

where  $l$  is the height of the vessel. The hoop stress is therefore given by:

$$\sigma_y = \frac{\Delta p R}{t} \quad (2.40)$$

However, as in the case of the spherical TVV, the cylindrical TVV will not have smooth walls, but rather walls with a number of local curvatures. Figure (2.13) will therefore also apply to cylindrical vessels. This will also serve to reduce the hoop stress. In the case of the tubular TVV,  $\sigma_y$  will be almost entirely determined by the curvature of the individual tube. Figure (2.15) shows that  $\sigma_x$  is due to  $F_{end}$  and therefore will not be given by equation (2.38). In this case the following must be true:

$$(2\pi R_i t + 2\pi R_o t)\sigma_x = F_{end} \quad (2.41)$$

which can be simplified to give:

$$\sigma_x = \frac{F_{end}}{2\pi t(R_i + R_o)} \quad (2.42)$$

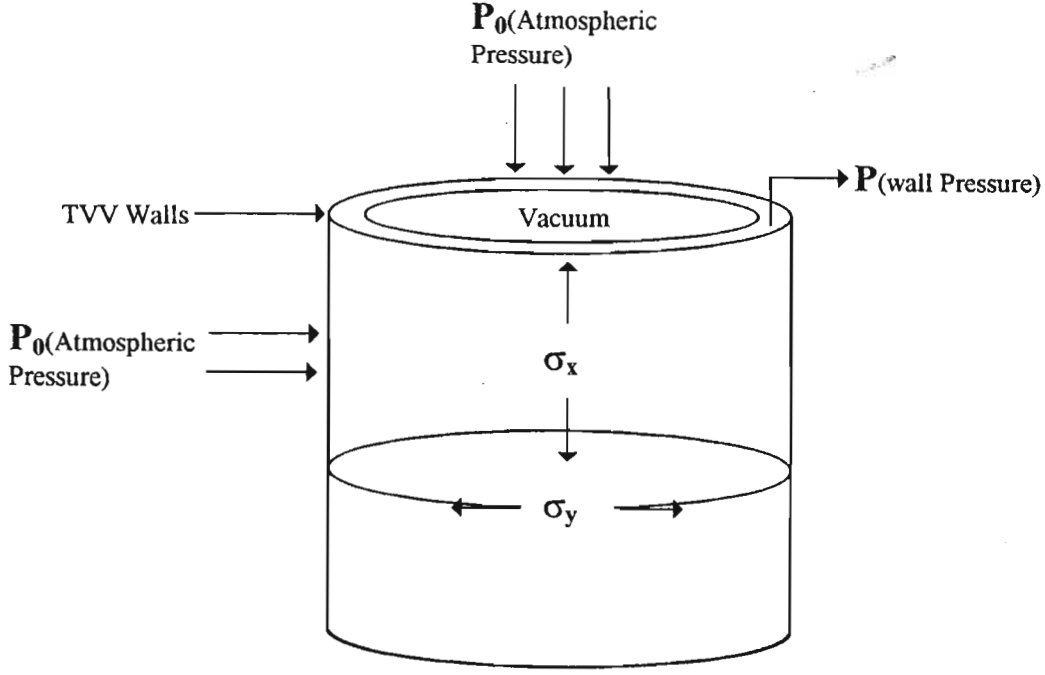


Figure 2.15: Tension in the Walls of a Cylindrical TVV (End Plate not shown)

Equation (2.8) can be manipulated to provide a suitable substitution for  $R_i$ . If the substitution is made, the following is obtained:

$$\sigma_x = \frac{F_{end}}{2\pi t(2 - p_0/p)} \quad (2.43)$$

An alternative expression for  $F_{end}$  is provided by equation 2.17). If this is used the above equation becomes:

$$\sigma_x = \frac{R_o P_0 (1 - p_0/p)}{2t(2 - p_0/p)} \quad (2.44)$$

If  $p \gg p_0$ , the following approximation can be made:

$$\sigma_x \approx \frac{R_o p_0}{4t} \quad (2.45)$$

In the case of a tubular TVV, the situation is slightly different. The cross-sectional area of the TVV walls in the plane perpendicular to the axis of symmetry is  $2\pi R_i t n$ . We therefore have:

$$2\pi R_i t n \sigma_x = F_{end} \quad (2.46)$$

If we use equation (2.17) to provide a substitute expression for  $F_{end}$  we obtain:

$$\sigma_x = \frac{R_o^2 p_0 (1 - p_0/p)}{2R_i t n} \quad (2.47)$$

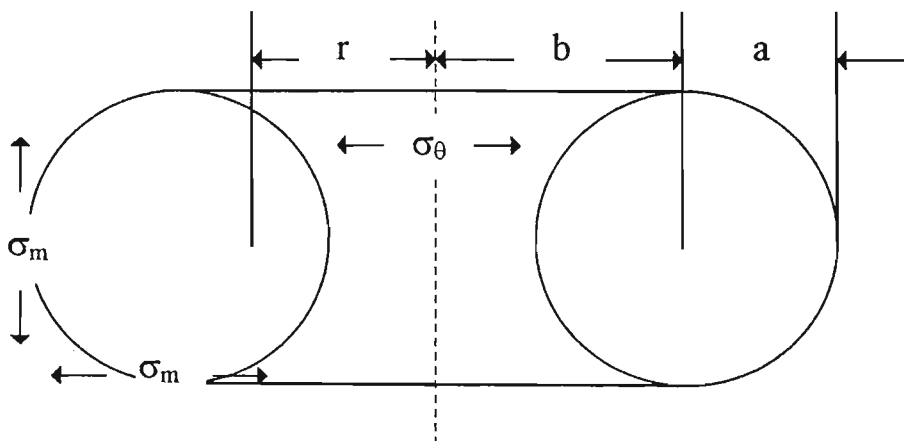


Figure 2.16: Diagram of a Torus under internal Pressure

If we make the approximation,  $2\pi R_o = 2\pi R_t$ , we find that:

$$\sigma_x = \frac{R_o p_0 (1 - p_0/p)}{\pi t} \quad (2.48)$$

. If  $p \gg p_0$ , then we can make a further approximation:

$$\sigma_x \approx \frac{R_o p_0}{\pi t} \quad (2.49)$$

which is very similar to the non-tubular expression.

### 2.4.3 Tension in a Torus

A diagram of a torus under internal pressure is given by figure (2.16). The torus under internal pressure is similar to the cylinder in that it has two tensions associated with it. The meridional stress,  $\sigma_m$ , is the hoop stress which exists in the plane of the axis of symmetry and is associated with the radius,  $a$ . The second stress,  $\sigma_\theta$ , is so labelled as it exists perpendicular to the axis of symmetry and acts in the direction of rotation about this axis.

The hoop stress is given by Cook and Young[19] as the following:

$$\sigma_m = \frac{\Delta p a (r + b)}{2rt} \quad (2.50)$$

The other stress component is given by:

$$\sigma_{\theta} = \frac{\Delta pa}{2t} \quad (2.51)$$

It may be noted that if  $b \gg a$ , the hoop stress will be given by:

$$\sigma_m = \frac{\Delta pa}{t} \quad (2.52)$$

The hoop stress is identical to that of the cylindrical case. The second stress is also identical to that of the cylinder and has the same value of the stress in the sphere. This is half the value of the hoop stresses. As the tubular and toroidal wall TVV's are the most useful configurations, it is clear that the hoop stresses are the most likely to cause rupture.

#### 2.4.4 Specific Material Examples

Table (2.1) gives the yield strengths of various metals, polymers and ceramics. The yield strength is the amount of stress a material can withstand without permanent deformation. Using equation (2.38), the yield pressures of a spherical TVV wall can be calculated for the materials listed, taking into account varying radii of curvature and thicknesses. The results are shown graphically in figures (2.17) to (2.23).

Graphs could also be given for the tensile stresses in the cylindrical vessels. However, the figures given illustrate the advantages of placing materials in tension. Polymers are very poor materials for TVV manufacture in that small  $t$  values can only be employed in small vessels. Metallic TVV's represent a considerable material saving as compared to regular vacuum vessels in compression. However, examination of ceramic materials reveals that the utilisation of novel materials in TVV construction allows for the existence of extremely thin walls. Comparison of Aluminium alloy and Silicon Carbide shows that the latter can have walls almost one hundred times thinner than that of the former.<sup>3</sup>

### 2.5 Inflatable Vacuum Vessels

One of the primary advantages of a TVV is that certain designs can be folded away, hence saving space when not in use. This also makes transportation of

---

<sup>3</sup>SiC may not be a practical material for the construction of TVV's. It is used here purely for illustrative purposes due to its high tensile strength and relatively small density.



Table 2.1: Yield Strengths of Various Materials

Material	Yield Strength/( $MPa$ )
Steel	
Structural	280
1% C hot-rolled	580
Stainless 302, cold-rolled	600
Aluminium Alloy	
1100-H14	110
2014-T6	410
Brass	
Cold-rolled	420
Annealed	100
Polymer	
Polyamide (nylon)	40
Polyurethane elastomer	30
Polyvinyl chloride (rigid PVC)	53
Ceramic	
Concrete	25
Glass (soda)	1500
Silicon	3200
Silicon carbide (SiC)	9800

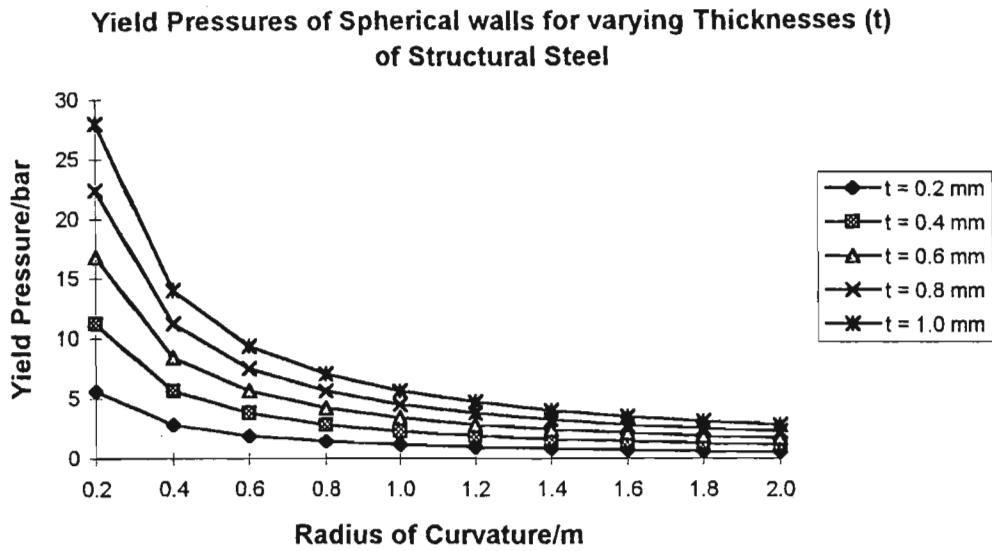


Figure 2.17: Yield Pressures of Structural Steel

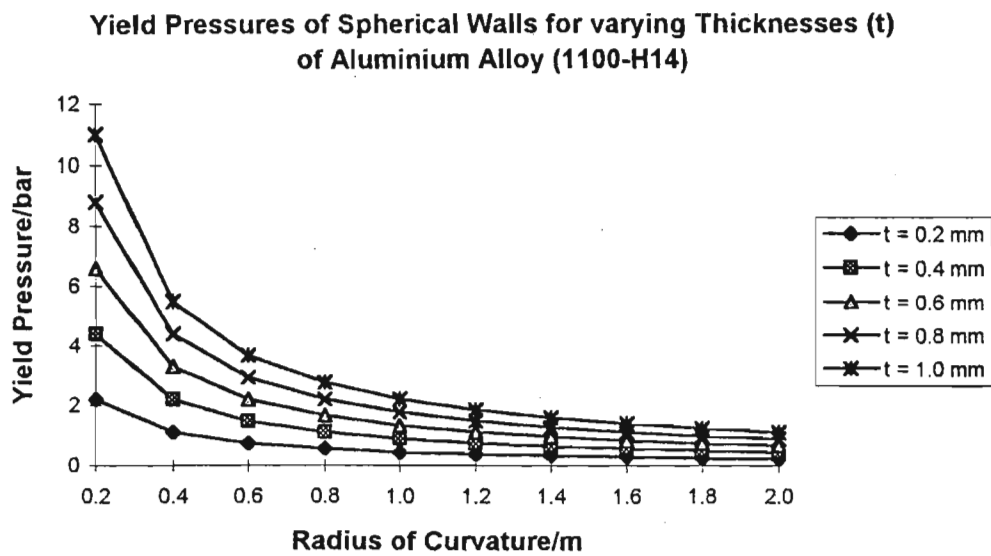


Figure 2.18: Yield Pressures of Aluminium Alloy (1100-H14)

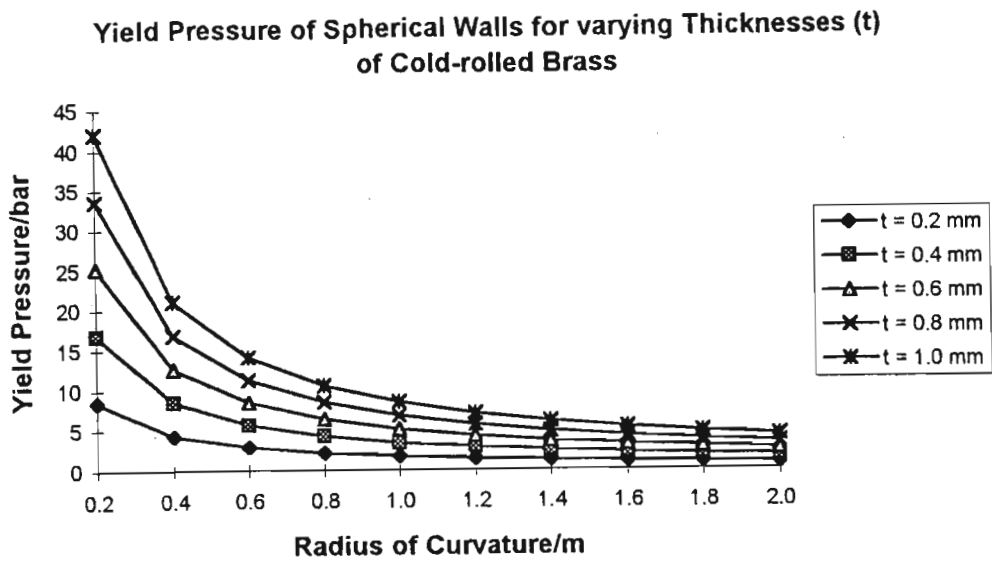


Figure 2.19: Yield Pressures of Cold-rolled Brass

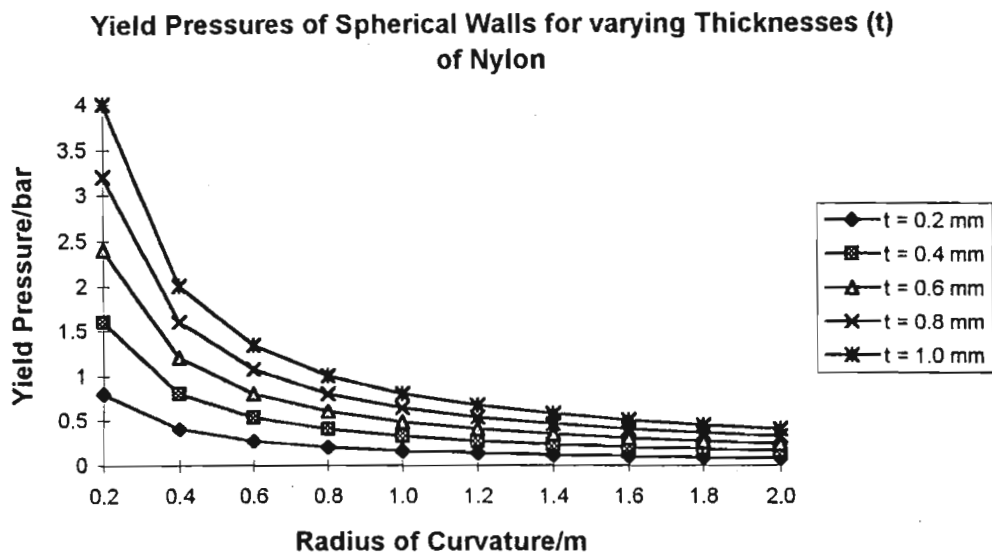


Figure 2.20: Yield Pressures of Nylon

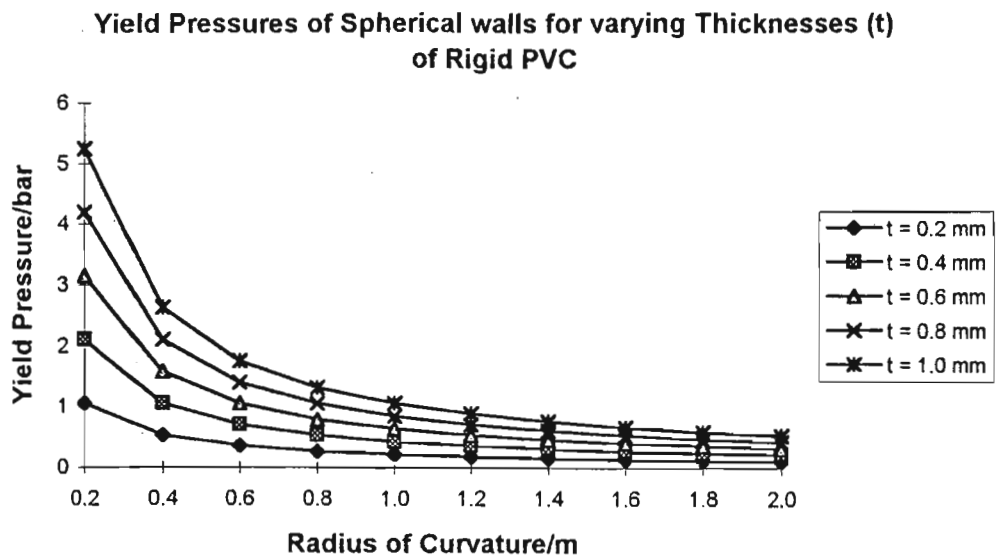


Figure 2.21: Yield Pressures of Rigid PVC

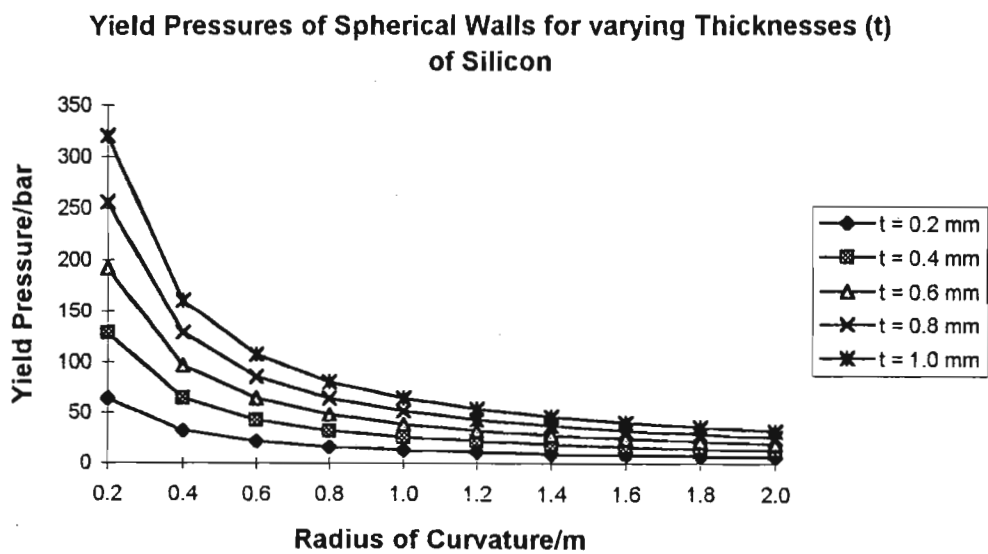


Figure 2.22: Yield Pressures of Silicon

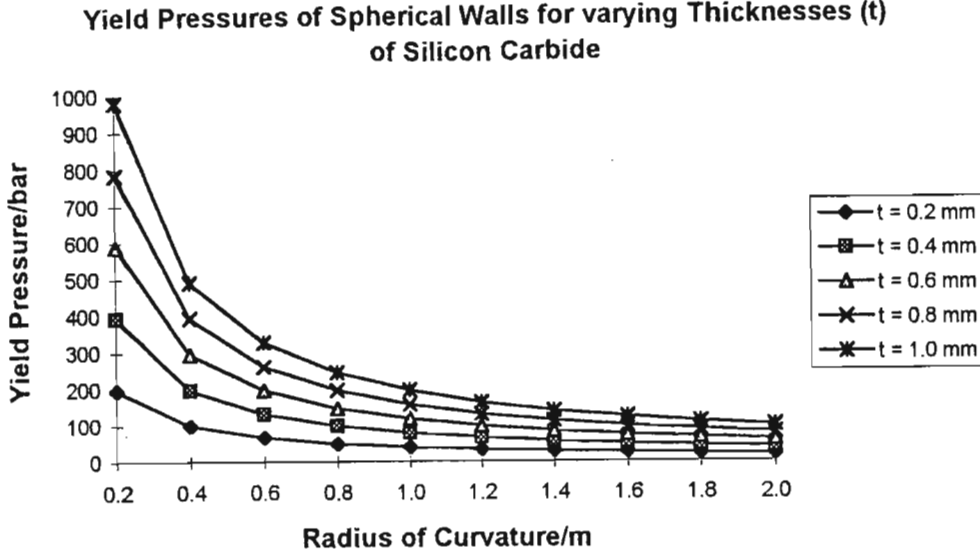


Figure 2.23: Yield Pressures of Silicon Carbide

such a vessel more cost effective. These particular chambers can be inflated when necessary.

The inflatable TVV allows for the existence of vacuum chambers that behave as lifting bodies. Development of inflatable TVV theory has shown that for certain configurations, the weight of the chamber is less than the buoyancy force.

Once again, the spherical TVV model is extremely useful in the development of a mathematical model. This will be used here to demonstrate the principle. In a spherical model, the intermediate volume of gas is given by:

$$V = \frac{4}{3}\pi(R_o^3 - R_i^3) \quad (2.53)$$

Employing the spherical TVV theory, the following equation can be derived by using equation (2.3) to provide a suitable substitution for  $R_o$ :

$$pV \approx 4 \left[ \left( \frac{p}{p - p_0} \right)^{3/2} - 1 \right] R_i^3 p \quad (2.54)$$

This is very approximately the mass of gas in kilograms if  $p$  is expressed in *bars*. The weight can therefore be expressed as  $p_{bar}Vg$  where  $g$  is the acceleration due to gravity. The equivalent weight of air for the total volume

of the chamber at 1 *bar* will be  $V_o g$  where  $V_o g = \frac{4}{3}\pi R_o^3 g$ . If the buoyancy force is taken into account, the equivalent mass of gas is:

$$W_g = g(p_{bar}V - V_o) \quad (2.55)$$

Substituting for  $p_{bar}V$ , the following is obtained:

$$W_g \approx 4R_i^3 g \left[ \frac{p^{3/2}}{(p - p_0)^{1/2}} - p \right] > 0 \quad (2.56)$$

This would indicate that a TVV could never be "lighter than air". Compounded with this is the fact that the above equations do not take into account the weight of the TVV components.

However, if gases which are less dense than air are employed, the problem can be overcome. If helium, for example, is used to pressurise the intermediate volume and the density of air is considered to be identical to that of nitrogen for practical purposes, then the buoyancy force,  $F_b$ , may be represented as follows:

$$F_b = \left( V_o - \frac{\rho_{He}}{\rho_{N_2}} p_{bar}V \right) g \quad (2.57)$$

In order to make a more realistic assessment, the weight of the chamber components,  $W_m$ , have to be included. If the material density is  $\rho_m$ , the weight will be given by  $W_m = \rho_m V_m g$ . A more complete description of the buoyancy force is given by:

$$F_b = \left( V_o - \frac{\rho_{He}}{\rho_{N_2}} p_{bar}V - \rho_m V_m \right) g \quad (2.58)$$

The vessel will be buoyant when the term in brackets is positive. Figures (2.24) to (2.26) provide graphical illustrations of the above equation with regards to spherical vessels of varying wall thicknesses and  $R_i$  values. The basic TVV theory developed at the beginning of this chapter is applied in order to determine  $R_o$  and therefore  $V_o$  and  $V$ . Three materials: structural steel, aluminium alloy(2014-T6)) and silicon carbide are selected. In the case of the metals, this is due to the large disparity in their density values although their yield strengths are similar. This allows one to see the effect of density on the buoyancy force. Silicon Carbide is selected due to the fact that it has a similar density to the aluminium alloy but a far greater yield strength. This allows one to see the effect of this factor on buoyancy. The graphs do not list the thickness of the walls but for each the minimum

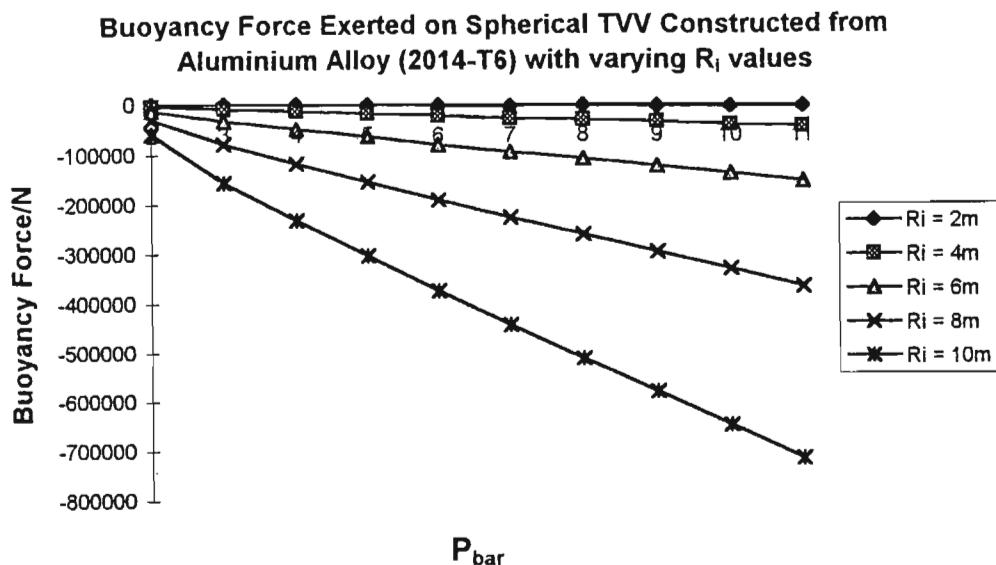


Figure 2.24: He Pressurised Spherical TVV with Aluminium Alloy Walls

thickness before material yield was employed in order to study vessels with the least possible mass. The aluminium alloy has a density of  $2710 \text{ kg/m}^3$  whilst that of structural steel is  $7860 \text{ kg/m}^3$  which is identical to that of 1%*C*, hot-rolled Stainless 302. Silicon Carbide has a density of  $2850 \text{ kg/m}^3$ .

The positive regions on the y-axis are the regions where the vessel becomes buoyant. Comparison of the steel and aluminium alloys shows the rather obvious fact that the less dense the material used, the easier it is for the chamber to achieve buoyancy. However, it is clear that neither material can be used in the construction of a buoyant TVV. However, the use of a novel material, as in the case of Silicon Carbide, which has a low density and extremely high tensile strength, allows a vessel to become buoyant. In this case, with an internal radius of 10 *m*, and a wall pressure of 11 *bar*, only a little more than half a millimetre of material thickness is required.

The graphs clearly illustrate that the larger the vessel, and the smaller the pressure in the intermediate layer, the more likely it will be for the chamber to become "lighter than air". This means that only large chambers can become buoyant. However, it is only with regard to the larger vessels that weight becomes a problem, particularly with regard to thin walled vessels. A major advantage of the TVV is that for very large vessels, the

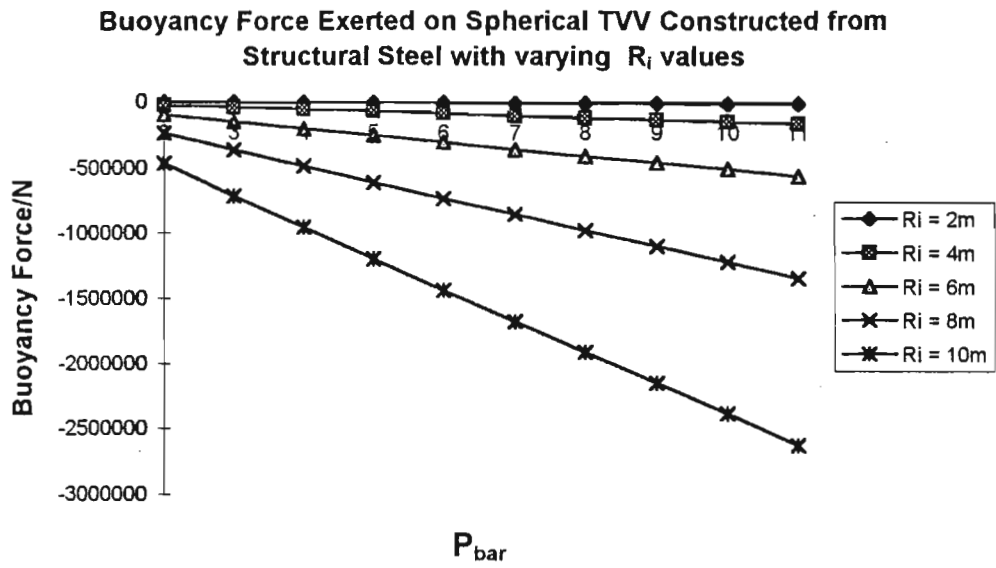


Figure 2.25: He Pressurised Spherical TVV with Structural Steel Walls

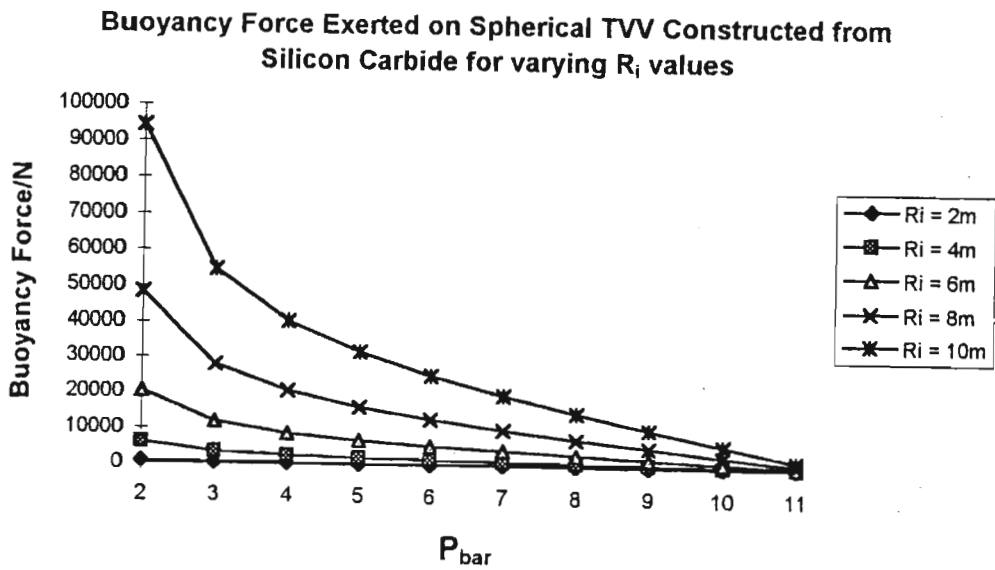


Figure 2.26: He Pressurised Spherical TVV with Silicon Carbide Walls



weight can be reduced considerably, even to the point that it is reduced to zero. The small pressures required have the advantage of alleviating the stresses on the walls.

## **2.6 Conclusion**

The theory developed in this chapter indicates that TVV's are viable alternatives to compressional vessels. The TVV can also compete with other thin wall designs. This is due to the fact that it can incorporate novel high tensile materials into its structure. The vessel is also potentially inflatable which means that it can be folded away when not in use. Inflatable TVV theory also indicates that large chambers can become buoyant under certain circumstances.

## Chapter 3

# Low Vacuum Tubular TVV Experiments

### 3.1 Aim of this Chapter

The projects described in this chapter are tubular TVV experiments undertaken in order to study the dynamics of large TVV's. The tubular wall design was chosen due to the cost effectiveness of this approach and the relative simplicity of manufacture. Previous work with this type of TVV, performed on a smaller scale by A. Forbes, is described in Chapter One. This consisted of "proof of principle" experiments which were performed on a small scale as were the other early TVV experiments. Once the viability of the TVV was established, the construction of larger vessels became a necessity. There are several reasons for this.

Firstly, small scale tensional vessels do not represent as great a financial saving as would a larger vessel when compared with alternative designs. The reduced overall forces allow for the use of thinner walls in compression. It would be uneconomical, therefore, to employ more complex designs. Also, cheaper alternative designs (eg. glass vessels) are available for small vessels.

Secondly, large TVV's are useful to industry if large vacuum vessels are required due to the cost savings involved.

Thirdly, TVV's must demonstrate a capacity to achieve and maintain a high vacuum. Our research required that a vessel be large enough to support an internal guard vessel. The chambers described in this thesis were incapable of maintaining a high vacuum within their double-walled structure. The experiments described in this chapter could only produce vacuums of several *torr*. The only means of producing a useful vacuum with the ves-

sels available to us, was through the implementation of a guard chamber included within the TVV wall. This would be placed over the necessary high vacuum apparatus. It is hoped that future designs will incorporate technology that will negate the need for such a vessel.

The aim of this chapter therefore, is to demonstrate the feasibility of larger TVV's. This is accomplished through the description of a series of experiments conducted with a tubular TVV design. The chamber was scaled up in size after each successful test. This design simplified the replacement of tubes in the event of collapse. This facilitated numerous observations being made over relatively short spans of time.

The experiments were purely structural and therefore not intended to produce a high vacuum. Rather, they were a forerunner to the later high vacuum experiments described in the next chapter. These would not have been possible without knowledge of the structural integrity of the larger TVV's.

## 3.2 TVV Dimensions

The terminology used to describe tubular TVV dimensions in the previous chapter will be used throughout the remainder of this thesis. The  $n$  value will be referred to as the radial number and the  $m$  value will be referred to as the longitudinal number. The first large models were manufactured with a radial number of thirty. Chamber size was increased through progressive doubling of the longitudinal number. This is because the tubes interlocked when stacked vertically (along the cylindrical axis of symmetry) and therefore one layer of  $n$  tubes could be placed above the other. The longitudinal numbers employed were:  $m = 1, 2, 4$  and  $8$ . However, later experiments had  $n = 24$  and  $m = 3$  in order to facilitate future high vacuum experiments, which required that the dimensions of the TVV wall conformed to those of the high vacuum apparatus.

The tubes were soft drink cans, predominantly coca-cola cans for sponsorship purposes. They were employed for their symmetry and ability to interlock when stacked vertically making the manufacture of chambers a relatively easy task. Their extremely thin walls and light weight in metal as well as their high mechanical strength were other contributing factors. The cans were still full of liquid with an internal pressure of  $1,5 \text{ bar}$  gauge. Pressure tests performed by Mr. R. Bodger at the UND Mechanical Engineering Department revealed that the cans rupture when a force of  $3000N$  is applied transversely (perpendicular to the axis of symmetry) and when

7680N is applied vertically.

The 340ml cans were used, the dimensions of a typical can having  $l = 11,9\text{cm}$  and  $R_t = 3,3\text{cm}$ . The wall thickness is  $300\ \mu\text{m}$ . This gives the can a cross-sectional area of  $78,5\ \text{cm}^2$ . When subjected to  $p_0$ , a force of 785 N will be experienced. This is an order of magnitude lower than the force required for rupture. Added strength is given to the can in compression by a ring stiffening hoop at its base. The top of the can is also ring stiffened in that the wall is corrugated at this point. If the internal radius of a concentric circle of thirty cans is calculated using the above dimensions, one obtains an  $R_i$  value of  $28\text{cm}$ , a value confirmed by measurement. The surface area of the end plates over the evacuated area and the volume of the vessel itself can easily be calculated. Using equation (2.20) the surface area is found to be  $0,25\ \text{m}^2$ . This means that the force at the end plates is  $2,5 \times 10^3\ \text{N}$ . Assuming an even distribution of force, each can will experience a force of  $8,3 \times 10^2\ \text{N}$ , once again an order of magnitude lower than the that required for rupture. In our early experiments, supporting columns are added to the chamber interior, further distributing the load. The calculated value is therefore to be regarded as a maximum value.

The internal volume of a vessel can be calculated using equation (2.19). A model with a longitudinal number of unity has a volume of 30 litres. This means that an  $n = 30$  chamber will have a volume of 30m litres. Once again it must be stated that this is a maximum value due to the volume occupied by internal supports in those models requiring them.

### 3.3 Note about Plasma Instabilities

During the course of experimentation various instabilities manifested themselves. Tubular vessels with large  $n$  values were expected to become unstable through amplification of small geometric misalignments as discussed in the previous chapter. Plasma research was found to be useful in this regard. Instabilities in cylindrical columns of plasma bare at least a superficial resemblance to those encountered in large tubular TVV's.

There are two main catagories: instabilities that occur when a vertical column shifts out of alignment with the axis of symmetry, and instabilities that manifest themselves when the concentric ring of tubes becomes asymmetrical.

The vertical instabilities can be subdivided into two catagories, the sausage and the kink[20]. Figure (3.1) provides an illustration of the plasma instabilities. In the case of the tubular vessel, these occur for  $m > 1$ , the

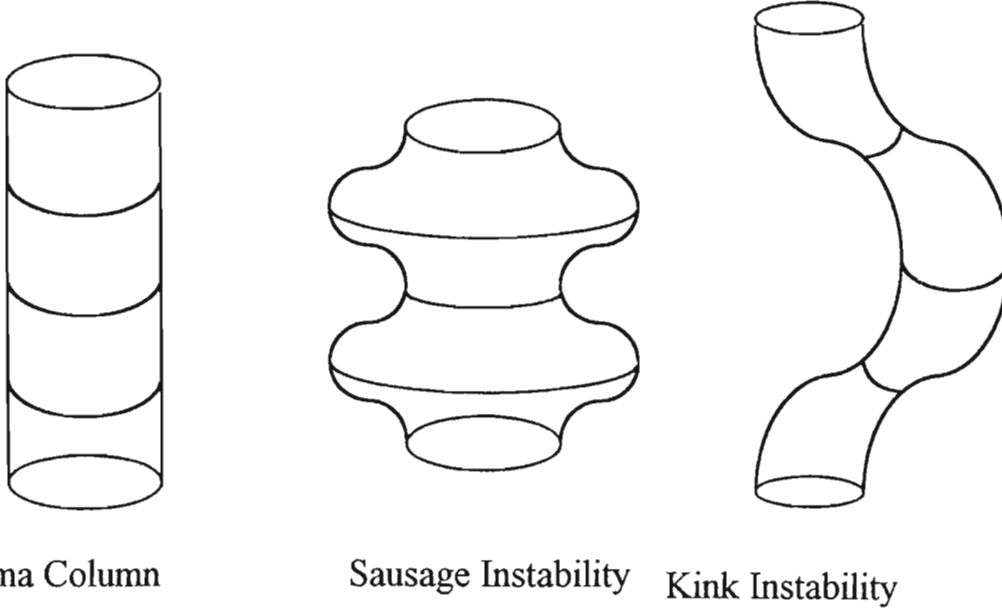


Figure 3.1: Plasma Column alongside Sausage and Kink Instabilities

sausage corresponding to the stacked tube columns bending inwards at particular levels while the kink corresponds to the entire vessel leaning over to one side.

Figure (3.2) is an illustration of the flute instability[20] in a plasma column otherwise known as the interchange. This corresponds to asymmetries in the circular arrangement of the tubes. For our purposes it was convenient to separate the flute and interchange into two separate categories. The flute corresponds to general amplification of geometric misalignments of the tubes while interchange occurs when a tube is "sucked in".

### 3.4 General Experimental Outlay

A small Edwards High Vacuum rotary pump produced the required structural vacuum. This was attached to a tube of very narrow bore (4,5 mm) to ensure a slow pump rate. Any instabilities manifesting themselves would have to do so slowly reducing the risk of implosion and allowing for a more comprehensive study of the dynamics of the vessel. The tube was inserted between the top parts of two of the cans on the bottom layer. This was true of all experiments described in this chapter. The vacuum measurements were taken with a mechanical gauge which was connected to the vacuum

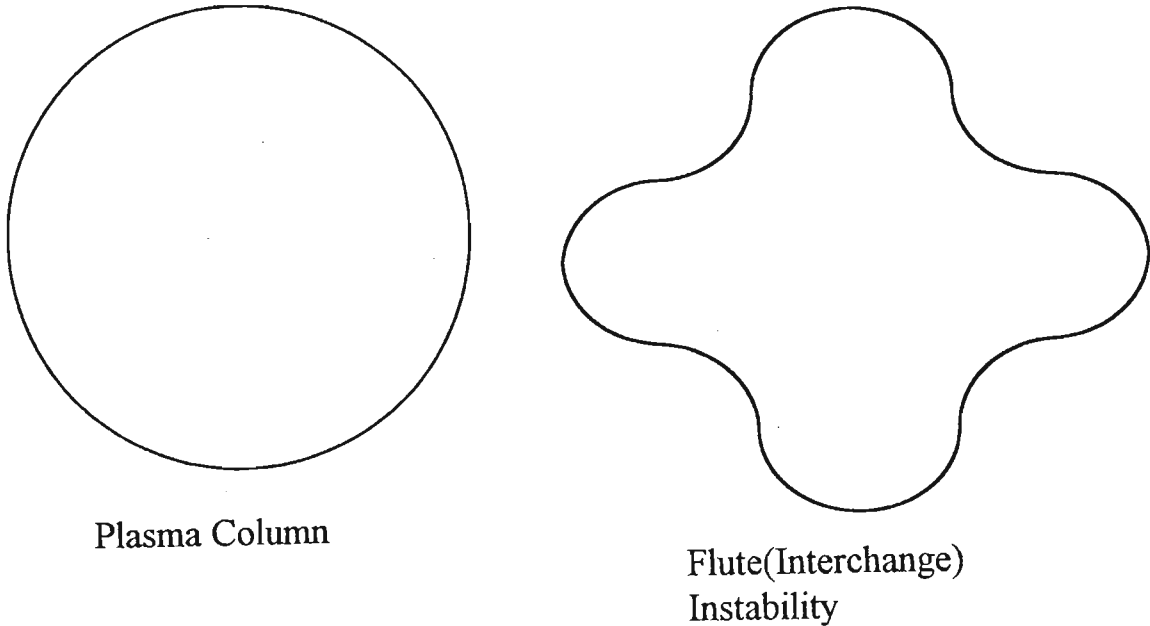


Figure 3.2: Plasma Column alongside Flute(Interchange) Instability

hose through a T-piece.

Two aluminium plates (each 1 *mm* thick) were used as end plates. Supporting columns were inserted into the vessel before evacuation due to the fact that these plates had almost no structural stability of their own. These were generally in the form of eight pillars of stacked soft drink cans equal to the height of the chamber. One pillar would be central with the other seven arranged around it in a concentric ring. The focus of these experiments was the behaviour of the tubular walls rather than the end plates and therefore the end plates were compressional.

Initially it was believed that the walls might seal themselves as the vessels were pumped down. However, this turned out not to be the case and therefore sealing material was required. Putty served this purpose during the initial experiments, ostensibly due to the cost effectiveness of this material being employed in a novel experiment. Continued use proved necessary due to the fact that the TVV "breathes" and therefore requires a flexible sealant. Most glues would flake off after hardening as the chamber alternatively contracted and expanded. Putty largely self sealed the TVV during evacuation, although this material does leak and therefore tends to produce frustrating delays as the leaks have to be found and sealed. The existence of a leak that could not be located sometimes prevented an experiment from

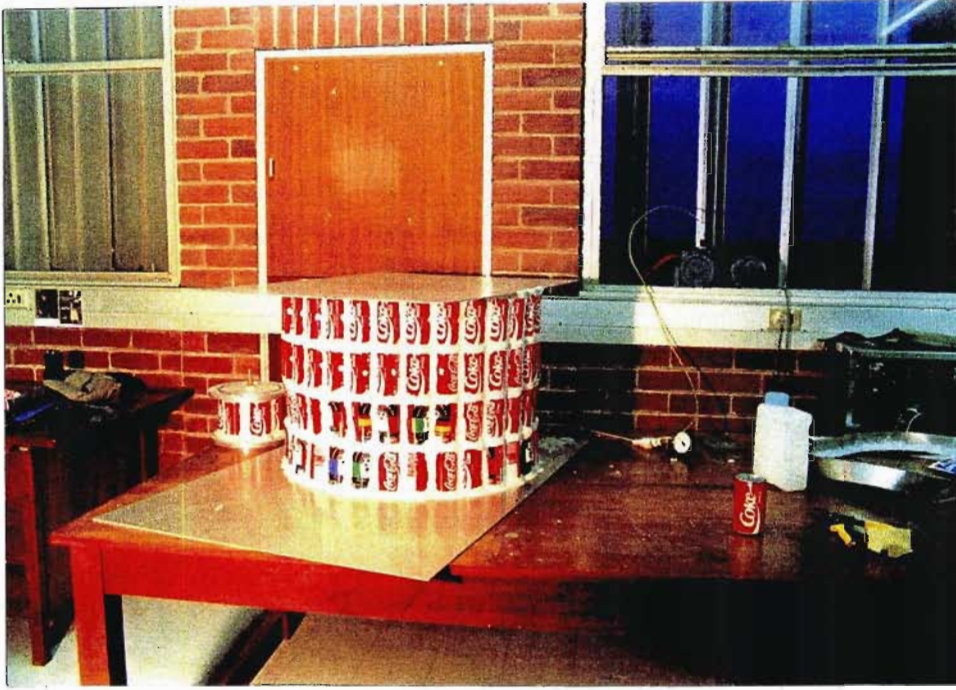


Figure 3.3: General Apparatus

obtaining a better structural vacuum although never to the extent of more than 0,1 bar. This was still acceptable for experimental purposes. Figure (3.3) shows an ( $m = 4$ ) TVV with the gauge and pump in the background. Figures (3.4) and (3.5) give a closer view of the rotary pump and the vacuum gauge.

### 3.5 Presentation of Experimental Results

This thesis includes the results of a number of experiments performed with a variety of TVV designs. It is therefore impractical, with the exception of the high vacuum work, to report on all the experiments at length. The majority will be presented in such a way as to give a description of the setup, results, and particular observations noted. A discussion of the results from a group of experiments will be given at the end of each chapter.

### 3.6 Single Layer Experiments ( $m = 1$ )

Two major experiments were set up to examine the single layer TVV.



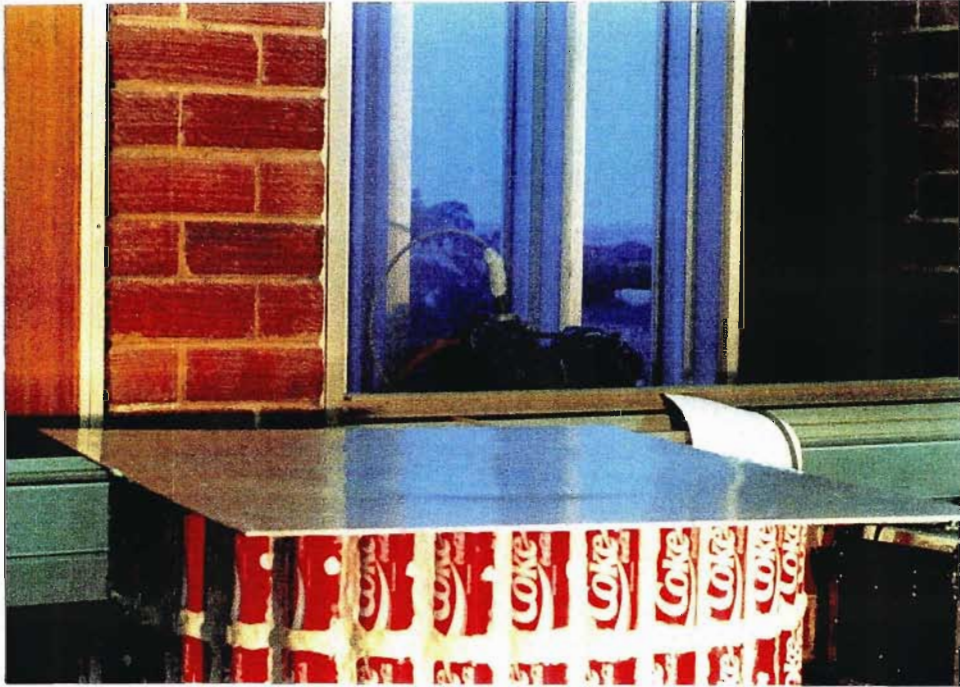


Figure 3.4: Edwards High Vacuum rotary pump



Figure 3.5: Mechanical Vacuum Gauge





Figure 3.6: Tubular TVV( $m = 1$ ) with Sand-filled Bowl as Interior Support

### 3.6.1 Experiment 1

The aim of the first experiment was to examine the behaviour of an  $n = 30$  tubular wall constructed from soft drink cans. In order to create a TVV model that could be scaled up and eventually used in a high vacuum experiment, knowledge of the wall stability was required. The volume to be evacuated was very small. A large bowl filled with sand was placed within the chamber to provide structural support. Figure (3.6) is a picture of the vessel without the top plate.

#### Apparatus

The only new apparatus added to the general schema was the bowl itself. This had a diameter only slightly smaller than that of the vessel. This was also true of its height. The bowl had a flat base with a diameter only slightly smaller than its maximum diameter. The interior was filled with sand which

provided the necessary support for the top aluminium end plate.

This meant that the evacuated volume was small in comparison to the size of the chamber. However, the cans themselves were still subject to the same pressure that would be experienced were the entire volume to be evacuated. This first experiment would therefore provide the knowledge as to whether or not soft drink cans would rupture if subject to the forces typical of larger vacuum vessels.

## Results

When the pump was activated, the chamber did not immediately evacuate due to the existence of leaks which perpetuated themselves through the putty seal. Plugging the leaks was a relatively trivial matter of adding more putty or pushing putty from the chamber itself over the problem area. Once evacuation began, the leaks became audible enough to be heard and several people were instrumental in finding and sealing them.

The mechanical gauge recorded 0,94 *bar*. None of the cans ruptured during the experiment. However, a better gauge reading could not be obtained.

## Observations

While sealing the leaks was simple enough, finding them could take hours. This was actually the most time consuming part of the experiment. The experiment was successful in that the cans proved to be strong enough and stable enough to be used in future TVV's. More importantly, the TVV principle was shown to apply to larger chambers.

The cans moved in during evacuation and the opposite was true when the chamber was repressurised. This meant that the continued use of a putty insulator would be necessary for the immediate future in that TVV's have to "breathe". Any tubular TVV design has to accommodate this.

### 3.6.2 Experiment 2

The second experiment differed from the first only in that the bowl was removed. The support structure of vertically stacked cans outlined earlier was implemented giving the chamber a much larger volume to be evacuated. Having established the stability of the chamber wall, the aim of this experiment was to prove that a large TVV could contain a large evacuated volume.



Figure 3.7: Tubular TVV with Supporting Columns

### Apparatus

The bowl was replaced with eight column support structure described earlier. This gave the chamber an approximate internal volume of 27 litres. Figure (3.7) is a picture of the internal arrangement.

An aluminium rim was placed along the internal radius to provide support in maintaining symmetry. The rim was 1 mm thick by 5 cm wide by 180 cm long. This was folded into a ring with the same diameter as the chamber and glued to the bottom plate at regular intervals. The seal was strengthened with silicon sealer placed along the entire inner circumference.

### Results

When approximately two-thirds of the air had been removed, one of the cans began to crumple and was "sucked in", depressurising the chamber. When the top plate was removed it was found that the rim had buckled inwards and that several other cans had also moved out of alignment, particularly in

the vicinity of the rupture. The glue and silicon sealer had been pulled away where the rim had buckled and the damaged can had leaked considerably. However, examination of the can showed no sign of a major rupture. The liquid must therefore have leaked through microscopic pores in the can wall.

The experiment was then repeated, only this time the rim was replaced by the bowl of the previous experiment. However, in this case the bowl was empty except for the cans used for supporting the top plate which were inserted into the bowl. This ensured that the chamber volume remained essentially unchanged. The bowl's outer rim was simply used to replace the aluminium rim in maintaining the symmetry.

The experiment was successful in that a gauge reading of 0,99 *bar* was obtained. This time none of the cans ruptured.

### Observations

The buckling of the rim due to the rupture showed the catastrophic effects of instabilities on a tubular TVV. In this case an interchange instability was noted. This means that it is important to have a reasonably firm support structure in order to maintain symmetry in a TVV of this nature. If such a structure is absent or inadequate, the effects of instabilities can be amplified to the point of implosion.

Examination of the ruptured can illustrated that the leaks can be microscopic and that soft drink cans have a finite lifetime when used in TVV walls and therefore have to be replaced on a regular basis. If any can leaks, it loses frictional contact with its neighbouring cans and is pulled inwards, allowing air back into the chamber.

The gauge reading was higher than in the previous experiment, indicating that the a leak had limited the effectiveness of that chamber. From a structural point of view this discrepancy was not serious but the indication is clear that leaks limit the effectiveness of the chamber. This has serious implications for any high vacuum experiments employing a guard vacuum chamber. If the guard vacuum is not good enough, there could be sufficient pressure on the guard vessel to cause implosion. Finding the final leaks in order to improve the vacuum proved to be a frustrating and time consuming process which certainly could lengthen the duration of any high vacuum experiment.

### 3.7 Double Layered Experiment ( $m = 2$ )

This experimental setup was very similar to that used before, the difference being that the scaling procedure was followed and a second layer of cans was placed above the previous TVV wall. This doubled the size of the vessel. The previous experiments had shown that the TVV wall was stable (with the proviso that symmetry is maintained and that leaking cans are replaced). The aim of this experiment was to prove that vessels with longitudinal numbers greater than one were stable.

#### Apparatus

A second layer of 30 soft drink cans was added to the TVV wall of the previous experiment producing a vessel of approximately 54 *litres* in size. The bowl was removed although the supporting columns were retained. Each of these was doubled in height through the addition of a second can. Stability was provided by the interlocking nature of the top and bottom ends of the soft drink cans.

In order to replace the bowl in maintaining symmetry, two bicycle rims were added, one to the top of the chamber, and the other to the bottom. The top rim was held in place with putty and both were padded with cardboard to reduce the hazard of a can being ruptured by contact with the rim edges.

The rims had an approximate diameter of 58 *cm* and were slightly too large for the vessel wall. This created a gap in the wall which was rectified through the addition of a rubber tube inserted between two of the cans.

#### Results

A gauge reading of 0,98 *bar* was obtained. None of the cans collapsed.

#### Observations

This version took much longer to pump down due to an increase in the number of leaks resulting from the larger wall size. There was also a tendency of the top plate to lift at its edges. This was due to a slight vertical displacement in the downwards direction of those parts the plate not directly supported by the supporting columns. This was also noted in the previous experiment. The top of the TVV wall as well as the support columns created clear indentations on the plate when the chamber was evacuated. This would certainly have provided additional frictional support as would the interlocking nature of the cans.





Figure 3.8: Four layer Tubular TVV

When the top plate was removed, marks were noted on the cans due to the rims indicating that the rims were taking some of the strain.

### 3.8 Four Layered Experiment ( $m = 4$ )

The vessel was again doubled in size through the addition of two more layers of thirty cans each to the wall. Figure (3.8) is a picture of this TVV. The aim of this experiment was not only to scale up the chamber size but also to examine the dynamics of a vessel with  $2R_i/ml$  close to unity.

#### Apparatus

The vessel was again scaled up in size, this time through the addition of a further sixty cans to the wall. These were arranged in two layers of thirty cans each, doubling the longitudinal number. The supports were also doubled in vertical height, giving the vessel an overall volume of approximately 108 litres. The supporting columns were also doubled in height, creating eight supporting columns of four cans each.

Three bicycle rims were used to maintain symmetry, one at the top and another at the bottom as before. The additional rim was placed in the

middle. These had been cut and welded to ensure a perfect fit to the inner radius of the chamber. The rubber tube could therefore be discarded.

## Results

This experiment was run several times and a gauge reading of 0,99 *bar* was obtained. The vessel could be run for several hours without collapse. However, the two bottom layers did buckle inwards in places in a V-formation. This sausage instability is shown clearly in figure (3.9).

## Observations

This vessel had an interesting geometry with its vertical height almost equivalent to the vessel diameter, effectively the size and shape of an average sized chamber. The results obtained indicate that the TVV structure is stable, the buckling of the bottom layers being to the lack of support (no rim placed between these layers). This was the first manifestation of a vertical instability.

Again, indentations created by the supporting cans due to the vertical forces on the top end plate, could be seen. This phenomenon, as noted in the previous experiment, provides additional support in preventing the inward migration of the cans. This effectively increases the value of  $\mu_e$ .

## 3.9 Eight Layered Experiment ( $m = 8$ )

The vessel was yet again doubled in size through the addition of 120 cans. The aim of this experiment was to study the behaviour of TVV's of this nature when the vertical height significantly exceeded the chamber diameter.

## Apparatus

The vertical height of the TVV wall was doubled through the addition of a further four layers of 30 cans each. Columns of soft drink cans, eight layers high, were deemed to be too unstable for use in supporting the end plates. A makeshift support was created from metal disks and tubes and placed in the centre of the chamber. The tubes made up the bulk of the length, the disks being employed to facilitate contact over a broader surface area with the end plates. This is shown diagrammatically in figure (3.10)

Bicycle rims continued to be used in maintaining the symmetry of the wall. This time, five rims cut to size, were employed. One was placed at the



Figure 3.9: Sausage Instability in TVV Wall



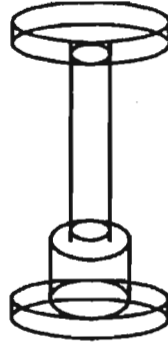


Figure 3.10: Diagram Showing Support Structure for Eight Layer TVV

top, another on the bottom and the other three were placed at the junctions of every second layer.

### Results

This experiment was run three times. The first run did not produce any useful results due to the collapse of a can in the sixth layer from the bottom which allowed air back into the chamber.

The second run produced the best result. No cans collapsed. The gauge gave a reading of 0,91 *bar* after evacuation.

During the third run, four cans in the fourth layer from the bottom began to collapse (two of these were next to each other). This was at a reading of 0,80 *bar*. Repressurisation was stopped through the addition of putty and a reading of about 0,70 *bar* was obtained before the two adjacent cans were pulled in with the two cans above them.

### Observations

This chamber was almost twice as high as it was wide. Vertical instabilities again manifested themselves, the entire chamber leaned over slightly to one side. This was probably due to a fault in the construction of the chamber, but may have been exacerbated by the evacuations. This behaviour is an example of a kink instability. Sausage instabilities again appeared in the layers that had no bicycle rims between them. That such instabilities can lead to implosion is illustrated by the fact that the imploded cans belonged

to such layers. This means that some means should be found to maintain symmetry in every layer. The alternative would be to use single tubes. This would eliminate the sausage instabilities and possibly the kink as well. A minimum of internal support would therefore be necessary to prevent interchange.

The failures once again illustrate the fact that the cans have a limited lifetime and therefore any TVV's constructed from these materials have to be rebuilt on a regular basis.

### 3.10 Tubular TVV for High Vacuum

The experiments outlined in this chapter so far have illustrated that these tubular TVV designs are stable enough to warrant high vacuum experiments. Ruptures occurred but chambers did maintain vacuum values of several torr over a period of several hours. A thin walled internal guard vessel would not collapse under this background pressure whilst maintaining a high vacuum. The TVV walls could last long enough to make such a vacuum achievable. The guard vessel would be placed within the TVV over an appropriate high vacuum pump. Further low vacuum experiments were designed to facilitate this in terms of providing a stable outer TVV wall capable of maintaining a fore-vacuum for several hours. The wall of a standard compressional high vacuum vessel was replaced by a tubular TVV wall with a radial number of thirty, placed over an oil diffusion pump. This radial value was chosen for its symmetry as well as the fact that the tensional wall had to be large enough to replace the original compressional wall but small enough to fit on the base. The longitudinal numbers chosen were:  $m = 1$  and  $m = 3$ . The top plate of the compressional vessel was also used by the TVV. This was thick enough such that no internal columns were required to support it. The original chamber is shown in figure (3.11). This vessel has a height of 50 *cm* and a diameter of 54 *cm* giving it a volume of 57 *litres*. Figure (3.12) shows the rotary pump employed in these experiments and the connection to the chamber above it. The connecting pipes pass through a valve which was set to "roughing" for the low vacuum experiments. This is the setting required to establish the necessary fore-vacuum in a chamber before the oil diffusion pump can be used to establish a high vacuum. This series of experiments only required a fore-vacuum as they were designed for structural studies. The rotary pump was more powerful than the model used in the previous TVV's and the pipes had a much larger aperture than the extremely narrow tube employed earlier. The pump rate was therefore much faster.

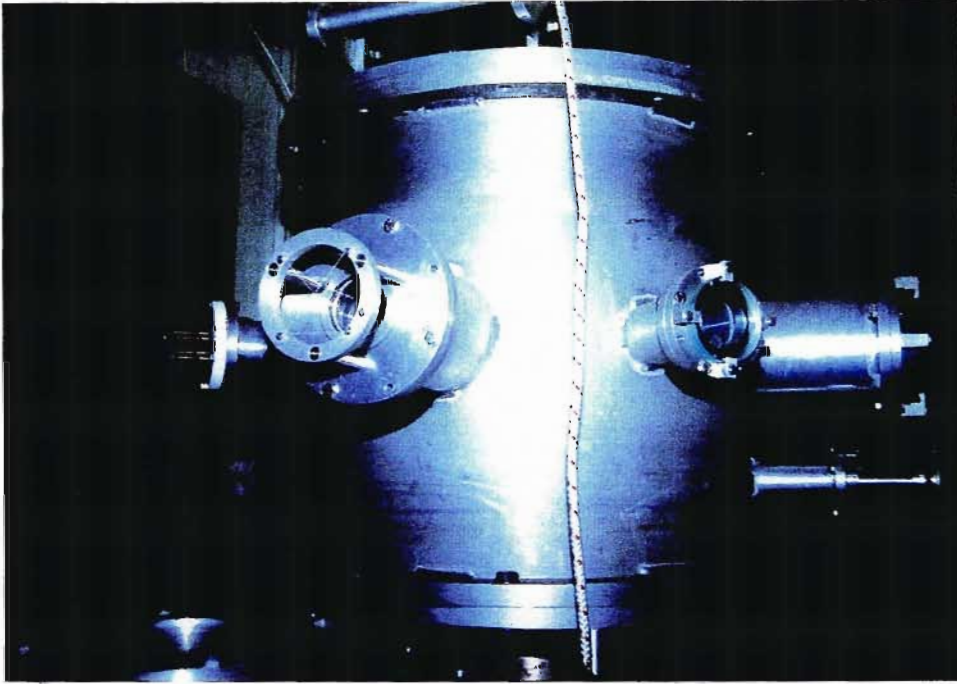


Figure 3.11: Original Compressional Vacuum Vessel

Once again, equations (2.19) and (2.20) can be used to calculate the internal volume and the end plate surface area exposed to vacuum. One finds that  $S_e = 0,15 \text{ m}^2$ . This means that the top plate will experience a force of  $1,5 \times 10^4 N$ . Distributed evenly, each tube will be subjected to a force of  $6,3 \times 10^2 N$ . The internal volume will be  $18 \text{ m litres}$ .

### 3.10.1 Experiment 1

An  $m = 3$  TVV wall replaced the compressional wall of a high vacuum chamber. The TVV wall consisted of  $340 \text{ ml}$  soft drink cans sealed with putty as before. This chamber had an internal volume of  $54 \text{ litres}$  which is almost identical to that of the original compressional vessel. The aim of this experiment was to prepare a tubular TVV wall for later high vacuum work. As mentioned above, this wall had to fit over a high vacuum pump. The  $m = 3$  value was chosen due to the fact that this gave the TVV a vertical height closest to that of the original chamber. This also was small enough to reduce the effects of vertical instabilities.

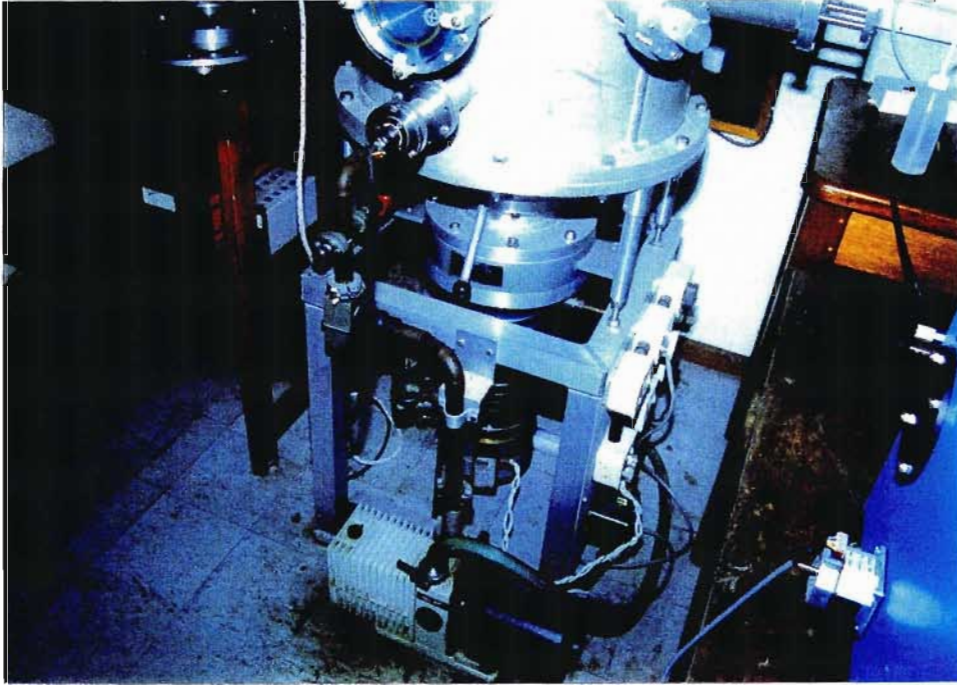


Figure 3.12: Rotary pump with connection to main chamber

### Apparatus

The tubular TVV wall was constructed in the usual way. No bicycle rims or other agent was used to maintain symmetry. Instead, standard setting resin with filler was placed at each confluence point of four cans in the hope that this would be adequate to withstand the initial excess forces due to initial geometric misalignments. The chamber was built over the oil diffusion pump which was separated from the rest of the chamber through a butterfly valve which was filled with sponge in order to prevent liquid from seeping into the pump in the event that a can should rupture. Further precautions were taken in that plastic was placed around the inner perimeter of the chamber. The vessel is shown in figure (3.13).

### Results

Shortly after the activation of the pump, one side of the chamber began to move inwards. There were five columns involved in this motion. After the initial slow movement, two columns were propelled to the other side of the chamber at extremely high velocity. The impact shifted the entire chamber approximately five centimetres.

When examined, at least one of the cans involved in the impact was



Figure 3.13: Proposed Tubular TVV Wall for High Vacuum Experiments

found to be leaking.

Figures (3.14) and (3.15) show the imploded columns and the shift in the TVV wall.

### Observations

The implosion illustrated how small effects due to asymmetry can be magnified with catastrophic results. This means that it is insufficient to hold the chamber together with strong glues. The effects of instabilities require the use of additional agents (eg. bicycle rims) in order to maintain symmetry.

The implosion also confirmed that instabilities would manifest themselves faster with a more powerful pump. Previously, the air would be allowed back into the chamber before any significant damage could be done to the chamber as a whole.

#### 3.10.2 Experiment 2

The chamber was rebuilt with a single layer ( $m = 1$ ) configuration. Due to the implosion of the previous vessel, it was decided to build a smaller chamber as a precautionary measure. This vessel had an internal volume of 18 litres.





Figure 3.14: Implosion photographs with Columns shifted to the opposite side of the chamber

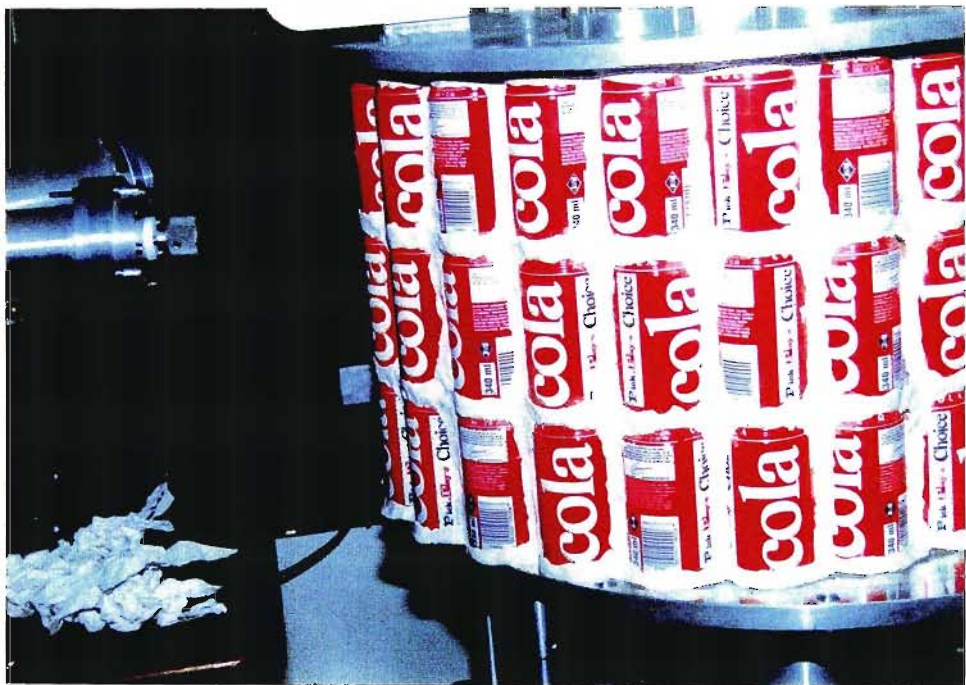


Figure 3.15: Shift in TVV

### Apparatus

Two 16 *inch* bicycle rims were introduced to the top and bottom parts of the chamber to prevent implosion. No resin was used. The rim radius was almost a centimetre and a half shorter than the inner TVV radius allowing the vessel to "breathe". The rims were padded with rubber and both were supported through the use of putty.

### Results

The chamber was evacuated without collapse. The evacuation time was reduced by the introduction of a more powerful pump. The rims did not mark the cans.

### Observations

The need for supports (such as the rims) to maintain symmetry was confirmed for small  $R_t/R_i$  ratios. Also the need to give a TVV room to "breathe" showed the necessity of taking into account the dynamical nature of the system.

#### 3.10.3 Experiment 3

The vessel was again scaled up to an  $m = 3$  configuration.

### Apparatus

Two more layers of 24 cans each were added to the TVV wall, restoring the chamber to its original volume. A third 16 *inch* rim was placed centrally as shown in figure (3.16).

### Results

This chamber also did not implode after evacuation. It was also noted that leaks are easier to find with a faster pump rate.

### Observations

This type of TVV could be scaled up which means that a high vacuum experiment could be done with the current TVV walls.



Figure 3.16: Internal view of rim stabilised TVV

### 3.11 Discussion and Conclusion

The experiments described in this chapter have proven that tubular TVV's are feasible from a purely structural point of view. The difficulties encountered have been due to the extremely rudimentary technology employed in a novel experiment. This was to save costs but none the less large vacuum vessels were constructed with walls of only  $300\ \mu\text{m}$  thickness. An unfortunate consequence of the use of  $340\ \text{ml}$  soft drink cans has been the development of vertical instabilities (the kink and the sausage). This was due to a combination of the scaling procedure and the fact that these cans have relatively large  $R_t/l$  ratio. Earlier in the chapter it was suggested that in future these instabilities may be removed through the use of single tubes. The interchange instabilities can only be removed through maintaining a high level of symmetry. This requires the use of hoops. These should not behave as ring stiffeners in a thin walled vessel although in these early experiments it cannot be denied that this probably did happen to a certain extent. Another feature of the cans mentioned at the outset of the chapter is that they are strengthened by ring stiffeners both at the bottom and at the top of each can.

Attempts were actually made to measure the change in the internal pres-



sure of the cans as an  $m = 1$ ,  $n = 30$  vessel was evacuated. No significant change was detected which indicates that the intercan forces were balanced by the compressional elements. This would also explain why the can tops did not rupture. This occurs at 5 to 6 *bar*.

This is useful in that it allows one to calculate the tension in the walls. For the outer wall,  $\Delta p$  is 1,5 *bar*, while for the inner wall,  $\Delta p$  is 2,5 *bar*. The maximum hoop stress is therefore experienced by the inner wall and is calculated to be:

$$\begin{aligned}\sigma_y &= \frac{2,5 \times 10^5 \text{ Pa} \times 0,033 \text{ cm}}{3,0 \times 10^{-4}} \\ &= 27,5 \text{ MPa} \\ &= 275 \text{ bar}\end{aligned}$$

This value is approximately one order of magnitude below the yield strengths of most metal alloys.

A similar calculation can be performed for  $\sigma_x$  for an  $n = 30$  vessel:

$$\begin{aligned}\sigma_x &= \frac{0,28 \text{ m} \times 10^5 \text{ Pa} \times (1 - 10^5 \text{ Pa} / 2,5 \times 10^5 \text{ Pa})}{3,14 \times 3,0 \times 10^{-4} \text{ m}} \\ &= 17,8 \text{ MPa} \\ &= 178 \text{ bar}\end{aligned}$$

assuming that  $R_o = 28 \text{ cm}$ . Once again, this is one order of magnitude less than that required for rupture to occur.

It has to be admitted that failures did occur but these were never due to large ruptures. Examinations of damaged cans proved that the leaks were microscopic in scale. Future improvements in the technology of these vessels should eliminate this problem.

In conclusion, then, it can be stated that the initial tubular TVV experiments were sufficiently successful to justify a high vacuum experiments. Having proven that the tubular TVV principle is valid structurally, the next step was to show that a high vacuum was obtainable.

## Chapter 4

# High Vacuum TVV Experiments

The tubular TVV wall is capable of supporting a large evacuated volume. However, the walls employed in our designs have inherent weaknesses which prevent a high vacuum being obtained within the double walled structure. Vacuums of several torr are typical of the performance of these vessels and cannot be improved upon with our current technology. It is hoped that this situation will improve with future developments. In the meanwhile it is necessary to overcome this problem through the addition of a third wall added within the confines of our vessel. A guard chamber is thus placed inside a conventional TVV in order to make high vacuum work possible.

### 4.1 General Experimental Outlay

The basic apparatus consisted of a tubular TVV design with the walls constructed from soft drink cans. A thin walled guard vessel ( $300\text{ }\mu\text{m}$  in thickness) was placed within the larger structure and sealed over a diffusion pump.

The tubular TVV used in these high vacuum experiments was the  $n = 24, m = 3$  model which had been tested and deemed reliable. The wall was constructed from 340 *ml* soft drink cans and sealed with putty. Bicycle rims were added for stability and thick walled end plates from a conventional vacuum vessel were employed.

A  $300\text{ }\mu\text{m}$  rectangular sheet of stainless steel was rolled into a tube and welded together at the ends to form the cylindrical body of the internal guard vessel. Two such vessels were manufactured, each having similar

dimensions. Both were slightly smaller than the TVV in height and slightly larger than the butterfly valve in diameter. Each was sealed at the top with a transparent material to allow visual access. The base was sealed over the diffusion pump with an appropriate sealant.

In order to avoid implosion during the roughing process it was important to ensure an even pump rate for both inner and outer chambers. Even a relatively small fluctuation in the pressure could damage the guard vessel. Both sections, therefore, needed to be evacuated simultaneously. To facilitate this, a rotary pump was connected to both chambers. However, in order to carry out the high vacuum experiments, it was also necessary to be able to evacuate the inner chamber separately. Ultimately this was accomplished by the diffusion pump but a second rotary pump had to be connected to provide the intermediate vacuum and the backing for the high vacuum.

All of this required the addition of new plumbing. An opening above the butterfly valve (which separated the diffusion pump from the vessel to be evacuated) provided a point of entry into the inner chamber. The bung which sealed this opening was removed and replaced with a mechanical vacuum gauge. To this was attached a hand operated valve which would allow the internal and external chambers to be evacuated simultaneously or separately. This was in turn attached to a flexible tube which connected to a T-piece to which two plastic pipes were attached. One of these was connected to the external chamber through the TVV wall. The other was connected to a rotary pump. This tube had a smaller pipe inserted within to reduce the pump rate thus ensuring even evacuation between the chambers. The second rotary pump was connected to the inner chamber. The exhaust nozzles of the rotary pumps were also connected to a T-piece with an exhaust hose to vent the fumes.

Two vacuum gauges were connected, a mechanical gauge and a pirani gauge. The mechanical gauge was used to measure the vacuum of both chambers during the roughing procedure. A disadvantage of its location was that it could not measure the vacuum in the outer chamber after closure of the valve which meant that if the guard vacuum became progressively worse due to leaks, this might go undetected with possible harmful consequences to the inner chamber. This situation was later rectified by moving its location to the opposite side of the valve. This gauge was only used as a guide when roughing down the chamber and therefore was not required for any fine measurement. It served adequately as an indication of the guard vacuum and allowed determination of when to pump the chambers separately. The pirani gauge served a similar function with regards to the internal vacuum chamber. The gauge proved reliable down to  $10^{-1}$  torr but could not be

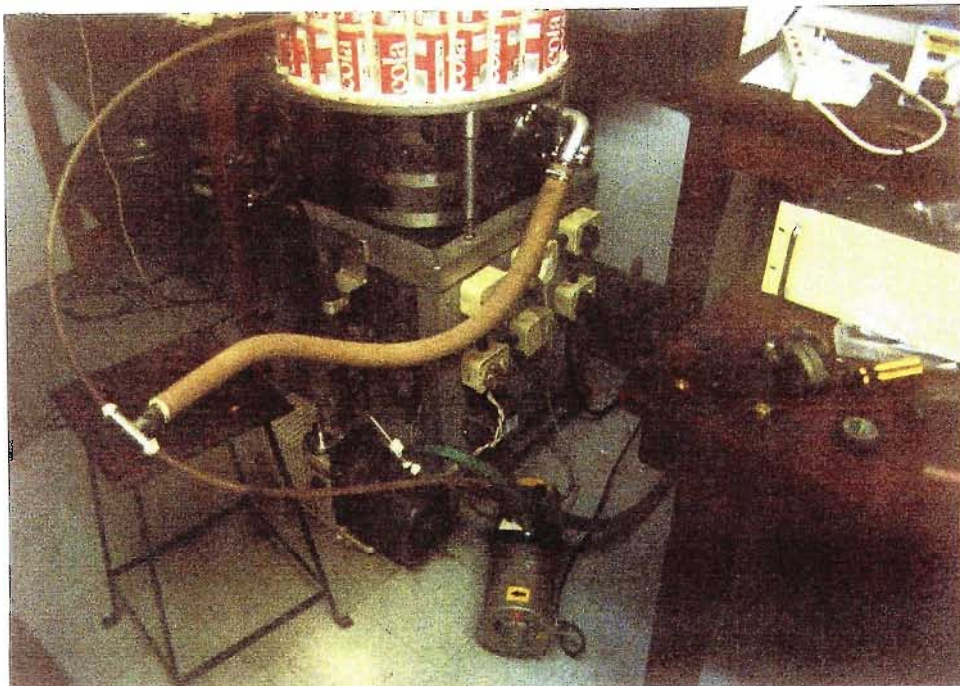


Figure 4.1: External Plumbing Arrangement

trusted below this value and would not move below  $3 \times 10^{-2}$  torr. This served well for the early high vacuum experiments which did not require measurement below these values or simply required knowledge of when to open the butterfly valve and begin evacuation of the inner chamber with the diffusion pump. An ionisation gauge was later added to give the required accuracy for the later high vacuum experiments.

Figure (4.1) shows the plumbing arrangement. The tube that enters the TVV wall can clearly be seen connected to the smaller of the two rotary pumps. The T-piece connects it to the inner chamber. This particular connection is shown in figure (4.2). The valve when closed allows the chambers to be pumped down separately. The mechanical gauge is also shown connected to the inner chamber.

A general procedure was established during the course of experimentation. Firstly, the rotary pump connected to both inner and outer chambers would be activated and the leaks in the TVV walls would be sealed as the chambers were evacuated together. The second rotary pump could be used



Figure 4.2: Valve connecting inner chamber with mechanical gauge

to back the diffusion pump at this stage. Once 80% to 90% of the air had been removed, the second pump could be set to roughing to assist with this process without the danger of creating a pressure differential large enough to implode the inner chamber. This would accelerate the process and often create a sufficiently good vacuum to push the mechanical gauge to the end of its scale. Both chambers could then be separated through closure of the valve. The primary rotary pump would maintain the guard vacuum while the secondary pump would continue evacuation of the inner chamber obtaining values in the  $10^{-1}$  *torr* range. These were registered on the pirani gauge. Heating of the diffusion pump would be maintained during this stage, the diffusion pump specifications such that this heating should continue for 20 minutes before attaining maximum efficiency. After this period of time the butterfly valve would be opened if the use of the diffusion pump was required. In this case the ionisation gauge (if available) could be activated if the pirani gauge was registering its lowest value ( $3 \times 10^{-2}$  *torr*).

## 4.2 The first guard chamber

The first of the two guard vessels was a crude structure, the purpose of which was to give information regarding the implementation of such a design within a TVV. This was necessary to ensure that future improved guard vessel designs could be utilised safely once the fundamental problems had been overcome. This vessel consisted of a 300  $\mu\text{m}$  stainless steel sheet approximately 30,5 *cm* in width, which was rolled into a tube approximately 20,5 *cm* in diameter. This was spot welded by the author and sealed at the top with a perspex dome approximately 6 *cm* in height. The dome was sunken into the chamber to a depth of about 0,5 *cm* giving the chamber an overall height of about 36 *cm*. The bottom was sealed over the diffusion pump. If one ignores the volume of the dome which was small compared with the total, then the volume of the guard vessel is found to be approximately 10 *litres*. Figure (4.3) is a picture of this vessel.

The red rectangular prism in the background of figure (4.3) is the pirani gauge sensor. This is connected to a bend in the pipe and therefore will give a poorer reading of the internal vacuum than is actually the case.

### 4.2.1 Experiment 1

This first experiment was conducted without the use of the diffusion pump. The aim was to find out whether or not it was possible to pump down both the internal and external chambers simultaneously without damaging the

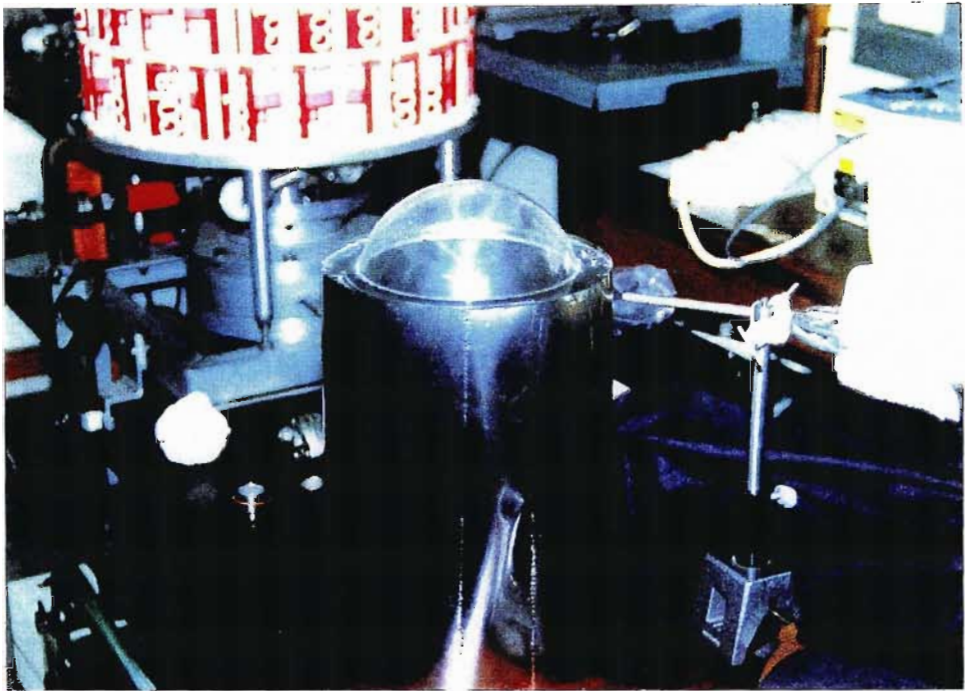


Figure 4.3: The First Guard Vessel





Figure 4.4: Guard Vessel within TVV structure

guard vessel. It was also necessary to find out if the chambers could be pumped down separately once the fore-vacuum had been obtained.

### Apparatus

The guard vacuum chamber was sealed at both ends with putty. The primary rotary pump was less powerful than the secondary and the mechanical gauge was still in its initial position allowing only measurement of the internal vacuum after valve closure. Figure (4.4) is a picture of the guard vessel placed within the TVV walls.

### Results

The TVV performed as in previous experiments and the internal chamber did not implode although some buckling did occur. Once more than 80% of the air had been removed, the secondary pump was activated. The combined



action of the pumps removed sufficient of the remaining air to bring the mechanical gauge to the end of its scale. After closure of the valve the secondary pump continued evacuation of the guard vessel and the pirani gauge recorded a value of  $4 \times 10^{-1}$  torr. This could not be maintained (presumably due to the buckling).

### Observations

The experiment showed that it is indeed possible to pump both the inner and outer chambers simultaneously without a catastrophic implosion. However, the internal chamber did buckle slightly and was shown to require at least some degree of reinforcement. Putty was also shown to be a dubious sealant in that it is too flexible to provide any degree of required support. The experiment also showed that the inner and outer chambers could be pumped down separately. The vacuum obtained was poor. This may have been due to the buckling but may also have been due to the poor quality of putty as a sealant in high vacuum applications. However, it must be stated that this experiment did not make use of the diffusion pump and was only intended to produce a vacuum in the intermediate range.

#### 4.2.2 Experiment 2

This experiment was essentially identical to the previous one except in this case the diffusion pump was activated. The aim was to establish a high vacuum in the guard vessel.

### Apparatus

The apparatus was the same as before although a reinforcing ring of stainless steel was added to the bottom of the guard chamber. Due to the buckling, it was deemed necessary to make use of this support as a ring stiffener.

### Results

The experiment proceeded successfully and after separation of inner and outer chambers a value of  $3 \times 10^{-1}$  torr was obtained on the pirani gauge. After heating diffusion pump the butterfly valve was opened. The vacuum progressively improved until a final reading of  $3 \times 10^{-2}$  torr was obtained.

Putty has a tendency to outgas as was indicated by the way in which the vacuum reading fluctuated before a final value was obtained. The experiment was repeated replacing the putty with standard setting resin with

filler. This was unsuccessful in that the guard chamber imploded. The experiment was then conducted again, this time successfully. After pumping with the diffusion pump a final reading of  $3 \times 10^{-2}$  torr was again obtained.

### Observations

The diffusion pump made a significant difference in that the recorded values improved by one order of magnitude. However, the pirani gauge was known to be unreliable in this range. The fact that the same minimum value was obtained using two different sealants strongly indicated that  $3 \times 10^{-2}$  torr was the bottom end of the scale for this particular gauge.

Several tests were conducted to check this hypothesis. A metal disk was placed over the butterfly valve and sealed with putty. After pumping with the diffusion pump, a minimum value of  $3 \times 10^{-2}$  torr was obtained. The same value was obtained when the disk was sealed with resin with filler. Also a glass plate was sealed over the butterfly valve using both putty and an O-ring in independent tests. In each case the same minimum value as before was obtained confirming that this was the minimum value of the gauge.

This discovery meant that the actual vacuum being obtained within the guard vessel required a more sensitive and accurate gauge to measure it. The ionisation gauge was chosen for this purpose.

### 4.2.3 Experiment 3

This involved the introduction of an ionisation gauge in order to facilitate more accurate and sensitive measurements. The aim was to obtain an actual value of the high vacuum in the guard vessel.

### Apparatus

The ionisation gauge was placed at the base of the guard vessel where a circular opening had been incised into the wall. The frontal aperture of the gauge was sealed to the chamber with resin with filler. The rest of the vessel was insulated with resin and an additional layer of putty was added for reinforcement.

The ionisation gauge connects to its external controller through eight wires. Usually, this gauge is placed externally to the vacuum vessel when in use thereby ensuring that a vactite connection is unnecessary. In this case, however, the connecting wires had to move through the TVV wall and therefore vactite insulation became a necessity. The original wire sheath was found to be a major source of leakage which prevented optimal performance



Figure 4.5: Connection of Ionisation Gauge to Guard Vessel

of the TVV which was necessary both for the protection of the guard vessel and to ensure optimal performance of the high vacuum system.

This problem was dealt with by placing the main sheath outside of the TVV and connecting to it with eight enamel wires which in turn were connected to the gauge itself. These passed through the TVV wall between two of the soft drink can walls, the enamel and putty providing insulation. Two sheets of mylar were also placed between the walls to ensure that the wires did not rupture the cans after evacuation. The setup with the ionisation gauge is shown with figures (4.5) and (4.6).

## Results

The experiment was conducted as previously and performance was normal. When the value of  $3 \times 10^{-2}$  torr was recorded on the pirani gauge, the ionisation gauge was activated. A value of  $1,7 \times 10^{-4}$  torr was obtained. This progressively worsened until a value of  $2,1 \times 10^{-4}$  torr was obtained



Figure 4.6: Wires passing through TVV wall

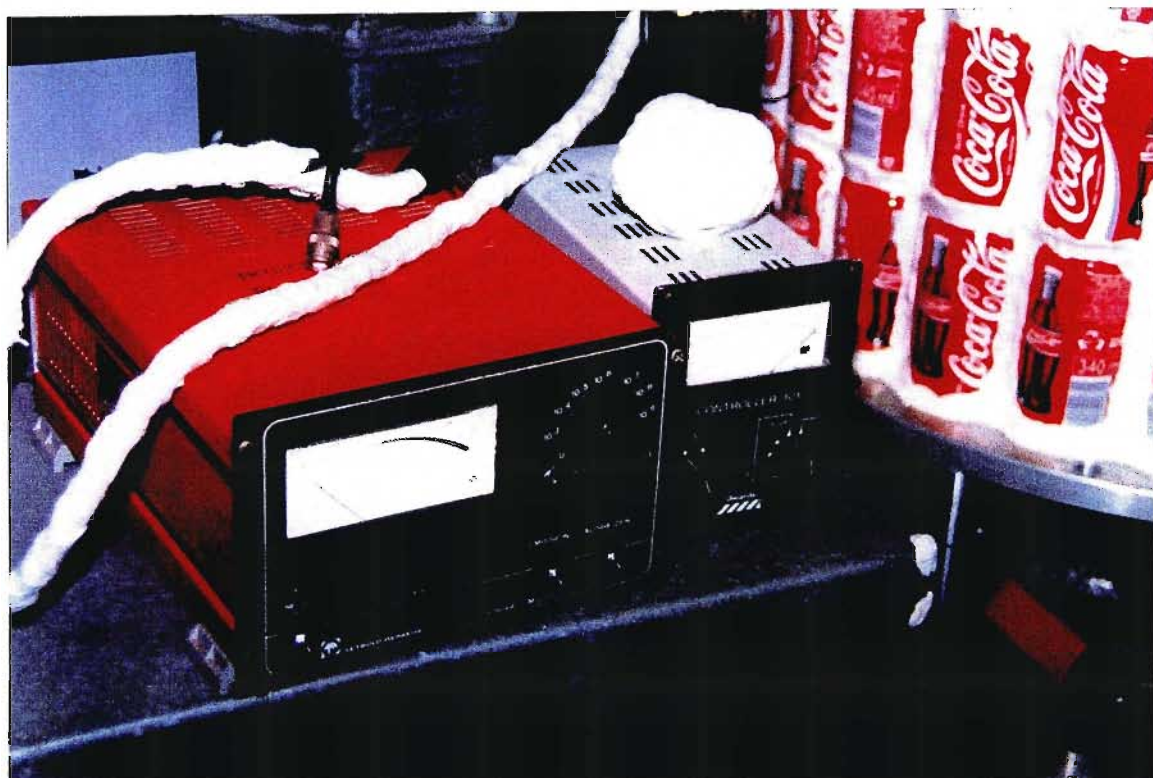


Figure 4.7: Pirani and Ionisation Gauge Heads

forty minutes after the initial activation of the ionisation gauge.

### Observations

The initial results showed that the guard vessel was achieving vacuum in the  $10^{-4}$  torr range. There were also good indications that values in the  $10^{-5}$  torr range were attainable. However, the arrangement with the enamel wires was extremely awkward and the internal vessel was a very flimsy structure in terms of supporting the weight of the ionisation gauge. This meant that it was necessary to find a way of attaching this gauge externally to the TVV. In order to further improve results, a new internal guard vessel was required, the previous design having served its purpose and being too crude to justify further use.





Figure 4.8: Second Guard Vessel placed over Diffusion Pump

### 4.3 The Second Guard Chamber

The second guard vessel was also constructed from  $300\ \mu\text{m}$  stainless steel. Less crude in design, this chamber was professionally rolled and welded by workshop staff. There was less propensity to buckle and a reinforcing rim was welded around the base. A glass window was placed at the top end of the tube to insure visual accessibility. This chamber was sealed over the butterfly valve with vacuum glue after the surface had been cleaned with ethanol. The window was sealed to the top in like manner. Figure (4.8) shows this vessel placed within the TVV.

#### 4.3.1 Experiment 1

This experiment was similar to the previous one but in this case the ionisation gauge was placed externally to the TVV. The new guard vessel did not, therefore, have to be modified to support this gauge and no modifications

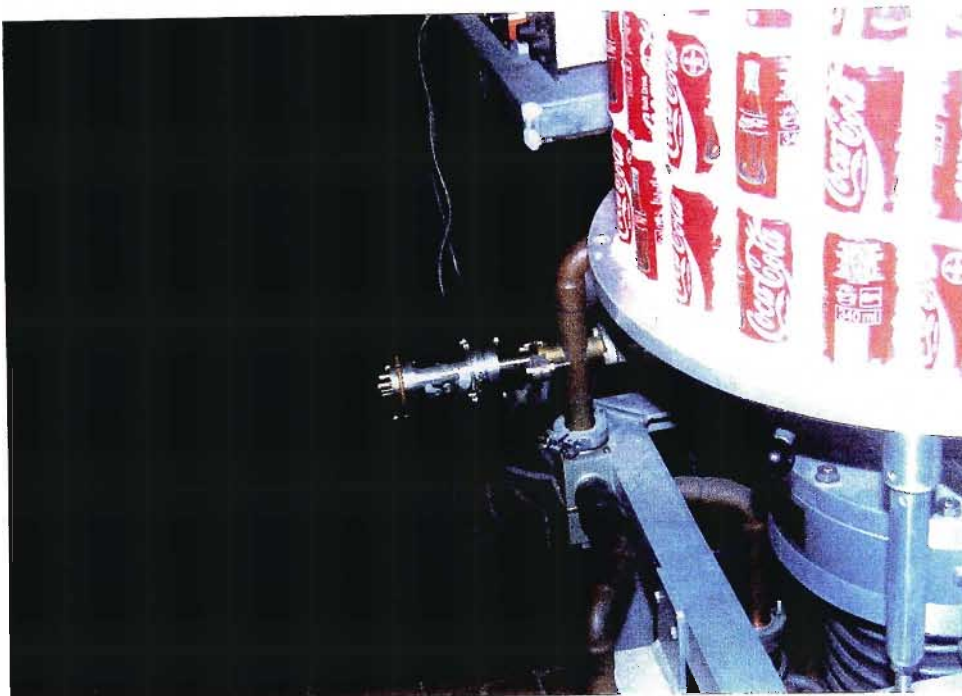


Figure 4.9: Ionisation Gauge connected externally to TVV

were required for the TVV wall. The aim was to find out whether the new guard vessel could support a better vacuum.

### Apparatus

The ionisation gauge was placed opposite the pirani gauge on the pipe connecting the secondary rotary pump with the guard chamber. A special flange had to be made to facilitate this connection. This join occurred after an elbow in the vacuum line which means that any vacuum measurements taken may give a poorer reflection of the actual situation within the internal chamber. This is shown in figure (4.9).

### Results

The TVV performed properly and the experiment ran smoothly without any damage to the new internal chamber. The ionisation gauge gave initial

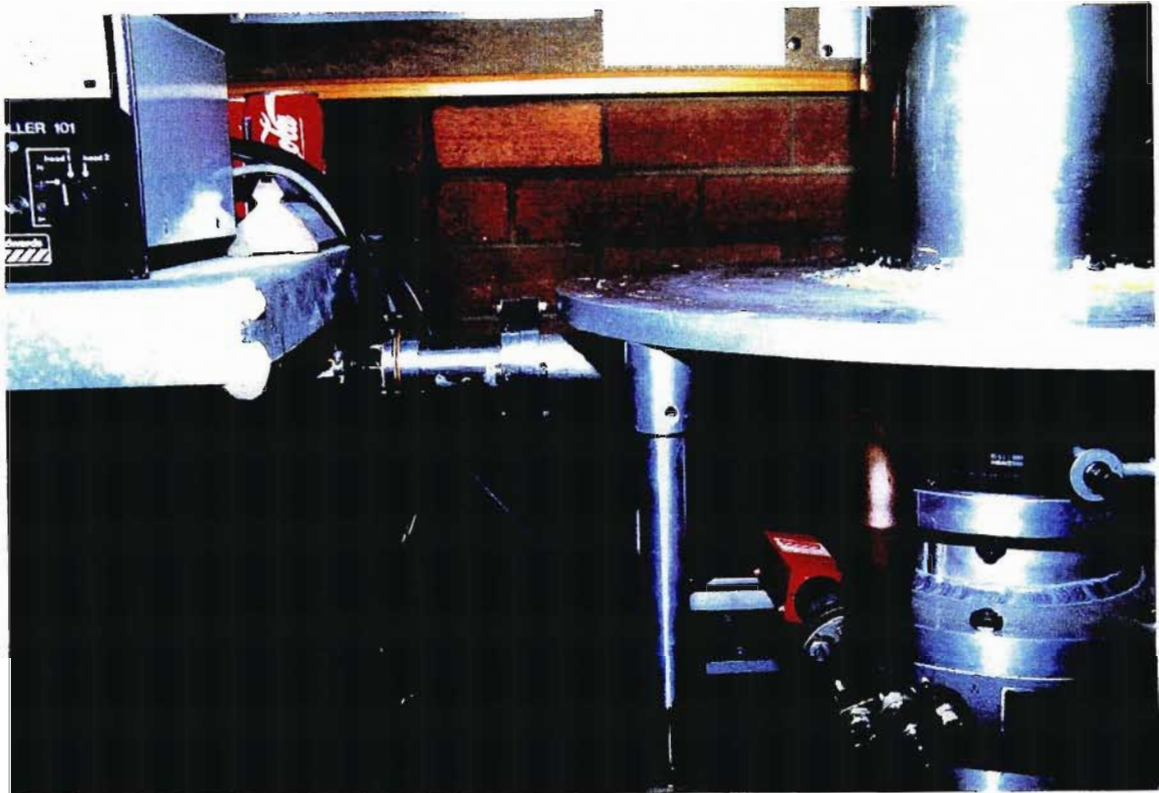


Figure 4.10: Ionisation Gauge with direct link to Internal Vessel

readings in the  $10^{-5}$  *torr* range and rose slowly through this range, peaking at  $2 \times 10^{-4}$  *torr*. A substantial improvement was achieved through the use of the degas operation. After degassing a value of  $8 \times 10^{-6}$  *torr* was obtained.

### Observations

The position of the ionisation gauge was shown to be unfortunate in that the vacuum readings obtained became progressively worse than anticipated. The initial readings were consistent with a value in the  $10^{-5}$  *torr* range.

### 4.3.2 Experiment 2

The ionisation gauge was moved to a new location where a more direct link to the guard chamber was obtained. This is shown in figure (4.10). The aim was to obtain more accurate measurements of the high vacuum.



## Apparatus

The ionisation gauge was moved to a location whereby it was connected to the internal chamber via a straight pipe with a larger aperture than previously. The distance to the gauge was also much shorter. These factors insured a more direct and therefore more accurate reading of the internal vacuum.

## Results

The experiment again encountered no mechanical problems and after 2 hours the ionisation gave a reading of  $2 \times 10^{-5}$  torr. This did not change over time and the experiment was allowed to run for 13 hours. No change in value occurred.

## Observations

The fact that the recorded value of  $2 \times 10^{-5}$  torr did not change over a number of hours indicates that this is the actual value of the high vacuum. The question remained as to whether this was a limitation of the diffusion pump or whether this was a limitation of the diffusion pump. The diffusion pump is rated to give a best vacuum of  $10^{-7}$  torr but the oil had not been changed for several years and had been known to produce vacuums in the  $10^{-5}$  torr range.

The only way to confirm this was to replace the TVV with the original compressional vacuum chamber. This was done and the experiment was repeated. The vacuum obtained in the internal chamber was  $2 \times 10^{-5}$  torr confirming that the limiting factor was the diffusion pump. If the oil were to be changed, it is almost certain that a better high vacuum would be obtained.

## 4.4 Conclusion

This chapter has demonstrated that a TVV is capable of producing a high vacuum through the inclusion of a guard vessel. The successive experiments described in this chapter have illustrated that it is structurally feasible to have such a vessel within the TVV walls. Also, of great importance, is the fact that as our technology improved so did our results. This indicates that improving high vacuum TVV's is a technological problem and therefore that the experiments show that high vacuum TVV's are practical.

## Chapter 5

# Further Tubular TVV Experiments

The two previous chapters have outlined experimental work performed with regards to creating large TVV's and proving that a high vacuum can be maintained within such vessels. The TVV's were tubular in nature for reasons already given. A number of observations were made with regards to the behaviour of tubular models but this happened in the context of producing a large, stable TVV that would ultimately be capable of supporting high vacuum work. The aim of this chapter is therefore to specifically focus on the dynamics of tubular vessels.

The disadvantage of using soft drink cans is that the pressure cannot be regulated. A series of tubular TVV's was designed such that the pressure within the walls could be measured and controlled.

### 5.1 Pressurisable Tubular TVV Experiments

Three experimental tubular TVV's were manufactured according to the same fundamental design, although each chamber was larger than its predecessor. All were made from soft drink cans modified to suit our experimental aims.

These vessels required thin sheet metal rolled into tubes. Soft drink cans already had the required shape and had metal walls  $300\text{ }\mu\text{m}$  thick. This was ideal for experimental purposes. The first two models were manufactured by the author whilst the final model was manufactured by workshop staff. The general technique used in making these chambers is described below.

Firstly, the cans are emptied of their contents. The empty cans are

then sand blasted in order to remove the anti-oxidant (the cans are made of ferrous material) coating to facilitate soldering. The top ends are then removed. The cans are paired off, the now open tops of each pair are soldered together to form a single unit with a thin solder seal in the middle. This soldering is generally done using an alkaline benzene based flux. Each unit has its top end defined by a hole made with a  $3\text{ mm}$  drill bit. This is necessary to facilitate the introduction of a copper tube for the purposes of pressurisation. Each unit has to be able to withstand pressures of 5 to 7 *bar* without the solder joint rupturing.

The required number of such units is then placed in a concentric circle and soldered to form the vacuum sealed wall of the TVV. Each unit is joined to the adjacent unit through a copper tube in order to facilitate pressurisation of the vessel. Flat metal end plates are employed in all of these vessels and these are either soldered on or sealed with putty.

#### 5.1.1 Experiment 1

The first model consisted of twelve 340 *ml* cans soldered together to form a TVV consisting of six units. The aim of this experiment was to test the basic TVV theory with a small scale vessel.

#### Apparatus

This was an chamber had a radial number of six, each unit standing 20,5 *cm* high and having a diameter of 6,5 *cm*. The mean diameter (diameter midway between the inner and outer diameters) was 14 *cm*. Two copper plates, each 1,5 *mm* thick were soldered to the top and bottom ends of the vessel. However, the original intention was to build an  $n = 8$  chamber. This was changed during construction resulting in an asymmetrical chamber. The internal volume of the space to be evacuated was approximately 0,6 *litres*. The top plate had a 6 *mm* hole drilled into the middle into which was inserted a stainless steel pipe of the same outer diameter. This in turn was connected to a plastic tube, which, at the opposite end, was connected to a rotary pump and mechanical vacuum gauge.

The units of the TVV wall were connected via 3 *mm* (outer diameter) copper tubing, allowing the units to be pressurised in such a way that only one unit was required to be connected to the pressure hose. This was connected to the vessel through a pressure regulator and valve. This allowed the TVV walls to be pressurised to 5 to 7 *bar*. A pressure gauge was attached to the hose. Pressure readings given regarding the TVV wall pressure in

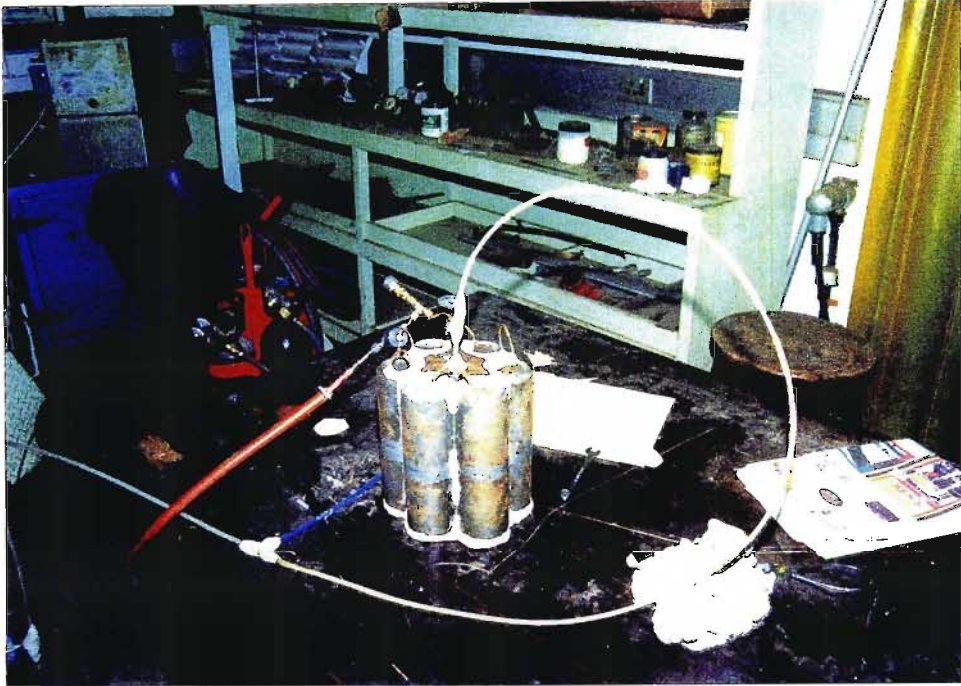


Figure 5.1: First Pressurisable Tubular TVV ( $n = 6$ )

this chapter are all given in terms of gauge pressure unless otherwise stated. The apparatus is shown in figure (5.1).

## Results

A standard procedure was developed for conducting experiments with this chamber. Firstly the pressure valve would be opened, pressurising the TVV wall to at least 5 *bar*. The air was then pumped out of the chamber. A putty seal was used.

The first time this experiment was run, a vacuum gauge reading of 0,80 *bar* was obtained. This could not be improved indicating the presence of internal leaks. The chamber did not collapse. The second run produced a reading of 0,60 *bar* indicating that the internal leaks were getting worse.

It was impractical to remove one of the end plates to repair the leaks as they were soldered on and removal might entail damage to the TVV wall. The most practical method of solving this problem was to reduce

the pressure in the TVV wall in order and thus reduce the intensity of the leaks. The air was pumped out of the chamber without pressurisation of the TVV wall. A value of 0,95 *bar* was obtained without collapse. However, when the inlet nozzle of the pressure hose (the hose was disconnected as the system was operating at atmospheric pressure) was covered, the chamber immediately began to collapse at that point. When the pressure hose was reconnected and the system pressurised the collapsed section resumed its shape. This is interesting in that it illustrates that this vessel is in a sense "inflatable".

### Observations

The chamber could withstand pressures of up to 5 *bar* within its walls for brief periods but the solder joints tended to leak after use for any significant length of time. After removal of the air from the chamber, the larger pressure differential across the inner wall produced internal leaks which were impossible to repair with the end plates soldered on. Future chambers of this nature would have to be constructed with the internal wall accessible for repairs.

The fact that the chamber could operate successfully without pressurisation so that the pressure differential across the internal wall was effectively 1 *bar* indicates that these structures have a rigidity of their own not completely explained by the simple TVV theory. The  $\Delta R/R_i$  ratio is difficult to determine as it is extremely difficult to measure  $\Delta R$  in this case. End effects are likely to contribute to stability. However, the surface area of the end plates exposed to the gauge pressure is small and therefore the normal force is not likely to be large enough to make friction a convincing explanation by itself. Another factor may be that it is more difficult for instabilities to manifest themselves. The most likely explanation is that the ring stiffening elements at the upper and lower extremities of the units provide stability in compression.

Buckling did occur after the pressure nozzle was closed preventing a flow of air through this orifice as air leaked internally. This section was repaired through pressurising the TVV walls illustrating that this chamber is inflatable to some extent. This also illustrated that the tubes which did buckle during the course of the tubular TVV experiments may have done so due to the evacuation of the tube itself. The internal pressure could have dropped below 1 *bar* as happened in this case. One cannot be sure that this was the case for TVV's with large  $n$  but it does appear that TVV's with small  $n$  do not require significant pressurisation.



Figure 5.2: TVV walls for  $n = 10$  vessel

### 5.1.2 Experiment 2

A second chamber was constructed similar to that used in the previous experiment. This made use of twenty 450 *ml* soft drink cans soldered end on end to form ten units making up the wall of the new TVV.

#### Apparatus

The second chamber in this series was larger version of the previous model. This had a radial number of ten, each unit being 27,3 *cm* high and 6,5 *cm* in diameter. The increased height of each unit is due to the fact that 450 *ml* soft drink cans were used in the manufacture of this vessel. The mean diameter of the chamber was 21 *cm*. This gave the internal volume a value of approximately 4,5 *litres*. Figure (5.2) picture which shows walls of this vessel.

The end plates were not soldered to the wall. Rather putty was used to seal them to the vessel walls so that they could be removed should the need

arise. The bottom plate was a circular aluminium plate 3,5 *mm* thick. The top plate was also aluminium 2 *mm* in thickness and was cut to fit over the wall.

## Results

As before, the units were pressurised to at least 5 *bar*. The air was then removed from the internal volume. A vacuum gauge reading of 0,67 *bar* was obtained before equilibrium was reached indicating the existence of internal leaks.

The experiment was run a second time but a reading of only 0,20 *bar* was obtained. The leaking had increased to the point that the chamber was effectively useless in terms of sustaining even a low vacuum. An attempt was made to repair the vessel by sealing the leaks through soldering. This did not have any significant effect. It was then decided to run the experiment with the TVV walls at atmospheric pressure in order to reduce the intensity of the leaks. The pressure hose was disconnected in order to facilitate this.

When the pump was activated a vacuum reading of 0,75 *bar* was obtained. The chamber did not collapse. The experiment was run again and this time the pressure inlet nozzle was covered in order to obstruct the through flow of air. Some of the units started to buckle at a reading of 0,65 *bar*.

## Observations

This experiment confirmed many of the observations made with the previous vessel. The solder joints tended to rupture at pressures of 5 to 7 *bar*, particularly the inner walls which had to support the greater pressure differential.

The vacuum gauge readings obtained were lower than in the previous experiment and this may in part be explained by the simple TVV theory. The  $\Delta R/R_i$  ratio is smaller in this case and hence the chamber should according to this theory be less stable than its predecessor.

However, this chamber was similar to the previous TVV in that it displayed a rigidity that could not be explained purely by the simple theory. Once again buckling did occur but only after the chamber inlet nozzle had been covered, confirming that collapse occurred when the absolute pressure in the units dropped to below 1 *bar*. The frictional forces due to the end plates are greater for this vessel than those experienced by the previous vessel. Once again it appears that the most likely explanation for this unusual stability is the stiffening rings situated at the upper and lower extremities.



The compressional components of this vessel cannot be ignored.

### 5.1.3 Experiment 3

The third TVV of this particular series was constructed by workshop staff and was a slightly larger version of the previous chamber. This was designed in order to make possible a high vacuum experiment. Once again soft drink cans were used to provide the basic material for the TVV wall. Twenty-four 450 *ml* cans were soldered together to form a TVV wall consisting of twelve cylindrical units.

#### Apparatus

This was an chamber had a radial number of twelve. The height was identical to that of the previous vessel the same cylindrical units were used in its construction. The chamber was somewhat larger than that of experiment 2 due to the addition of two units to the wall. The mean diameter was 25 *cm* giving the chamber an internal volume of approximately 7,4 *litres*.

Once again each unit was connected to the adjacent tube by means of a small copper tube. The pressure hose connection was soldered to one of the units and a pressure gauge was attached. The gauge employed previously was a crude device used to give a more approximate pressure value. The device used in this experiment was intended to give more accurate readings. A pressure regulator and valve were also added to the system in order to make pressure regulation efficient.

A thin steel top plate was soldered to the TVV wall. This plate was made to fit tightly between the unit tops in order to ensure a good seal. An identical sheet was soldered to the units at the bottom. A hole 19,1 *cm* in diameter was cut into this sheet and a ring of metal 5 *mm* in thickness of the same outer diameter was attached. The inner diameter of the ring was 18,4 *cm* and an O-ring groove was cut into it. This was done to ensure accessibility to the inner chamber so that repairs could be made if necessary as well as to create the possibility of a high vacuum experiment. The chamber could be sealed over an oil diffusion pump should such an experiment be conducted.

During the first tests of this chamber, the TVV was sealed to the bottom plate used in the the previous experiment by means of an O-ring lubricated with high vacuum grease. A 6 *mm* hole was drilled into the bottom to admit the vacuum hose. The same vacuum system as that of the previous experiment was used to test this TVV. The chamber with its associated





Figure 5.3:  $n = 12$  Vessel Painted to Prevent Rust

vacuum and pressure apparatus is shown in figures (5.3) and (5.4).

### Results

The chamber was pressurised to 4 *bar*. The vacuum pump was activated and an equilibrium was established at 0,60 *bar*. The air was readmitted to the chamber and a pressure of 4 *bar* was maintained in the TVV walls. After forty minutes this had declined to 3 *bar* indicating the presence of a slow leak. As in the previous experiments the leak occurred through the internal solder joins.

The experiment was run several times without significant improvement. The solder joins always leaked internally and had to be repaired. A larger rotary pump was employed and values of 0,80 *bar* were obtained on the vacuum gauge. Leaks still remained a problem and also occurred as a result of the deformation of the top plate. These too had to be repaired.

A tensional pattern formed on the top plate due to the deformation of

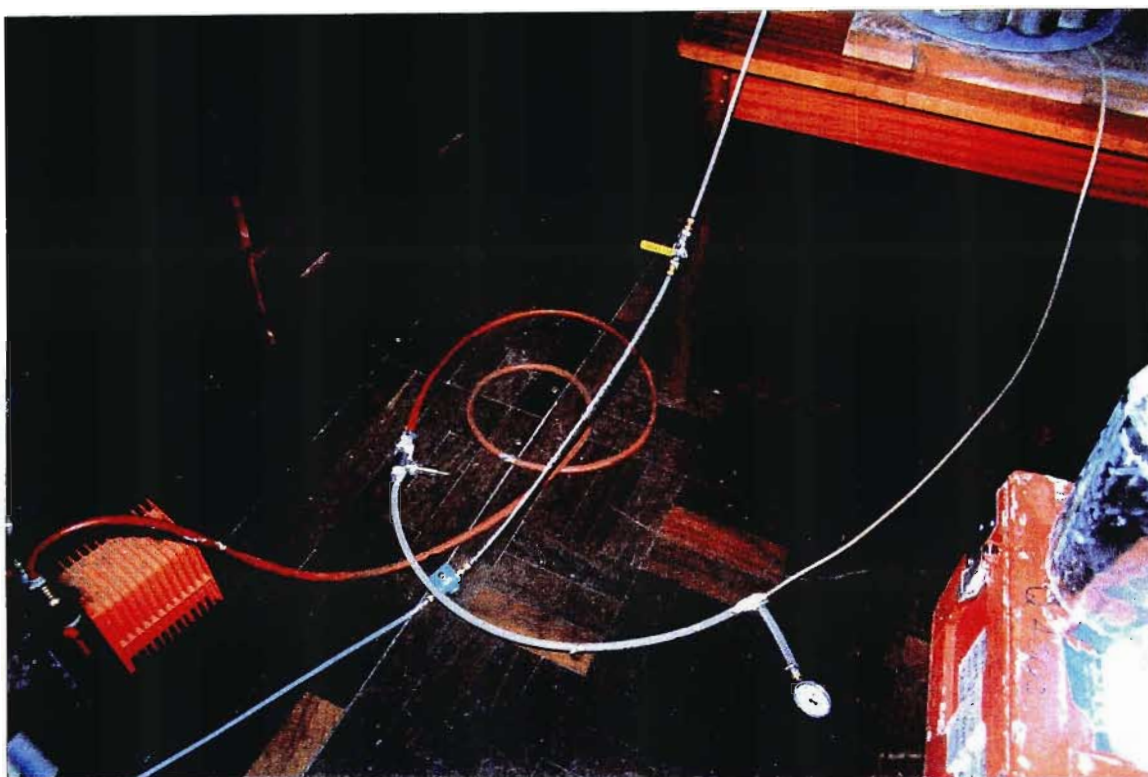


Figure 5.4: Vacuum and Pressure Apparatus

this structure. Once the pattern had formed, the plate became relatively stable and leaks were generally confined to the internal solder joins. In order to deal with this it was decided to operate the TVV at lower wall pressures. This would also test whether or not the structure remained stable at lower pressures as was the case with the two previous TVV's. The TVV was pressurised and the vacuum pump activated. The pressure in the tubes was allowed to drop to 1,5 to 2 *bar*. Vacuum gauge readings of 0,85 *bar* were obtained and the chamber did not collapse.

### Observations

Once again this type of TVV was found to have an internal rigidity not fully explainable with the simple TVV theory. The solder joins continued to leak indicating that they are not strong enough for this type of chamber and that in future other means will have to be used. It may be more practical to employ single tubes that do not require solder joins.

The tensional pattern formed on the top plate was extremely complex and would require a finite element analysis to gain a better understanding. The unit tops were distorted into oval egg-shapes. This may be explained by the tension of the top plate pulling the units inward. There was no distortion of the unit bottoms. Any movement was restricted due to the solid bottom ring. The other chambers did not produce such patterns. The fact that the tube ends were distorted but did not collapse clearly shows the effects of their ring stiffening properties in maintaining stability. Although the tensile forces due to the top plate were sufficient to cause distortion, they were still not capable of causing structural failure. This certainly provides further proof of the need to take into account the compressional components of tubular TVV's.

## 5.2 Experiments with $p = 1$ *bar*

The experiments outlined so far have illustrated that the pressure inside the walls of a tubular TVV can be as low as atmospheric pressure. The tests performed with chambers with  $p = 1$  *bar* illustrated that at least for small  $n$ , the vessel walls only collapsed when the tube interiors were partially evacuated. This means that the internal surfaces of the tubes were supporting the vessel against the atmosphere.

In order to gain a better understanding of the behaviour of TVV's with low  $p$  values it was decided to examine the behaviour of tubular walls constructed from empty soft drink cans.

## Apparatus

Soft drink cans (340 ml) were once again used as tubular TVV walls. A hole was punctured into the side of each can which was then emptied of its contents. The cans were arranged into a concentric circle and sealed together with putty. This wall was then sealed to the aluminium base used in the previous experiment. A second circular aluminium plate of the same thickness was used as the top plate. The vacuum apparatus was the same as that used in the first two experiments described in this chapter. The holes in the cans were made to face outwards such that they were not exposed to vacuum as this would place the can walls in compression. This would otherwise cause the can to collapse.

## Results

Two chambers were made: an  $n = 6$  model and an  $n = 8$  model. When the first tests had been run with the  $n = 6$  vessel, two cans were simply added to the structure in order to create the  $n = 8$  vessel. The tests have all been grouped together as one experiment due to their similarities.

When the  $n = 6$  vessel was pumped down no inwards movement was noticed. There was only a minor distortion of the outer walls. The vessel was, however, stable. When the  $n = 8$  vessel was pumped down the same distortions were noted although they appeared to be somewhat more severe. However, more importantly instabilities manifested themselves in this vessel. Some of the cans moved inwards resulting in a formation of three cans in a line. In each case the vacuum gauge registered more than 0,8 bar indicating that from a structural point of view the forces being experienced were essentially those due to atmospheric pressure.

## Observations

The most important observation is the confirmation of the fact that larger vessels experience greater instabilities. This is obvious for large  $n$  as compared to vessels with small  $n$  but in this case the increase in  $n$  was by no means dramatic.

It must also be noted that an increase in  $n$  also results in an increase in the surface area of the end plates exposed to vacuum and therefore the normal force. If one calculates the distribution of the forces across the cans, the force experienced by each can in the  $n = 8$  model is significantly greater than that experienced with the  $n = 6$  version. This means that the frictional forces due to the end plates should be greater for the larger model which

would suggest that stability should be greater. However, this is clearly not the case although it must be noted that in the  $n = 8$  case these end forces were great enough to prevent implosion. It appears that with this vessel, the flute instability can no longer be restrained by these forces.

### 5.2.1 Discussion and Conclusion

The experiments described in this chapter have shown that the basic tubular TVV theory is inadequate when used to describe such vessels with walls that have their own rigidity. If the walls of the TVV were to be completely flexible (as in the case of an inflatable chamber) then one might expect the theory to correlate more closely. Clearly the end effects play some role in holding the cans and preventing instabilities. However, for chambers with large radial numbers, the development of instabilities cannot be held in check by the end forces and they are rapidly amplified. Vessels with larger radial numbers tend to rupture more easily whereas chambers with smaller values tend to be more self supporting.

This clearly favours vessels with fewer tubes. However, if one desires a chamber with a significant internal volume, then it becomes impractical to have vessels such as  $n = 6$  models which have bulky walls. If one increases  $n$  then the ratio of internal volume to the TVV wall volume increases. One therefore has to balance the desire to avoid bulky TVV walls with the desire to reduce instabilities.

Another factor which reduces the necessary value of  $p$  is the use of stiffening rings at the base and top parts of the tubes. If strong enough they can effectively support the intertube forces which means that the tubes need only be at  $p_0$ . This means that only the inner walls of the tubes are in tension and even then the tensile forces are relatively small if they are not required to tolerate a pressure of several bars. The outer walls are not really necessary except for vertical support. Once again, a designer of such a vessel will have to balance the desire to reduce the material required for ring stiffening with the strength of material required as well as the desire to reduce  $\Delta R$ .

A little theory regarding tubes in compression is useful here. More detail is given in Appendix A. The buckling pressure of a circular ring is given by:

$$p' = \frac{3EI}{R^3} \quad (5.1)$$

where  $E$  is Young's Modulus of Elasticity and  $I$  is the second moment of inertia about the centroidal axis parallel to the axis of symmetry.  $R$  is the radius of curvature and  $p'$  is the load per unit length.[7, 18, 23] A cylinder

without stiffening rings has  $I = t^3/12$  and  $V_l = \pi(2R+t)t$ , while if stiffening rings are included, we have  $I = \frac{5}{6}th^2$  and  $V_l = 4\pi Rt$  depending on the symmetry of the rings. In this case,  $t$  is the thickness of the wall material and  $V_l$  is the volume of wall material per unit length.

If one substitutes the above values of  $I$  into equation (5.1), one discovers that  $t$  can be smaller for ring stiffenned tubes and therefore the volume of material in the walls can also be less.

In our case, the forces on the walls are both due to atmospheric pressure as well as the intertube forces and so will not be evenly distributed. Equation (5.1) will not give a complete description of the tubes under pressure. However, it does serve to illustrate the effects of ring stiffenners and hence illustrate that these components cannot be ignored. Compressional components are likely, therefore to play a role in future designs of tubular TVV's as these can also be instrumental in material savings.

## Chapter 6

# Cylindrical TVV's with Toroidal Walls

An alternative design to that of the tubular TVV is the toroidal wall TVV (TTVV) where the walls are essentially pressurised tori.<sup>1</sup> The basic theory is actually identical to that of a perfect double walled cylindrical tensional chamber. This makes the TTVV less prone to instabilities than the theoretically more complex tubular TVV's. The interchange, for example, is impossible as is the sausage. However, the kink may well occur if such a vessel is scaled up in size through the vertical stacking of additional tori. TTVV's can be constructed from circumferential tubes. However, in order to avoid confusion, the term tubular TVV will always be taken as referring to vessels constructed from longitudinal tubes.

This chapter outlines experiments performed in order to test the performance of the TTVV. Various tyres were used as the basic construction materials of the TTVV walls. The first tests were "proof of principle" experiments which were small in scale using childrens bicycle tyres. Car tyres were used from then on in order to create vessels of more useful size. Chamber volume was increased through the vertical stacking of additional tyres. Once a sufficiently large and stable vessel had been created, high vacuum experiments were conducted through the inclusion of a guard chamber in order to prove that a useful vacuum could be obtained. It must be stated at this point that the TTVV's described in this chapter could truly be described as being inflatable. This chapter can therefore also be regarded as describing "inflavac" experiments.

---

<sup>1</sup>The walls may not be perfect tori but the theory of a torus under internal pressure is useful in the development of theory describing tension in the TTVV walls.

## 6.1 Low Vacuum Experiments

In order to test the structural viability of the TTVV, a series of low vacuum experiments were conducted.

### 6.1.1 Experiment 1

The first TTVV created was small in size. This was the first vessel of its kind and knowledge of the stability of a small model was required before any attempt at building a larger version could be made. The TVV walls were made from childrens bicycle tyres.

#### Apparatus

The TTVV wall consisted of two 12,5 *inch* by 2,25 *inch* tyres. This means that each tyre had an outer diameter of approximately 32 *cm* and an internal diameter of approximately 20,6 *cm*. Each was supported by a plastic rim with a diameter of 20,5 *cm*. The tyres were sealed together with putty and a perspex dome was sealed to the top rim of the upper tyre by the same means. This gave the vessel an overall height of approximately 14 *cm*.

A rotary pump was used to remove the air from the vessel and a mechanical vacuum gauge was used to measure the vacuum obtained. The vacuum hose was inserted through the TPV wall between the tyres. The vessel itself was sealed to a welding bench.

#### Results

During the first run, a vacuum gauge reading of 0,95 *bar* was obtained. The tyres did not rupture but compressed visibly, particularly the bottom tyre. A second run gave a value of 0,98 *bar*.

Our first plasma experiment in a TVV was performed. Wires were placed between the tyres and the perspex dome and these were in turn attached to a 6 *kV* power supply. When voltage was applied, plasma sheaths formed around the wires. The size of the sheath varied in accordance with the quality of the vacuum as explained later.

The experiment was done in order to illustrate that one could obtain a plasma in a TVV. We also wished to demonstrate how TVV's can be used in order to provide relatively cheap demonstrations in a classroom or a lecture theatre.



## Observations

The most important observation was that the tyres did not rupture which means that the principle of the TTVV is valid, at least on a small scale. However, if the tyres did not rupture on a small vessel, then there was a distinct possibility that larger tyres could be employed to create a larger vessel. This would allow more quantitative data to be obtained as well as opening up the possibility of a high vacuum experiment.

The plasma experiment in this case was a "fun" experiment but it did illustrate the principle of how an inflatable vessel could be inflated on site and be used for performing examinations or physics demonstrations.

### 6.1.2 Note on Plasma Sheaths

A plasma sheath is the layer of plasma that collects around a charged electrode in a gas/plasma medium. In the case of our vacuum experiments, electrodes were inserted into a rarified gaseous medium.

Chen[21] gives a good description of plasma sheath formation. Charged particles will gather around an electrode of opposite charge. Assuming that by some means these charges are prevented from recombining on the surface, a cloud of plasma will tend to form. This is the sheath. The charged particles within the sheath would shield the outside region from any electric potential.

This is the ideal situation which can be applied to a cold plasma. A more realistic explanation has to take thermal motion into account. At the edge of the sheath, where the electric field is weak, some of the particles have enough thermal energy to escape. The shielding is, therefore, not perfect. The radius of the sheath is therefore defined as the distance from the electrode to the point where the potential energy is approximately equal to the thermal energy ( $KT$ ) of the particles. This radius, also known as the Debye length, is given defined mathematically by the following equation[21]:

$$\lambda_D \equiv \left( \frac{KT_e}{4\pi n e^2} \right)^{1/2} \quad (6.1)$$

where  $\lambda_D$  is the Debye length,  $KT_e$  is the thermal energy of the electrons (ions are assumed to be cold in this case due to their much greater mass),  $e$  is the charge of an electron and  $n$  is the particle density.

The important point to notice with regards to our vacuum work, is that the Debye length (and therefore the size of the plasma sheath) is inversely proportional to the material density. Therefore the better the quality of the vacuum, the larger the sheath.

### 6.1.3 Experiment 2

This was the first of a series of experiments involving the use of car tyres. This particular experiment involved the use of two car tyres although they were used separately in single layer ( $m = 1$ ) configurations. The same convention is used with regards to vertical stacking as in the case of tubular TVV's. There is no radial number associated with TTVV's, only the longitudinal number. No internal rims were required to stabilise the structure.

#### Apparatus

Two size 13 car tyres were used separately as TVV walls. The existence of a slight variation in size was inconsequential. All the tyres used in the experiments described from here on in the chapter were size 13 with minor variations. The internal diameters were all 33 *cm* and the external diameters were all effectively 59 *cm*. The height corresponded to the difference between the internal and external radii and was therefore 13 *cm*.

A size 13 tube was placed into the first tyre and a size 14 into the second. In order to prevent the inner tubes from escaping whilst in a vacuum, it was deemed necessary to clamp the tyres. In each case eight 6 *mm* screws were placed along the inner circumferences of each tyre which were then bolted together.

The experiment was qualitative in nature in that pressure readings were not taken after the tyres were pressurised. Also, no vacuum gauge was attached to the vacuum line. The aim was to find out if tyres of this size would rupture if used in a TTVV experiment. A rotary pump was used to evacuate the interior.

In each case the tyre would be sealed to a welding bench with putty and the top plate a compressional vacuum vessel was sealed to the top. The vacuum hose was placed through the bottom between the tyre and the welding bench.

#### Results

The smaller of the tyres did not rupture. The same was true of the larger tyre although parts of the tyre tube "ballooned out" between the clamps. The best term to describe this "ballooning" is the medical term, aneurism.

In attempting to find a solution to this problem, bicycle tyres were placed within the inner circumferences of each car tyre. These bicycle tyres were in turn equipped with supports. The tyre to be inserted into the smaller of the car tyres was equipped with two metal hoops joined together, one above



Figure 6.1: Rupture of inner tube

the other. The other was equipped with a flat metal sheet rolled to form a circular rim.

The experiment was run for a second time. Once again, the smaller tyre did not rupture but aneurisms developed in the second tyre and one of them burst causing the TVV to collapse. During each experiment the tyres were compressed noticeably, possibly to as much as two-thirds of their vertical height.

Figure (6.1) is a picture of a burst inner tube clearly illustrating the inability of the inner tube to withstand the pressures that develop in this TVV.

### Observations

The results obtained indicate that larger TVV's are viable and that the tyre experiments can be scaled up in size. The tyre fabric is strong enough to withstand the present tensile forces. However, the inner tube is made of

material that is far more elastic in nature and tends to stretch to the point of rupturing when exposed to vacuum. It is therefore necessary to ensure that in these experiments these tubes are firmly clamped within the tyre material and are not directly exposed to the vacuum, thus ensuring that the air pressure within the tubes and the tyre material are responsible for supporting the TVV.

The tyres were compressed in each case indicating the loss of volume associated with an increase in pressure when using a gas as the pressurising medium. There were no inward instabilities associated with this model.

#### 6.1.4 Experiment 3

This was a double layered ( $m = 2$ ) experiment. Initially one tyre was placed above the other and the two were sealed together with putty. However, every time the experiment was run one of the inner tubes would rupture causing the tyre to deflate. The other tyre would then be "sucked into" it. In order to have a successful double layer experiment it was deemed necessary to ensure that the inner tubes were firmly clamped inside the tyres.

#### Apparatus

The tyres from the previous experiment formed the TTVV wall. Each was provided with a size 15 tube. In order to clamp them, two 1 *cm* thick metal hoops were placed above and below the inner circumference of each tyre. These hoops had a diameter slightly larger than the inner diameter of the tyres. Both tyres were fitted with sixteen metal clamps, eight above and eight below which would clamp the top and bottom hoops respectively. The 6 *mm* screws were used to connect the upper and lower clamps. When the clamps were screwed together the hoops would seal the inner tubes within the tyres. The arrangement is shown in figures (6.2) and (6.3).

Each tube was pressurised to 2,5 *bar*. The tyres were sealed together with putty and the same rotary pump was used to remove the air from the system. The vacuum hose was inserted through the bottom of the TVV which was once again attached to the welding bench. The same top plate was used.

#### Results

The vessel compressed noticeably after activation of the rotary pump. In this case neither of the tubes ruptured and the vessel remained stable. The experiment was run successfully for periods of up to ten minutes. The figures



Figure 6.2: Clamping arrangement for car tyre



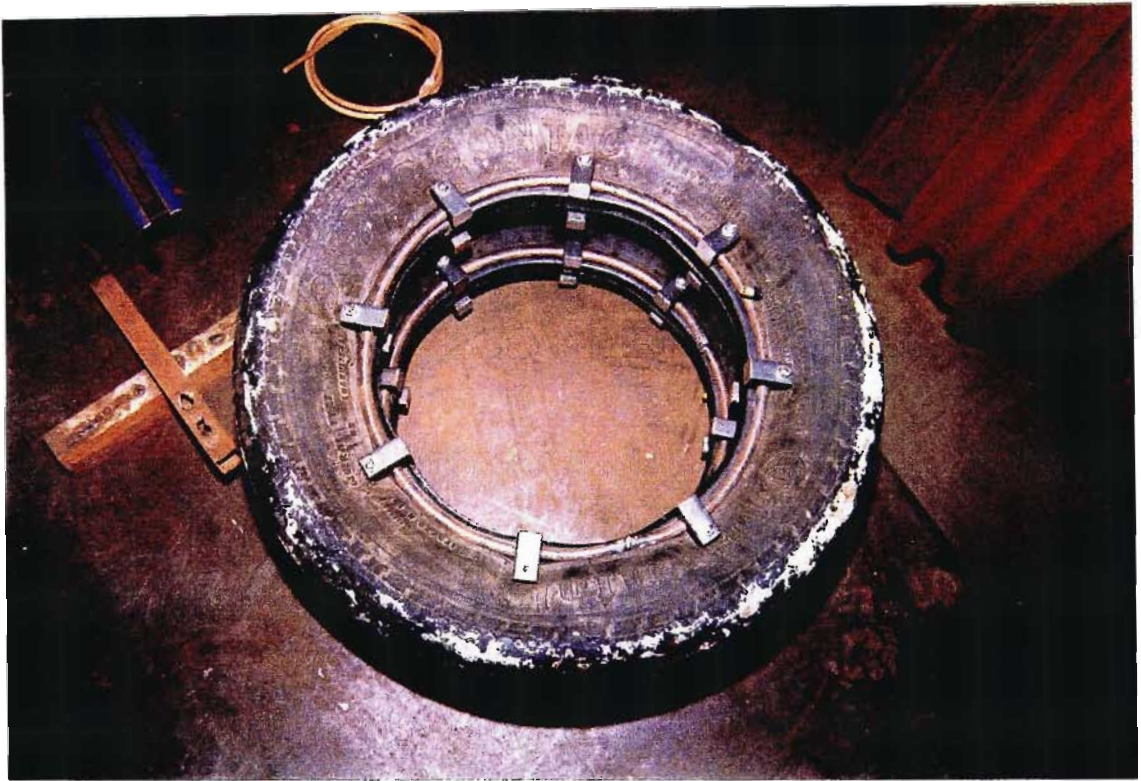


Figure 6.3: Internal structure of double layered TTVV

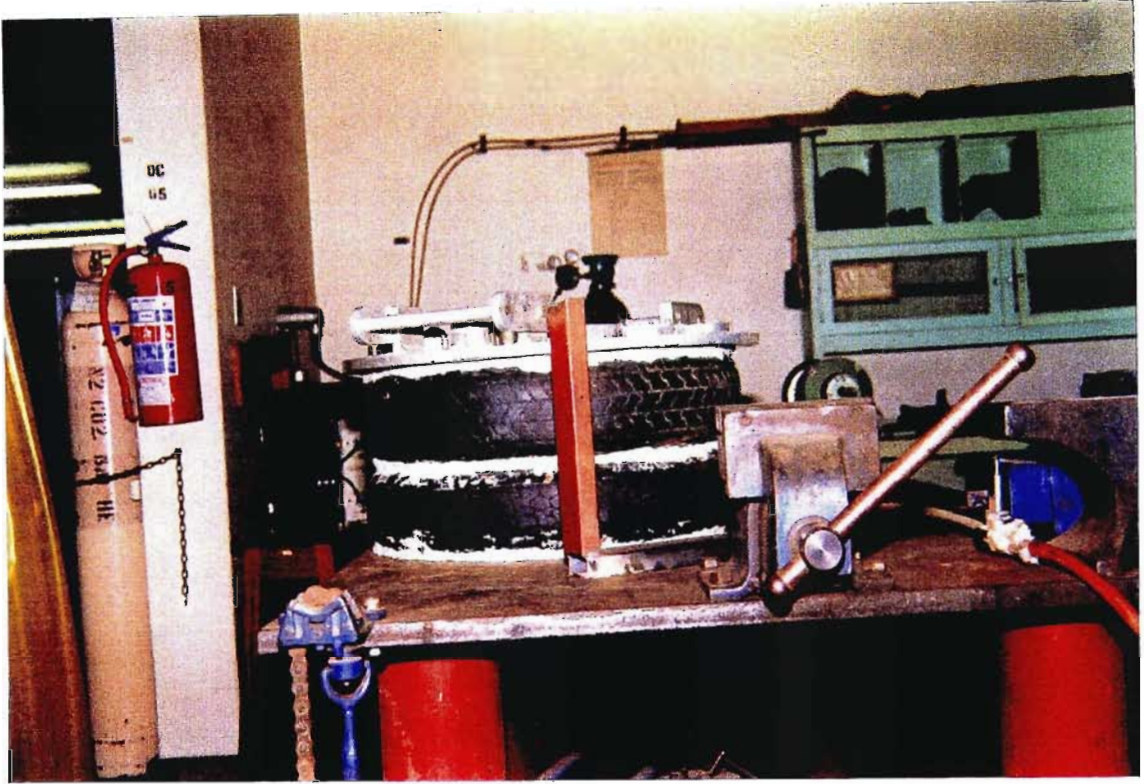


Figure 6.4: TTVV with ( $m = 2$ ) before evacuation

(6.4) and (6.5) are pictures of this vessel taken before and after evacuation respectively. They show how evacuation stresses the system such that the top plate descends which is indicative of a reduction in the tyre volumes. This means that there is an increase in the TTVV wall pressure, although this was not measured at this stage.

### Observations

When the tubes are clamped tightly within the tyres these vessels become stable and can operate over sustained periods. This indicates that they can be increased in size and possibly operated for long enough to make a high vacuum experiment possible. The next step was to build a TTVV large enough to contain a guard vessel and to ensure that it could be operated on a time scale of hours. This is the time required to heat an oil diffusion pump and to obtain a high vacuum in the inner chamber.

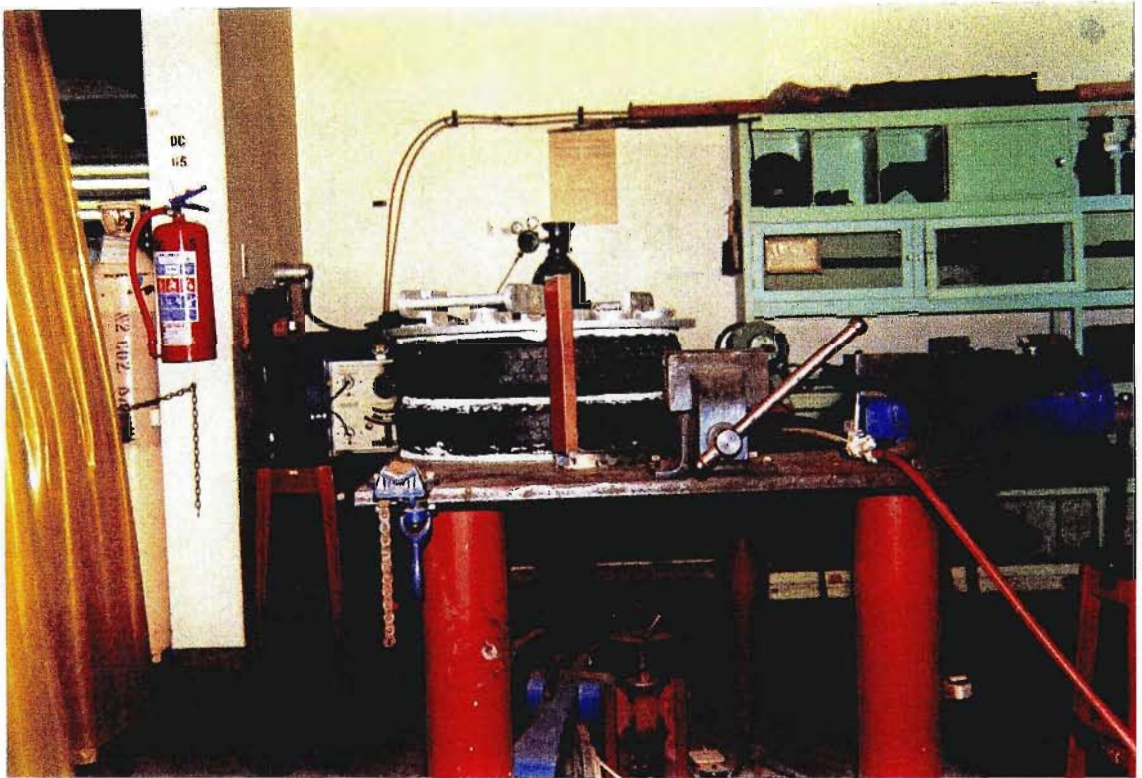


Figure 6.5: TTVV with ( $m = 2$ ) after evacuation



### 6.1.5 Experiment 4

The TVV was doubled in size through the addition of two more tyres creating a four layer ( $m = 4$ ) TTVV.

#### Apparatus

Except for two additional tyres, the apparatus was identical to that of the previous experiment. These had a slightly larger outer diameter although the difference was not significant. The internal diameters were identical. These tyres were modified in the same manner as before with regards to the clamping of their inner tubes. Into each was placed a size 15 tube. All of the tyre tubes were inflated to 2,5 *bar* and sealed together with putty.

#### Results

When the chamber was pumped down, once again the chamber compressed noticeably. Precautions were taken in that safety spectacles and ear muffs were worn in the event of possible explosive decompression of the TVV. This turned out to be unnecessary. Even, in previous experiments, when a tyre had burst, the event was not explosive.

The chamber stood 57 *cm* in height. After removal of the air the vertical height of the chamber was reduced to 51 *cm*. The tyre stacking was not completely symmetrical and after the vacuum pump was activated, there was a distinct tendency of the chamber to lean. This is a further example of a kink instability illustrating that vertically stacked TTVV's are indeed susceptible.

The chamber could be pumped down for an hour without collapsing. Figures (6.6) and (6.7) are pictures of the vessel before and after evacuation respectively. The reduction in the height of this vessel may be clearly noted.

#### Observations

This chamber had an interesting geometry in that it was approximately as high as it was wide as in the case of the  $m = 4$  tubular vessel. The increase in the longitudinal number resulted in the formation of instabilities in that the chamber had a tendency to lean to one side if one was not careful to stack the tyres symmetrically.

Despite the loss of vertical height with the accompanying loss of internal volume, the chamber remained enough to support the guard vessel which had

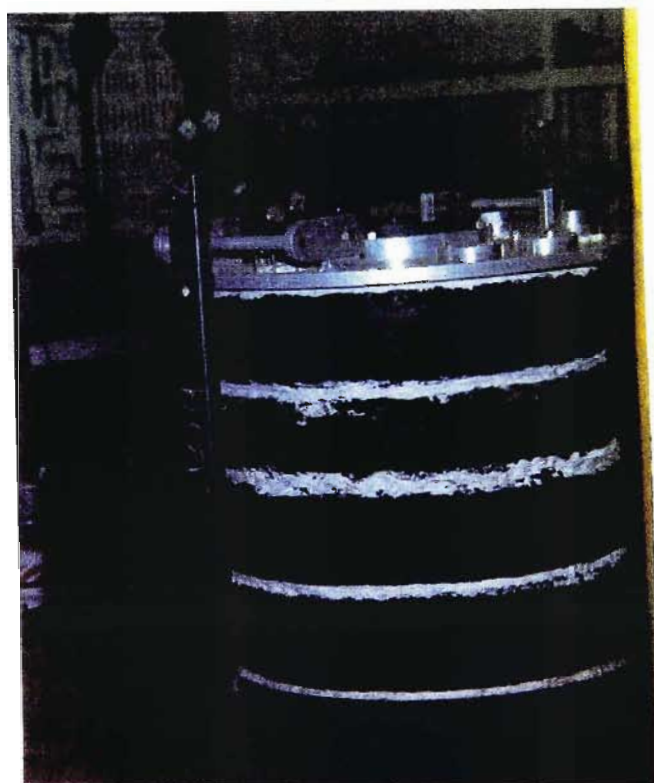


Figure 6.6:  $m = 4$  TTVV before evacuation

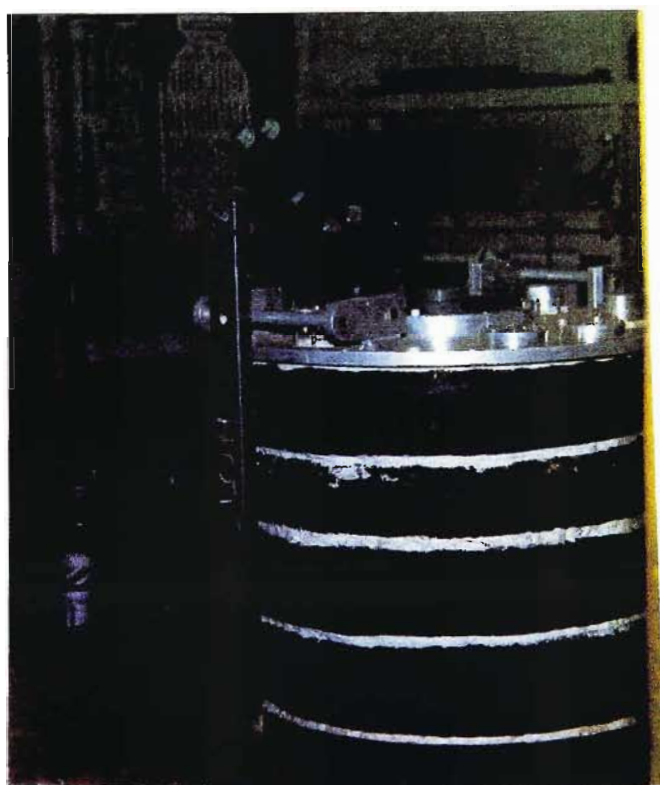


Figure 6.7:  $m = 4$  TTVV after evacuation



Figure 6.8: Guard Vessel used in High Vacuum Toroidal Experiments

been used in the tubular TVV high vacuum experiments. The chamber had remained stable long enough to make a high vacuum experiment feasible.

## 6.2 High Vacuum TTVV Experiment

This aim of this experiment to show that not only are TTVV's viable but that they are also capable of supporting a high vacuum. The four layer TTVV of the previous experiment was placed over the second guard chamber from the tubular TVV high vacuum experiments. The experiment was conducted according to procedures developed for the earlier high vacuum TVV experiments. Figure (6.8) is a picture of the guard vessel sealed over the oil diffusion pump.

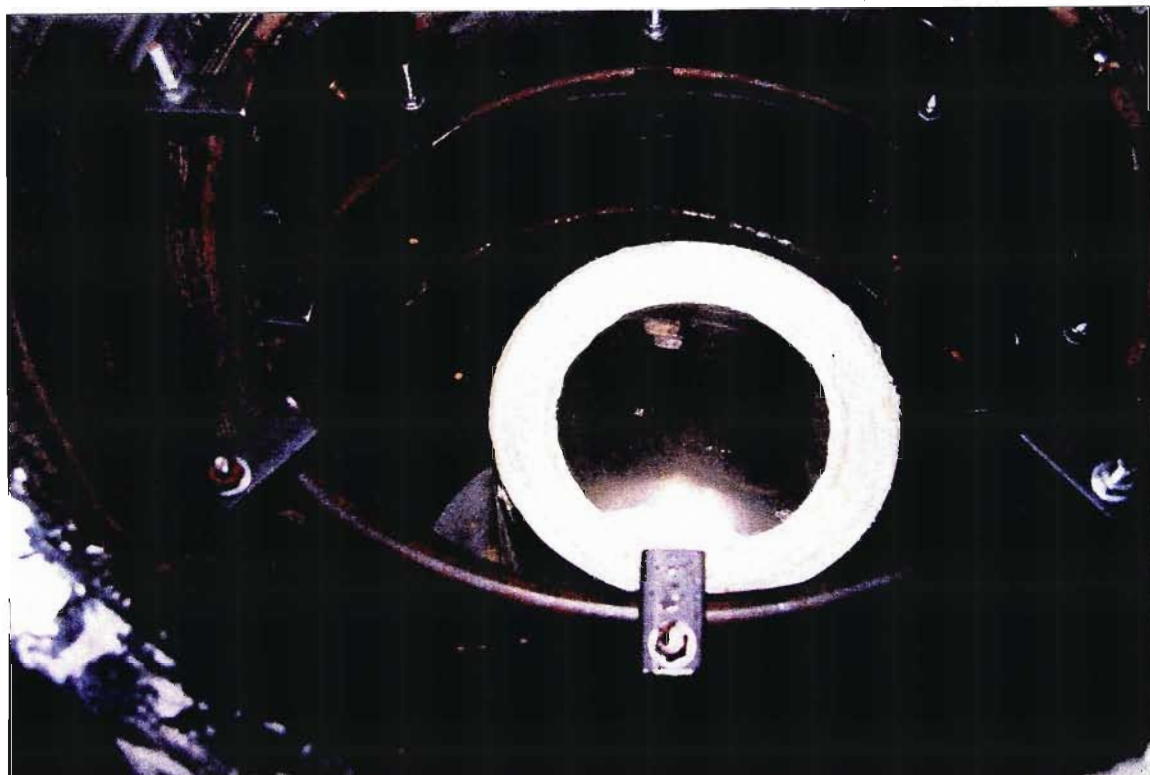


Figure 6.9: Guard Vessel within  $m = 4$  TTVV

### Apparatus

The apparatus was essentially a hybrid of the ( $n = 4$ ) TTVV apparatus and that of the tubular TVV high vacuum experiments. The four modified car tyres, sealed together with putty, were placed over the guard vessel and sealed to the base of the high vacuum apparatus with putty. The vacuum hose was placed between the bottom of the TVV and the base plate. The tyres now replaced the wall of the conventional vacuum vessel which previously stood over the diffusion pump. Figure (6.9) shows the TVV walls encompassing the guard vessel.

### Results

The internal and external chambers were both pumped down according to the standard procedure. Initially, the TVV tended to lean and this resulted in the development of a leak. The chambers had to be repressurised and the tyres arranged in a more symmetrical vertical pattern. However, this

particular run did succeed in removing over 90 % of the air.

The second run did not produce any problems with leaks. The mechanical gauge moved to the end of its scale after the second pump was activated, although there was a small amount of pressurisation in the outer chamber after separation of the internal and external vessels. After pumping the internal vessel with the rotary pump for some minutes, the pirani gauge reported a vacuum reading in the  $10^{-2}$  *torr* range. The diffusion pump was heated for twenty minutes and then the butterfly valve was opened. The ionisation gauge was used to take the further readings and after pumping for one and a half hours a final value of  $2 \times 10^{-5}$  *torr* was obtained. The TVV was pumped down for an overall period of two and a half hours.

### Observations

The most important observation is that a high vacuum was achieved and maintained for up to an hour. This proves that it is possible to produce high vacuum with an TTVV which in turn means that inflatable high vacuum vessels are a possibility.

Once again the kink instability manifested itself causing a loss of the vacuum. For TTVV's with significant vertical height relative to their horizontal diameters it is important to ensure that vertical symmetry is maintained.

The vacuum reading obtained is identical to that of the tubular TVV high vacuum experiments indicating that this may be the lower limit due to the vacuum system external to the TVV. In order to confirm this, the TTVV was removed and replaced with the compressional vacuum vessel which is normally used with this pumping apparatus. Once again the lowest vacuum reading obtained was  $2 \times 10^{-5}$  *torr* proving that this is the limit of the pumping apparatus. This means that a value in the  $10^{-6}$  *torr* range should be obtainable with a better vacuum system.

#### 6.2.1 Further Experimentation

The oil in the diffusion pump was replaced. This pump was then sealed and evacuated. After more than twenty-four hours of a reading of  $10^{-6}$  *torr* was obtained with the ionisation gauge.

The experiment with the high vacuum TTVV then recommenced and a reading of  $10^{-5}$  *torr* was obtained. However, a leak was discovered in the guard vessel. This means that there is no reason why this experiment should not be capable of producing a high vacuum of  $10^{-6}$  *torr* if the leaks are removed. The chamber was found to be stable enough to maintain a

high vacuum for up to 13 hours.

### 6.3 Discussion and Conclusion

The experiments outlined in this chapter have proven the TTVV is a viable alternative design for a vacuum vessel. Vertical instabilities do manifest themselves when several toroids are stacked one upon the other. However, TTVV's are far more stable than tubular vessels, not being prone to the interchange and the sausage instabilities. An advantage that tubular vessels possess is that they do not lose height during evacuation. However, it must also be said that these vessels do lose volume through "breathing". In terms of the experiments outlined in this thesis, the TTVV's have always been found to be more reliable. This makes them the better choice for the performance of high vacuum experiments.

Mention must also be made here of the notion of "inflavac" or inflatable vacuum technology. This is mentioned because of the inflatable nature of the TTVV's constructed. All the vessels created could be deflated when not in use. This hints at later TVV technology where this principle could be developed further such that when not in use, the vessel occupies very little volume. This is a distinct possibility if the structure is fully tensional. Thin walled end plates would be in placed in tension with the rest of the structure.

## Chapter 7

# Fully Tensional Cylindrical TVV

The most basic TVV possible is the spherical model which has the advantage that the wall comprises the entire shell which is therefore in tension. However, a more useful form is the cylindrical TVV which, in general, has the end plates in compression. It is, however, possible to place the end plates in tension and therefore to create a fully tensional cylindrical TVV. This is accomplished by utilising inverted domes as end plates.

### 7.1 Theory

The advantage of a dome as an end plate, as opposed to a flat sheet of material, is the amount of material required. Ross[15] points out that flat plates are inefficient as they have to withstand lateral pressure in flexure. Domes have a membrane stress which allows the use of ten times less material in order to withstand the same pressure. If placed in a convex to the vacuum vessel, the dome will have the advantage of increasing the overall volume. However, the disadvantage of such an arrangement is that the dome will be in compression and will therefore have the propensity to buckle. There are three main ways in which a dome in compression can fail [15, 24, 25]: buckling with the nose denting inwards, lobar buckling and axisymmetric yield. The first mode of failure occurs for hemispheric and oblate domes. The second occurs with prolate domes. The third mode of failure is universal. An oblate dome is defined as having an aspect ratio of less than two while a prolate dome has a value greater than two. This ratio is defined as



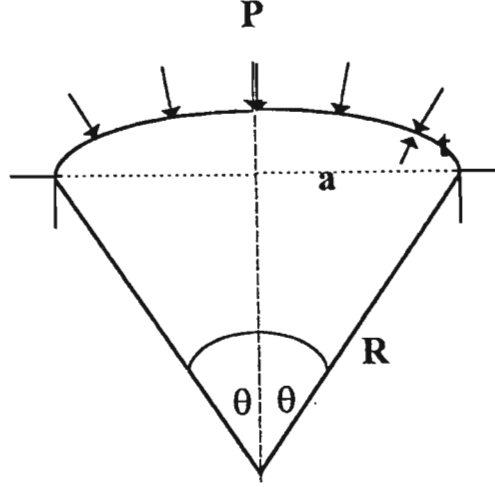


Figure 7.1: Dome Under External Pressure

follows:

$$\text{AspectRatio} = \frac{\text{Dome Height}}{\text{Base Radius}} \quad (7.1)$$

The ratio for a hemispherical dome will therefore be two.

The elastic instability pressure,  $P_{cr}$ , is given by the following semi-empirical formula[14, 24, 28]:

$$P_{cr} = \left[ 1 - 0.175 \frac{\theta - 20}{20} \right] \left( 1 - \frac{0.07R}{400t} \right) (0.3E) \left( \frac{t^2}{R} \right) \quad (7.2)$$

in the case of a spherical shell cap with a half-centred angle,  $\theta$ , between twenty and sixty degrees, and where:  $400 \leq a/t \leq 2000$ . This is illustrated by figure (7.1). It must be pointed out that  $E$  is the elastic modulus. Inverting the dome will place it into tension thereby overcoming the problem of buckling. The disadvantage is the overall loss of volume. However, this configuration, according to C.T.F.Ross[14], represents a saving in material of more than 50%. This is the conclusion reached after finite element analysis was performed using the THINCONe programme<sup>1</sup>. A dome, of similar

<sup>1</sup>The details of the simulation can be found in the references cited. I have only given an overview of the results in order to illustrate the advantages of placing a dome in tension

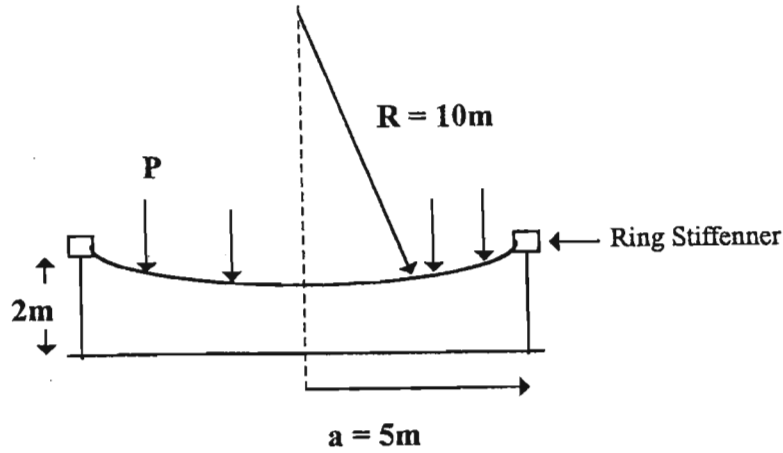


Figure 7.2: Simulated Dome Inverted Against Pressure

shape to that illustrated by figure (7.1), only inverted, was simulated, being placed over a cylinder and joined by a stiffening ring. This is shown by figure (7.2). The radius of curvature of the dome was selected to be twice that of the cylinder due to the fact that the maximum membrane stress of a sphere is twice that of a cylinder. The dimensions are given as follows:

Shell Thickness ( $t$ )	=	2 cm
Radius of Cylinder ( $a$ )	=	5 m
Radius of Dome ( $R$ )	=	10 m
Length of Cylinder	=	2 m
Elastic Modulus ( $E$ )	=	$2 \times 10^{11} \text{ N/m}^2$
Poisson's Ratio	=	0,3
External Pressure ( $P$ )	=	$4 \times 10^5 \text{ N/m}^2$

If the above values are substituted into equation (7.2), we find that

$$P_{cr} = 2 \times 10^5 \text{ N/m}^2$$

for a convex dome of the same dimensions. According to the results of the simulation, this is considerably less than that required for yield to occur in the inverted dome. If the value of  $t$  is increased to 3 cm, we get

$$P_{cr} = 4,64 \times 10^5 \text{ N/m}^2$$

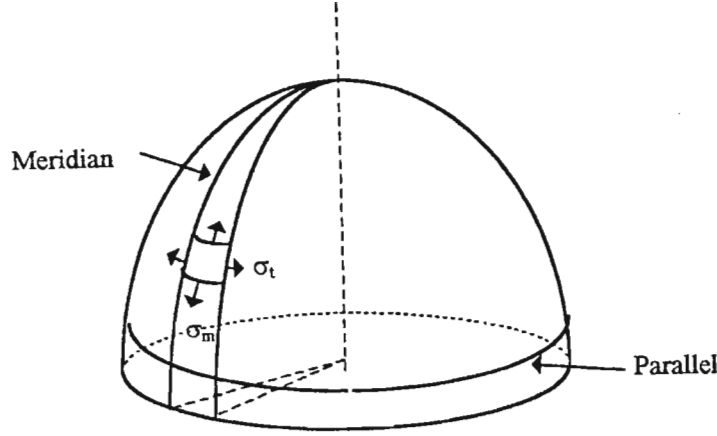


Figure 7.3: Tensional Stresses on a the Membrane of a Dome Under Internal Pressure

which is still insufficient to cause yield in the inverted dome. In fact, given geometrical imperfections in the convex dome, up to twice as much material, possibly more, is required in order to make this structure as strong as the inverted dome.

There are two membrane stresses associated with a dome in tension: the meridional stress,  $\sigma_m$ , which acts on a plane perpendicular to the meridian, and the tangential stress,  $\sigma_t$ , which acts on a plane perpendicular to a parallel. This is illustrated in figure (7.3). The figure is adapted from Riley, Sturges and Morris[22]. They give the formula for these stresses as follows:

$$\frac{\sigma_m}{r_m} + \frac{\sigma_t}{r_t} = \frac{p}{t} \quad (7.3)$$

## 7.2 Experimental

Two experiments which made use of this principle were conducted . In each case only the top end plate was tensional while the bottom plate remained compressional. Tubular TVV walls were used but the chamber could not be regarded as fully tensional due to the existance of the compressional plate. However, this is inconsequential as a single working tensional end plate was

required in order to prove the principle.

### 7.2.1 Experiment 1

#### Apparatus

A standard tubular TVV wall with a radial number of thirty and longitudinal number of four was constructed from soft drink cans and sealed with putty. The bottom plate was an aluminium sheet of 1 *mm* thickness which was sealed to a thick welding bench with putty in order to prevent buckling. Metal bowls with 60 *cm* diameters were placed over the top of the chamber, providing the tensional end plate. Each bowl measured 1 *mm* in thickness and had a depth of 17 *cm*. These too, were sealed with putty. Initially three bowls were used to increase the thickness in order to provide added mechanical strength. This was deemed necessary at this early stage as little was known about how this structure would behave.

#### Results

A reading of over 0,90 *bar* was obtained without any problems although the paint did tend to fleck off the bowls and the sausage instability became evident. The same result was obtained when one of the bowls was removed. When the experiment was run using only one bowl, the system became unstable, and one side of the bowl was sucked further into the chamber. This damaged the bowl in that the TVV wall made large indentations into the sunken part of the wall. Figures (7.4) and (7.5) are pictures of this TVV after having been run successfully.

#### Observations

These preliminary experiments show that in principle, a fully tensional TVV is possible. However, instabilities can develop and these need to be compensated for. A small misalignment with the single bowl resulted in damage to the end plate. This is hardly surprising as the force on this plate is approximately 30000 *N*. This arrangement had the smallest thickness for an end plate and therefore illustrates the need for increased precision with smaller wall thickness.

### 7.2.2 Experiment 2

A second experiment was designed with the intention of using a single tensional top plate. Structures were designed to provide stability.



Figure 7.4: Side View of TVV with Sausage Instability



Figure 7.5: Tensional End Plate

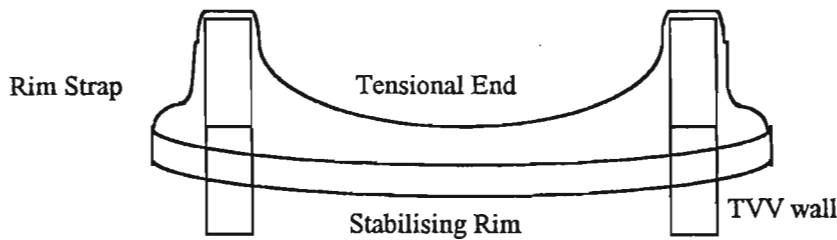


Figure 7.6: Diagram of TVV with Tensional End Plate

### Apparatus

This experiment employed an  $m = 2$  tubular TVV wall. This too was constructed from soft drink cans and sealed with putty. The top end plate consisted of a single bowl from the previous experiment. An aluminium plate served as the bottom plate.

The bottom plate was to serve as a self buckling structure which would stabilise itself as it was pulled up into a tensional structure. The top plate was stabilised by strapping its edges with thin metal bindings to a ring placed around the chamber. This is illustrated diagrammatically in figure (7.6).

Figure (7.7) is a picture of the bowl with the rim attached

### Results

This chamber too, could be pumped to over 0,90 bar without collapse.

### Observations

The results show that fully tensional chambers are indeed possible provided that they are provided with the appropriate stabilising structures to prevent movement of the end plates. The outward radial forces also remove the need for support structures such as bicycle rims, at least at the ends of the chamber.

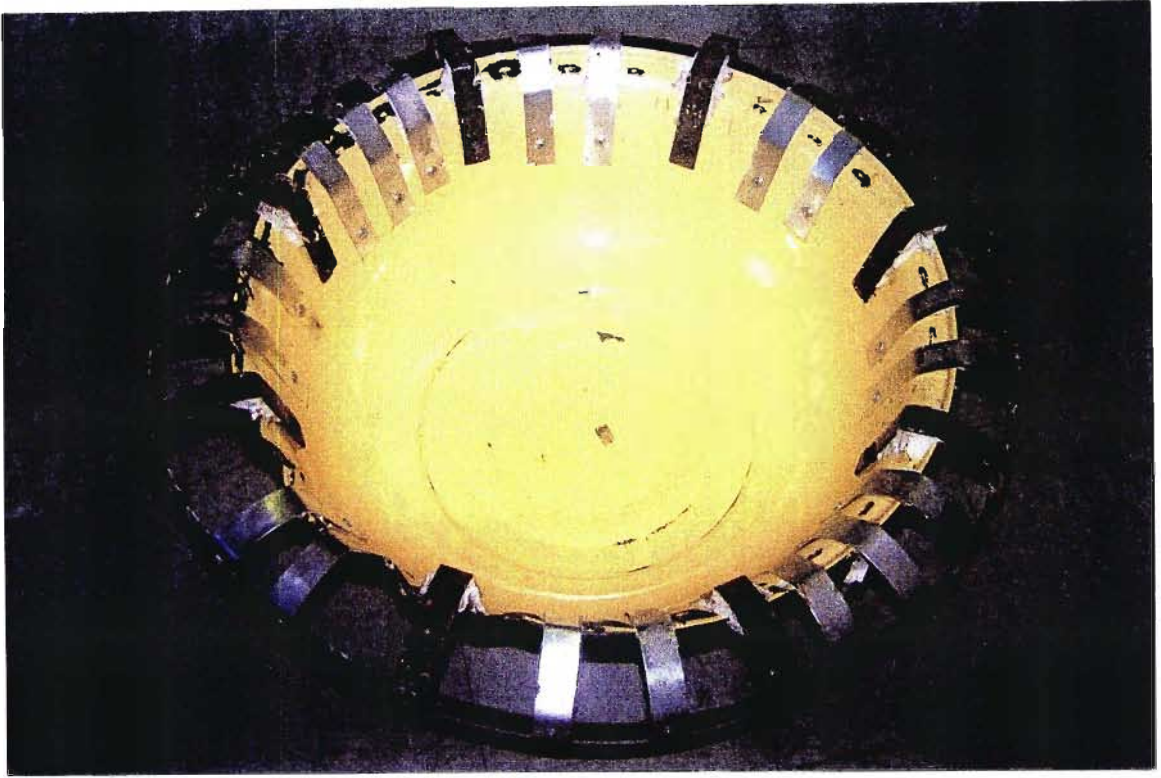


Figure 7.7: Bowl with Stabilising Rim Attached

### 7.3 Examination of a Deformed End Plate

In one of the tubular TVV experiments, the end plate, which was compressional, deformed due to the force of atmospheric pressure. This was initially a flat plate soldered to the top part of a vessel with a longitudinal number of one and a radial number of twelve as documented in a previous chapter. Deformation occurred due to the tensile stress becoming greater than the elastic limit of the material. The resulting patterns were deemed worthy of further study in that they were of a symmetrical nature and illustrate the deformation of a plate due to both compressional and tensional forces. Figure (7.8) is a picture of the deformed plate.

#### 7.3.1 Theory of the Deformation of a Circular Plate

The equilibrium equation for a thin, flat plate was first derived by Lagrange and is given by Voltera and Gaines[26] as:

$$\frac{\partial^4 w}{\partial x^4} + 2\frac{\partial^4 w}{\partial x^2 \partial y^2} + \frac{\partial^4 w}{\partial y^4} = \frac{1 - \nu^2}{EI} p \quad (7.4)$$

where  $I$  is the moment of inertia and is equal to  $t^3/12$ . In the case of a circular plate, which has been symmetrically bent with regard to its centre,



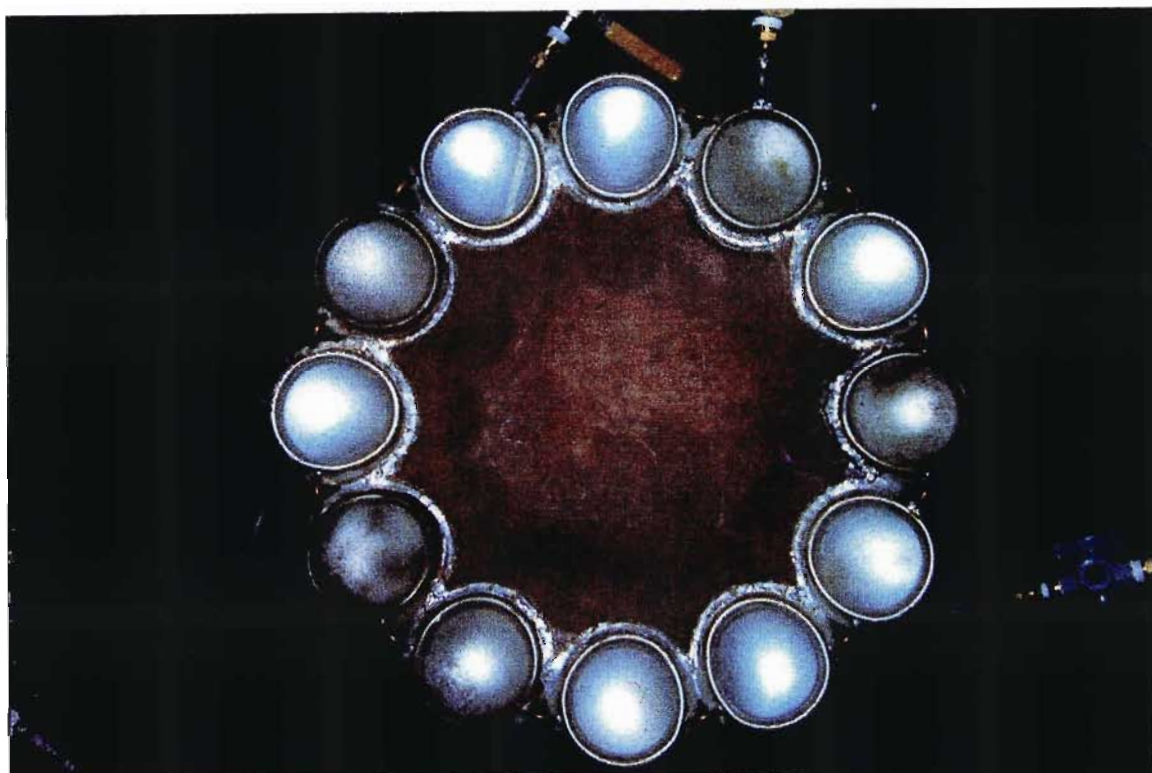


Figure 7.8: Deformed TVV End Plate

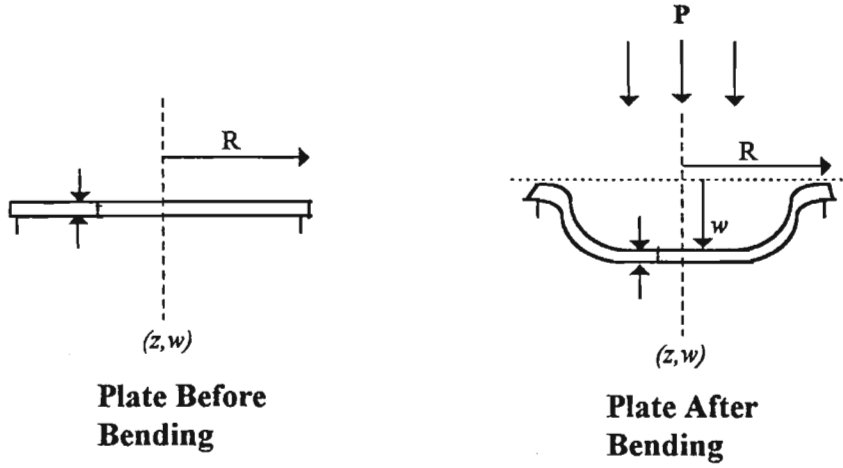


Figure 7.9: Bending of a Circular Plate Due to Uniform Pressure

the above equation can be transformed to the following:

$$\left( \frac{d^2}{dR^2} + \frac{1}{R} \frac{d}{dR} \right) \left( \frac{d^2 w}{dR^2} + \frac{1}{R} \frac{dw}{dR} \right) = \frac{p}{D} \quad (7.5)$$

where

$$D = \frac{Et^3}{12(1 - \nu^2)} \quad (7.6)$$

In this case  $w$  is the vertical displacement as illustrated by figure (7.9). Once again, there are two stresses associated with this plate,  $\sigma_R$  and  $\sigma_\theta$  which are illustrated by figure (7.10). These are given by the well known equations[26, 27]:

$$\sigma_R = \frac{E}{1 - \nu^2} (\epsilon_R + \nu \epsilon_\theta) = -\frac{Ez}{1 - \nu^2} \left( \frac{d^2 w}{dR^2} + \frac{\nu}{R} \frac{dw}{dR} \right) \quad (7.7)$$

$$\sigma_\theta = \frac{E}{1 - \nu^2} (\epsilon_\theta + \nu \epsilon_R) = -\frac{Ez}{1 - \nu^2} \left( \frac{1}{R} \frac{dw}{dR} + \nu \frac{d^2 w}{dR^2} \right) \quad (7.8)$$

The general solution to equation (7.5) is:

$$w = C_1 \log R + C_2 R^2 \log R + C_3 R^2 + C_4 + \frac{pR^4}{64D} \quad (7.9)$$

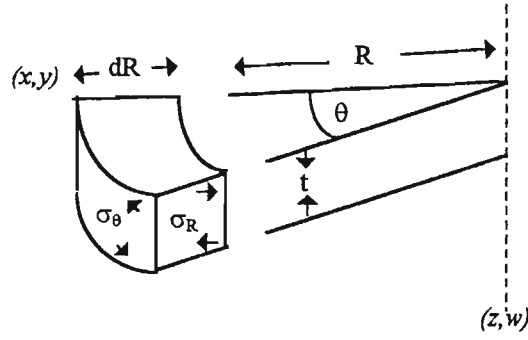


Figure 7.10: Stresses of a Circular Plate Bending due to Uniform Pressure

where the coefficients,  $C_1$  to  $C_4$ , are constants determined by the boundary conditions.

In the case of a cylindrical TVV, the end plate is firmly clamped at the boundaries. The load is due to the pressure and is distributed evenly over the plate. The first two of the constants in equation (7.9) must therefore be zero in order to prevent infinities from arising at  $R = 0$ . Also, at the boundary,  $w = 0$  and  $\frac{dw}{dR} = 0$ . If the radius of the plate is  $a$ , then at  $R = a$ , we have the following:

$$C_3 a^2 + C_4 + \frac{p a^4}{64 D} = 0$$

$$2 C_3 a + \frac{p a^3}{16 D} = 0$$

from which we obtain:

$$C_3 = -\frac{p a^2}{32 D}$$

$$C_4 = \frac{p a^4}{64 D}$$

This gives us:

$$w = \frac{p a^4}{64 D} \left( \frac{R^4}{a^4} - 2 \frac{R^2}{a^2} + 1 \right) \quad (7.10)$$

From equations (7.7) and (7.8) we now have:

$$\sigma_R = -\frac{3pa^2}{4t^3}z \left[ (3 + \nu)\frac{R^2}{a^2} - 1 - \nu \right] \quad (7.11)$$

and

$$\sigma_\theta = -\frac{3pa^2}{4t^3}z \left[ (1 + 3\nu)\frac{R^2}{a^2} - 1 - \nu \right] \quad (7.12)$$

The maximum deflection is found to be at the centre of the plate and is given by:

$$\frac{pa^4}{64D}$$

Equation (7.10) indicates that the shape of a circular plate after deformation will be parabolic. The shape of the deformed plate that we wished to study was of this nature in that it was flattened in the central area but steep toward the edges. However, in this case the edges consisted of twelve circular arcs, which meant that no simple analytical solution was available. In order to attempt to model the deformation of this plate, we therefore turned to finite element analysis.

### 7.3.2 Finite Element Analysis of Deformed Plate

The COSMOS programme was used for this purpose, simulating a thin plate of uniform thickness, with the boundary of twelve circular arcs at the edges which are present due to the  $n = 12$  vessel wall. The programme assumed a 0,2 mm thick plate with a standard Poisson's Ratio of 0,3. The strain was assumed to be linear elastic and the plate was subjected to a uniform pressure. This did not perfectly represent the actual plate but the simulation was intended to give a qualitative idea of how a thin metallic plate would deform.

The structure was created by placing together twelve identical segments. Each segment was bounded by two lines proceeding outwards from the plate centre and an inverted circular arc. Each segment was meshed with ten finite elements as is apparent from figure (2.38). Also shown are the nodal points, where the lines intersect. The program specifies how each nodal point interacts with the other in terms of the stress and strain parameters.

Figures (7.11) to (7.15) are the results. Figures (7.11) and (7.12) are three dimensional views of the plate both before and after deformation. The next two figures are two dimensional indicators of the von-Mises stress and

displacement respectively. The final figure is a side view of the displacement using different scales.

The von-Mises stress plot clearly shows that most of the stress exists at the plate edge, particularly in those parts of the circular arcs that are closest to the plate centre. With the actual plate itself, these were the places where it tended to pull away from the TVV wall. The stress progressively decreases as one moves inwards although there is a slight increase about halfway to the centre. This is interesting in that the displacement plots all show that the the centre of the plate tends to be flattened in comparison to the steep displacement which occurs at the plate edge.

This is indeed comparable to what we find in the deformed plate. The central region tended to be flattened when compared to the regions closer to the edge. While the simulation did give a slightly different representation of these regions, it did show most of the bending occurred here and that the patterns formed were symmetrical. This is also comparable to the theory developed earlier which shows that the centre should experience the maximum displacement and that this displacement should be parabolic in nature.

## 7.4 Conclusion

The experiments outlined in this chapter were successful in that end plates were placed in tension without any catastrophic implosion. There was only one case of damage to a plate due to asymmetry. The simulations gave a good approximation of the deformation of an end plate when subject to uniform pressure. The theory also confirms the parabolic nature of the deformation as well as indicating that domes placed in tension are very strong structures.

It may therefore be concluded that the construction of a fully tensional TVV does not necessarily require a spherical structure. Cylindrical TVV's can also be fully tensional as has been illustrated with the tubular design. The TTVV may be better in this regard as the end plate will then have a perfectly circular edge. This makes a fully inflatable cylindrical TVV possible in that the entire vessel including the end plate could consist of metal foil. Alternative materials with strong tensile properties could also be used.

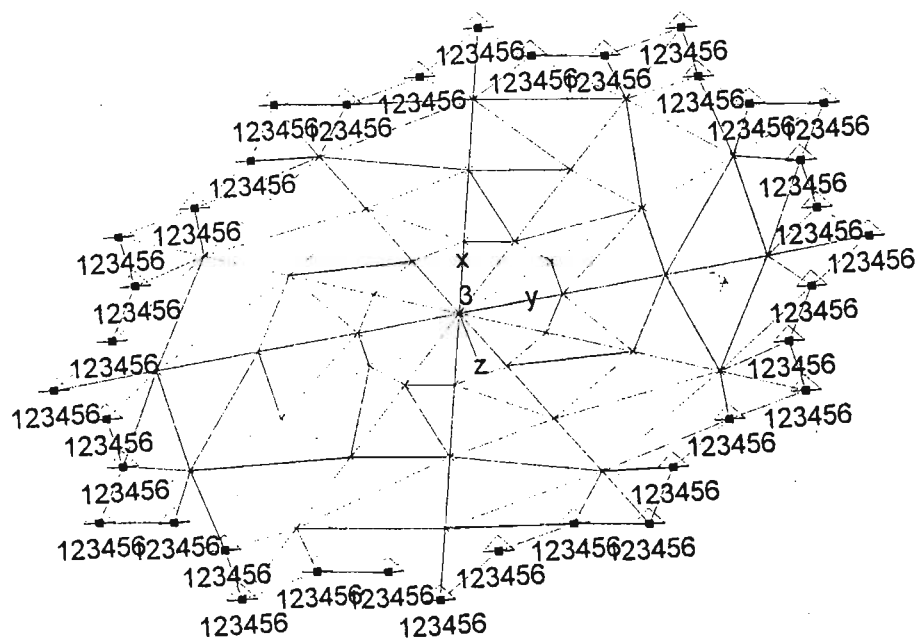


Figure 7.11: 3-D Plot of Plate before Deformation

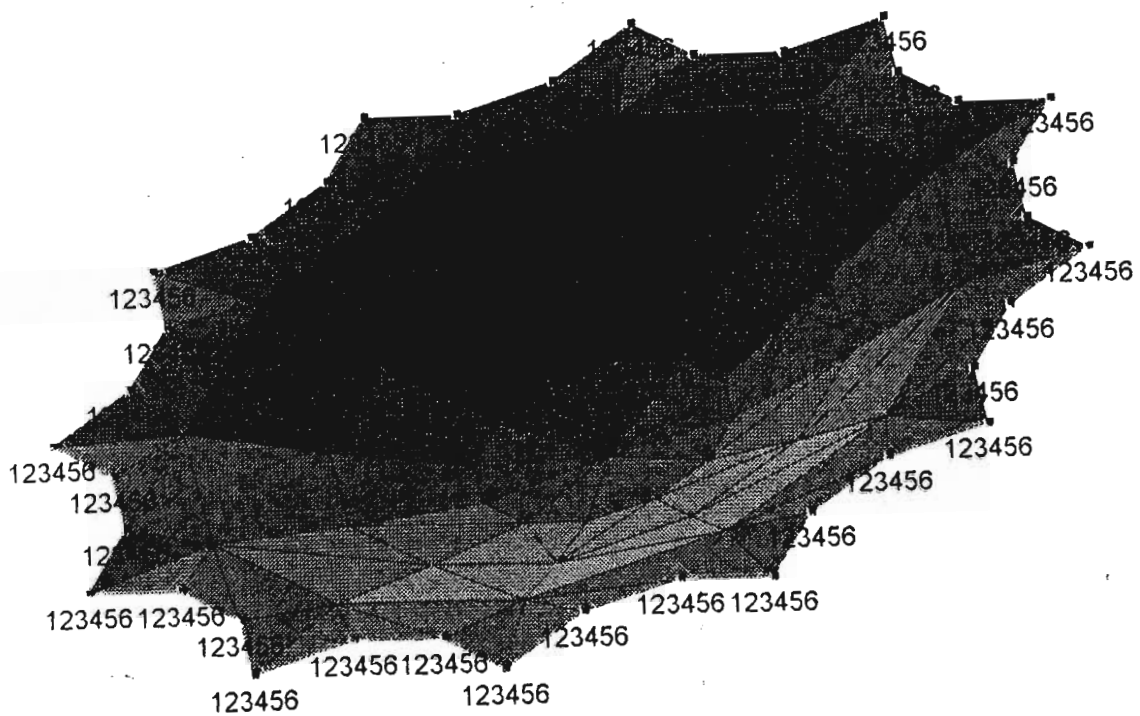


Figure 7.12: 3-D Plot of Plate after Deformation

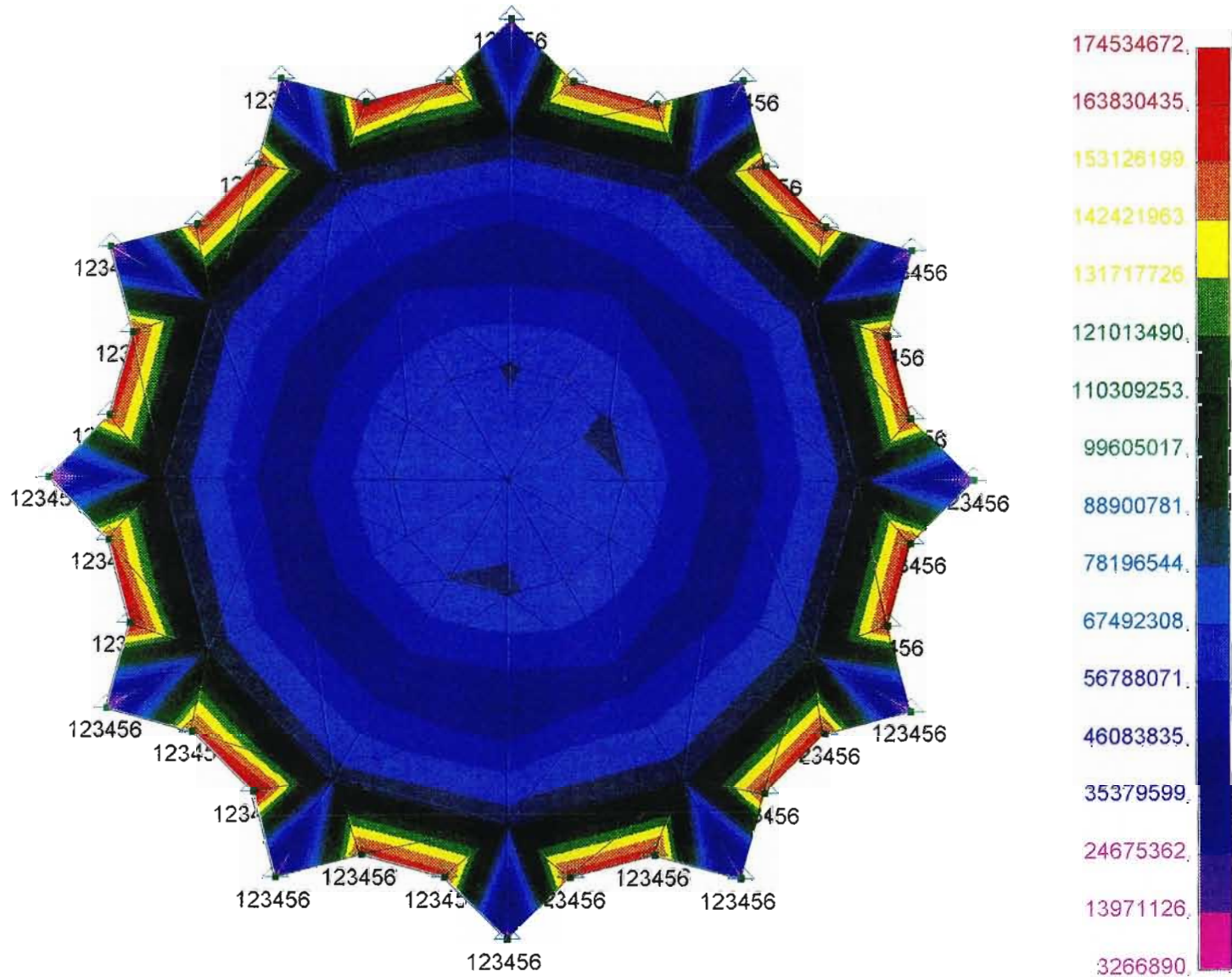


Figure 7.13: Plot of VonMises Stress on Plate



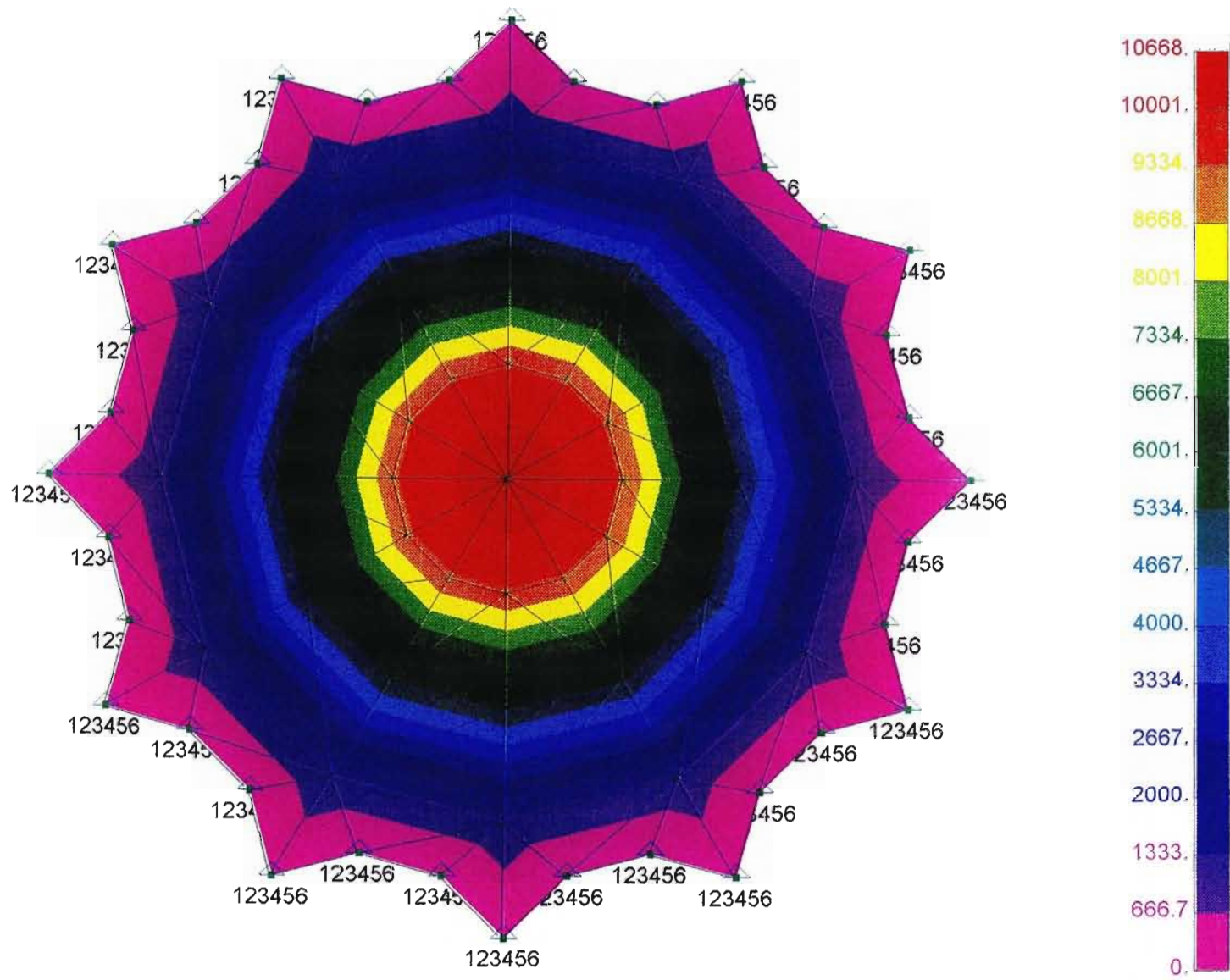


Figure 7.14: Plot of Total Displacement

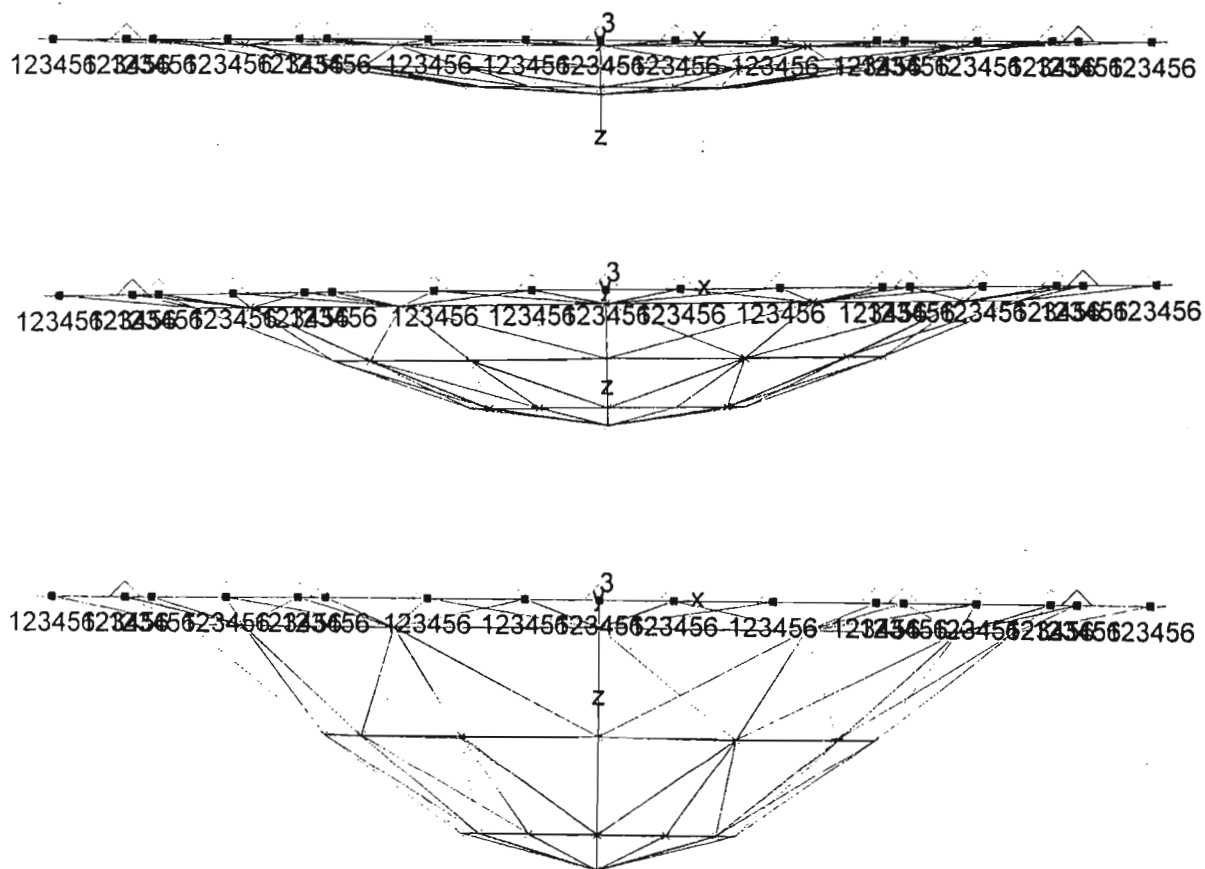


Figure 7.15: Side View of Displacement: Scale = 2%, 5% and 10% respectively

## Chapter 8

# The Spinning Vacuum Vessel

The main subject matter of this thesis is the tensional vacuum vessel, an alternative design to the standard chamber which has the walls in compression. In this chapter, a second novel vacuum vessel is proposed, one which allows for the use of thin walls, as does the TVV. This is the spinning vacuum vessel (SVV)<sup>1</sup>. The proposal is that a cylindrical vessel, spinning with sufficient angular velocity, reaches a point where the outwards force on the walls due to the centripetal acceleration is balanced by the inwards force due to atmospheric pressure, should the vessel be supporting a vacuum.

### 8.1 Theory

The theory can be represented mathematically as follows:

$$p_0 A = \frac{mv^2}{R} \quad (8.1)$$

where  $A$  is the area of a small section of the SVV wall and  $m$  is the corresponding mass of the volume of material. The  $v$  term is the tangential velocity and  $R$  is vessel radius. This is valid for a thin walled SVV.

According to the definition of the density,  $\rho$ , of a material, its mass,  $m$ , is given by  $\rho V$ , where  $V$  is the material volume. In the case of an SVV with a thin wall, the volume of a section will be given by  $At$  where  $t$  is the wall thickness. The mass of this section will therefore be,  $\rho At$ . Equation (8.1)

---

<sup>1</sup>Independently invented by the present writer. It is quite possible that this is not a new idea, but it came to our group without exterior knowledge.

can therefore be represented as follows:

$$p_0 A = (\rho A t) \left( \frac{v^2}{R} \right) \quad (8.2)$$

This can be simplified to:

$$p_0 = \frac{\rho t v^2}{R} \quad (8.3)$$

which allows one to deal with the vessel wall as a whole rather than in sections. It is preferable, when working with rotating objects, to work with the rotational velocity,  $\omega$ , rather than the tangential velocity,  $v$ , which can be represented by the term,  $\omega R$ . Equation (8.3) now becomes:

$$p_0 = \rho t \omega^2 R \quad (8.4)$$

which can be rearranged to give:

$$\omega = \sqrt{\frac{p_0}{\rho t R}} \quad (8.5)$$

This is the fundamental equation of the SVV. The desire on the part of any designer will be to reduce  $\omega$ . This will have to be done by increasing any of the values of the denominator in the square root bracket. Increasing the value of  $t$  is undesirable, however, due to the fact that the SVV concept was developed in part to allow for the use of much thinner walls and therefore less material. Alternative vessels are largely designed with larger vessels in mind as it is here that the greatest savings can be made. It is therefore favourable to the SVV that  $\omega$  is reduced with an increase in  $R$ . Denser materials are also favoured and therefore it is better to employ denser materials if they can be obtained cheaply.

Figures (8.1) to (8.3) are graphs which give the required rotational frequencies (measured in units of *rpm*(revolutions per minute)) of SVV's constructed from three different materials with varying parameters of  $R$  and  $t$ . The materials are Aluminium Alloy (1100-H14), Structural Steel and Phosphor Bronze (Spring Temper) which have densities of  $2710 \text{ kg/m}^3$ ,  $7860 \text{ kg/m}^3$  and  $8800 \text{ kg/m}^3$  respectively. The aluminium alloy, which is the least dense, requires the highest rotational frequencies, particularly with regards to small thicknesses. The denser materials require smaller rotational frequencies. However, for large values of  $t$ , these differences tend to become less dramatic. In fact, for the three larger values of  $t$ , even when comparing the different materials, the differences are relatively small despite the

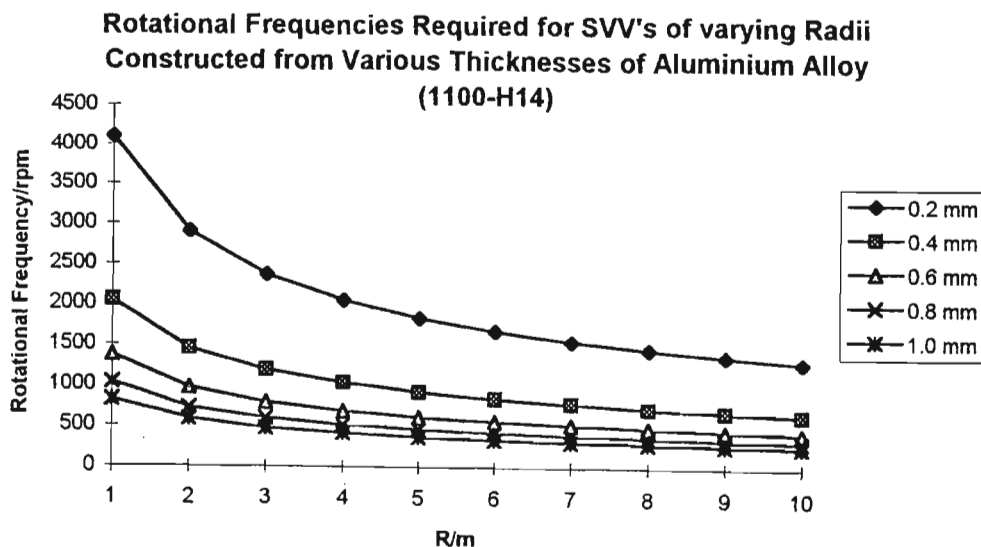


Figure 8.1: Graph of Required Rotational Frequencies of SVV's Constructed from Aluminium Alloy(1100-H14) with Regard to Varying Parameters

discrepancy with the densities. This gives a designer a greater range of materials to select if a larger  $t$  value is to be built. For large  $R$ , all the graphs tend to converge. In this region, values of around 500 rpm are typical. In fact the heaviest of the vessels (the vessel where all the variables have their maximum values), only requires a rotational frequency of 144 rpm which is less than 2.5 Hz. This indicates that SVV's, although a very novel concept at this stage, may indeed be feasible.

It should, however, be stated that the SVV does have certain drawbacks. Such a vessel will collapse if the rotation slows below a certain value. It is also difficult to attach pumps unless they rotate with the vessel or if not, will require a rotary seal. It also creates difficulties with regards to conducting experiments unless the experiments themselves rotate.

## 8.2 Experimental

It was decided to perform a "proof of Principle" experiment in order to test the veracity of the SVV concept. An experiment was performed, although on a small scale. A small cylinder was rotated at a relatively high rotational frequency on a lathe, while the air was removed through a vacuum hose.

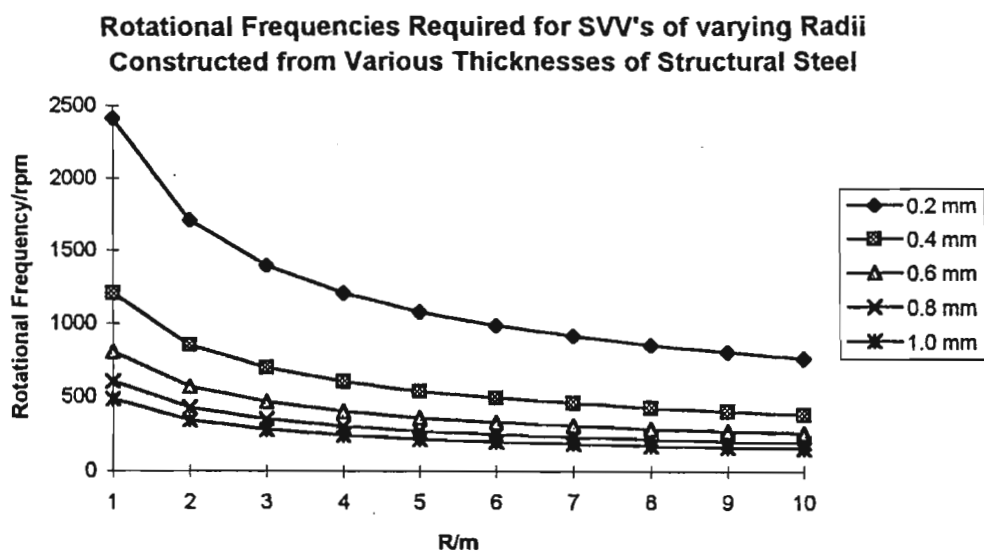


Figure 8.2: Graph of Required Rotational Frequencies of SVV's Constructed from Structural Steel with Regard to Varying Parameters

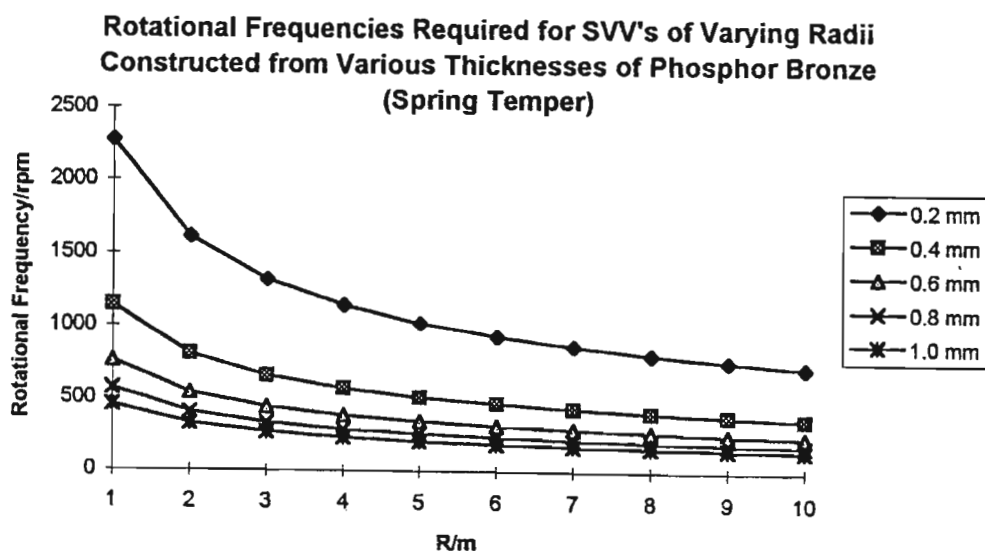


Figure 8.3: Graph of Required Rotational Frequencies of SVV's Constructed from Phosphor Bronze (Spring Temper) with Regard to Varying Parameters

## Apparatus

The cylinder used in this experiment was a typical soft drink can which was emptied of its contents and modified to suit our experimental aims. A 16 mm bolt was inserted into the bottom of the can. This would be held and rotated by the lathe in order to spin the can. The top end was removed and the interior was reinforced with putty which was deposited to a depth of roughly 1 cm. The top end was then sealed to a bearing which would allow rotation of the can while attached to a vacuum line. The bearing was inserted into a wooden block which held the cylinder in place in addition to preventing rotation of the exterior part of the bearing. A hole was drilled into this block in order to allow the admission of a vacuum hose. This hose was attached to a rotary pump. A mechanical vacuum gauge was also attached to the vacuum line through a T-piece. The modified can is shown sealed to the bearing in figure (8.4). This apparatus is shown attached to the lathe with the vacuum hose inserted into the wooden block in figure (8.5).

## Results

The cylinder was successfully spun at 1200 to 1500 rpm. The pump was activated and a value of approximately 0,5 bar was obtained. The rotation was stopped after the pump was switched off. The can remained intact, there was no sign of buckling. When the experiment was repeated, the same reading of 0,5 bar was obtained. However, this time the rotation was stopped before the pump was deactivated. This time the vessel buckled visibly. The can was again rotated at 1500 rpm without activation of the rotary pump. Some of the buckling was removed in this way.

## Observations

This experiment clearly shows that the SVV principle works in so far as it demonstrates the buckling resistance of a cylinder being reduced through rotation. The can did not buckle while in rotation but did so when this was not present to counteract atmospheric pressure.

Equation (8.5) is useful in performing a simple "ball park" calculation. A small volume of putty, approximately 1 cm<sup>3</sup>, was weighed and found to be 1,94 g. We can therefore say that the putty has a density of approximately 2000 kg/m<sup>3</sup>. The value of  $R$  is 0,033 m while the value of  $t$  is 0,0003 m. The vacuum gauge recorded half an atmosphere and therefore  $p$  can be taken



Figure 8.4: Modified Can with Bearing



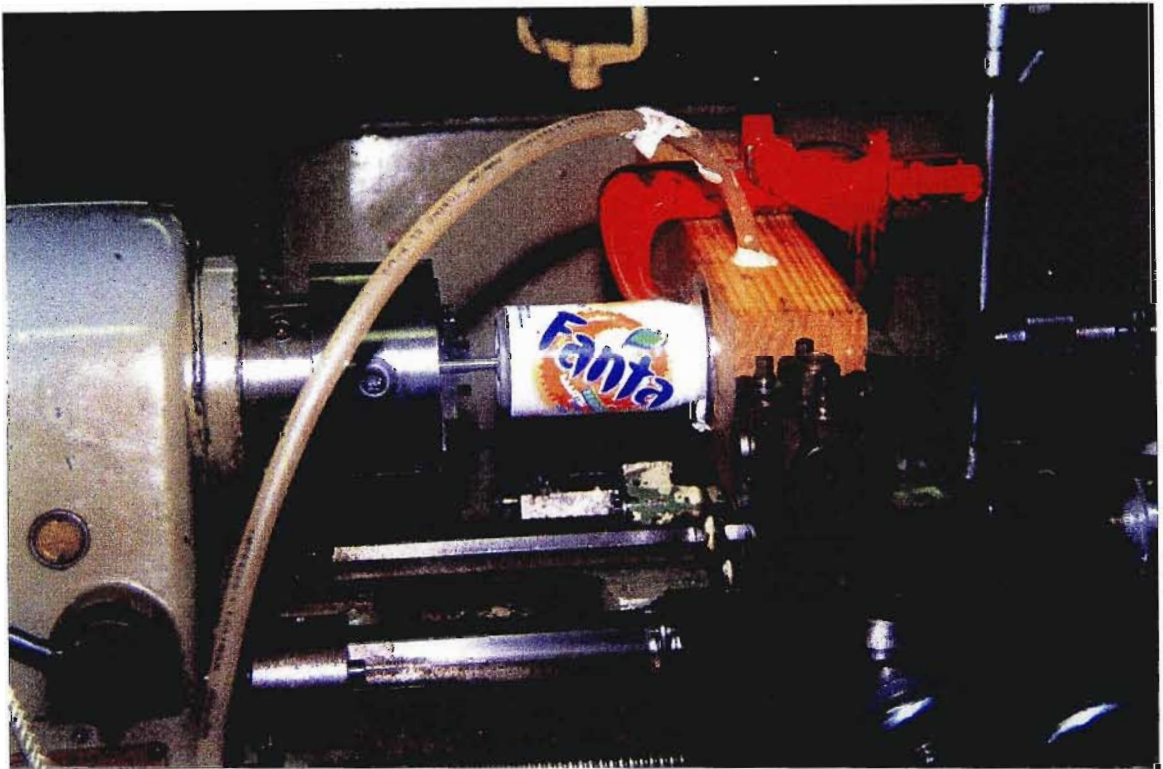


Figure 8.5: Modified Can Attached to Lathe with Vacuum Hose

as 50000 *Pa*. We therefore have:

$$\begin{aligned}
 \omega &= \sqrt{\frac{5 \times 10^4 \text{ Pa}}{(2 \times 10^3 \text{ kg/m}^3)(3 \times 10^{-4} \text{ m})(3,3 \times 10^{-2} \text{ m})}} \\
 &= 1,6 \times 10^3 \text{ rad/s} \\
 &= 2,5 \times 10^2 \text{ Hz} \\
 &= 1,5 \times 10^4 \text{ rpm}
 \end{aligned}$$

which is an order of magnitude higher than the 1500 *rpm* of the lathe in our experiment. However, it must be pointed out that the can did not buckle when the vacuum gauge gave a reading of 0,4 *bar* while the system was stationary. It should therefore be considered significant that an increase in the pressure of 0,1 *bar* could result in buckling of the can, when not in rotation. This does appear to illustrate the principle.

### 8.3 Conclusion

The theory clearly shows that the SVV principle can be used to create alternative vacuum vessels which require less material than is the case with standard vessels. Large vessels can be built which require small rotational frequencies which indicates that the idea may be technically feasible. Of course this remains to be seen with the construction of actual large scale vessels. One may question the use of such vessels in that ports cannot be attached to the walls. However, instruments could still be placed inside and readings taken. We propose that an SVV may be useful with regards to such processes as the electron beam welding of turbo fan blades. There are also difficulties with regards to sealing such vessels. However, such a vessel is novel and so it is difficult to say at this stage, how great the technical difficulties may be. What can be said, is that the first SVV has been constructed on a small scale with promising results.

## Chapter 9

# Conclusion

This thesis has explored the concept of vacuum vessels with walls that consist of two linked shells placed in tension through pressurisation of the intermediate space. Submersibles with tensional hulls have already been designed but the tensional vacuum vessel is novel. The early work on TVVs was carried out at this institution by Michaelis and Forbes as described earlier. The experiments performed by the author represent a continuation of this work.

Alternative vacuum vessel designs were also examined. These show a desire for the use of cheaper materials. There is also a preference for thinner walls and therefore designs which represent material savings. The TVV has this advantage and also allows for the use of novel materials with high tensile strength to be incorporated into vacuum vessel design. TVVs can also be made to fold away and can therefore be portable. They can even be inflatable and certain large vessels can become buoyant.

The initial work on TVVs performed by Michaelis and Forbes proved that the principle of a vacuum vessel with the walls placed into tension was viable. The work performed by the author had several aims.

Firstly, there was the desire to prove that larger versions of the earlier TVVs could be scaled up in size. This was accomplished through the construction of TVVs with walls constructed from soft drink cans and putty. Although there were some problems in that sometimes the cans would leak after prolonged use and stabilising rims were required in order to prevent instabilities, it was found that larger vessels could be evacuated for periods of several hours without collapse.

The second aim was to prove that a high vacuum could be obtained within a TVV. This was accomplished through the implementation of a thin

walled guard vessel which was sealed over an oil diffusion pump. Vacuum values of  $10^{-5}$  torr were obtained. There was good reason to believe that the  $10^{-6}$  range was obtainable with an improvement in technology.

The third aim was to examine the behaviour of vessels constructed from longitudinal tubes. Most of the vessels mentioned in this thesis were of this nature due to the cost effectiveness of this approach. It was found that one had to balance the desire to reduce the bulkiness of the vessel with the desire to increase its stability. One therefore could not have a vessel with a radial number that was too large or too small. The longitudinal number should be unity in these vessels in order to prevent vertical instabilities. It was also found that the compressional components could not be ignored. A TVV of this nature should incorporate compressional elements in order to increase stability and decrease the pressure required in the intermediate space and therefore the tensile stress of the walls.

The fourth aim was to examine the behaviour of cylindrical vessels with walls constructed from circumferential tubes. These vessels were also inflatable in nature. Tyres were used as the basic construction materials. Initially, childrens bicycle tyres were used in order to prove the principle but later experiments made use of car tyres. It was found that large vessels could be constructed and that high vacuum experiments could be conducted through the incorporation of a guard vessel. Vacuum values of  $10^{-5}$  torr were obtained. These vessels were also found to be far more stable than those constructed from longitudinal tubes, with only vertical instabilities manifesting themselves. There was little evidence of the need to incorporate compressional elements into these vessels.

The final aim was to examine the possibility of a fully tensional cylindrical TVV. All of the experimental vessels outlined in this thesis were cylindrical in nature as this is the most useful form of vacuum vessel design. This was accomplished by fitting large bowls to one end of a vessel manufactured from longitudinal tubes. Some deformation did occur due to instabilities which were the result of small asymmetries but this was rectified through the inclusion of a stabilising rim. A computer simulation of the deformation of a circular plate was also performed in order to find where the greater stresses were. The experiments illustrated that tensional end plates were viable.

Finally, a further novel vacuum vessel was examined. This was the spinning vacuum vessel, whereby the force due to the atmospheric pressure is balanced by the force due to the centripetal acceleration. A small scale experiment was conducted, evacuating a reinforced soft drink can which was spun on a lathe. Promising results were obtained.

The TVV is a novel idea and requires much further development. This

thesis has served to highlight the major ideas and has proven that such vessels are viable. What remains to be done is to improve the technology. This should result in much better high vacuums being obtained and far larger vessels being constructed. Vessels constructed from novel tensile materials should also be researched as well as buoyant vessels. There are also the challenges of learning how to attach ports to fully tensional TVVs.

However, the basic principles of the TVV have been proven and therefore it can be said that TVVs are indeed promising as alternative vacuum vessels.

## Appendix A

# Structures in Compression

Most vacuum vessels are structures in compression. With the exception of the fully tensional vacuum vessel, compressional forces cannot be ignored in TVV's. A certain knowledge of structures in compression is therefore required both to gain a better understanding of the compressional aspects of TVV's as well as for purposes of comparison with conventional vacuum vessels.

This appendix will examine tubes in compression due to the fact that this is the most common configuration for a vacuum vessel. Apart from the end plates, it is the tubes in the tubular TVV's that are also subject to compressional forces.

### A.1 Tubes in Compression

The stresses in a tube under pressure with  $t \ll R$  are identical in magnitude but opposite in direction to the tensile stresses in a thin walled cylinder. The axial stress is therefore given by

$$\sigma_x = \frac{pR}{2t} \quad (\text{A.1})$$

while the hoop stress is given by

$$\sigma_y = \frac{pR}{t} \quad (\text{A.2})$$

Failure will occur if these compressive stresses exceed the compressive yield of the material.

However, this is not the only mode of failure. A circular ring can collapse at a particular pressure due to radial instability. This may vary depending

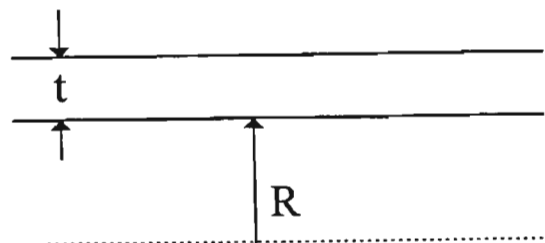


Figure A.1: Standard Thick Walled Tube:  $I_1 = t^3/12$ ,  $V_1 = \pi(2R + t)t$

on the geometric imperfections of the structure, but the buckling pressure of a circular ring is given by the following formula

$$p' = \frac{3EI}{R^3} \quad (\text{A.3})$$

where  $E$  is Young's modulus of elasticity and  $I$  is the second moment of inertia about the centroidal axis parallel to the axis of symmetry.  $R$  is the radius of curvature and  $p'$  is the load per unit length.[7, 18, 23]

Bennet has given a number of configurations for tubular walls in compression which illustrate the effects of ring stiffeners in allowing for the use of thinner walls. The following diagrams give six possible configurations starting with a standard thick walled tube which provides a reference.[7] Comparisons can be made with the other configurations in order to illustrate the material savings. The second moment of inertia and the volume of material per unit length are given in each case.

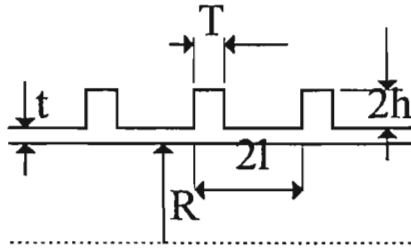


Figure A.2: Thinner Walled Tube with Ring Stiffeners:  $I_2 = \frac{5}{6}th^2$ ,  $V_2 = 4\pi Rt$  for  $T = t$  and  $l = h$

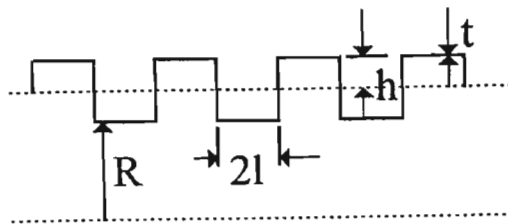


Figure A.3: Thin Walled Tube with Rectangular Profile:  $I_3 = (t/3l)(h^3 + 3h^2l)$ ,  $V_3 = 2\pi R(l + h)t/l$



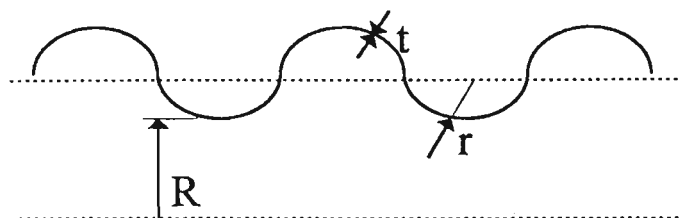


Figure A.4: Thin Walled Tube with Semicircular Profile:  $I_4 = \pi/4tr^2$ ,  $V_4 = \pi^2(R + r)t$

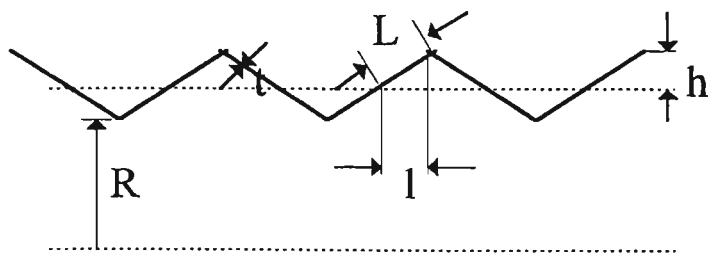


Figure A.5: Thin Walled Tube with Triangular Profile:  $I_5 = h^2Lt/3l$ ,  $V_5 = 2\pi(R + h)Lt/l$

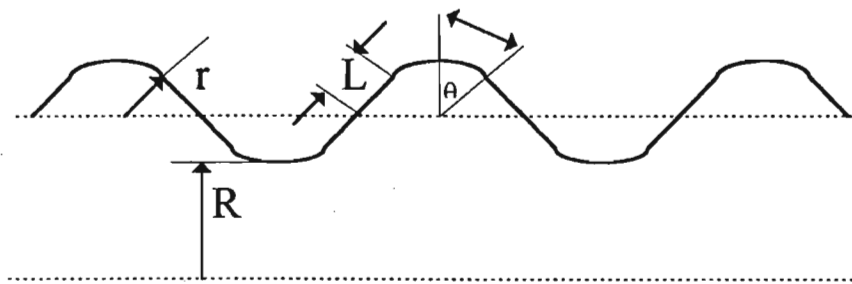


Figure A.6: Thin Walled Tube with Corrugated Profile

## Appendix B

# Simulation Programme for the Deformation of a Circular Plate

The simulation described in chapter seven concerning the deformation of a circular plate was performed using the COSMOS/M programme. The list of commands necessary to generate the plate including the finite elements and the load due to atmospheric pressure is given below.

```
C*
C* COSMOS/M Geostar V1.71
C* Problem : append2
C*
EGROUP,1,PLANE2D,0,1,0,0,0,0,0,
MPROP,1,EX,30E6,NUXY,0.3,
RCONST,1,1,1,2,0.2,0,
VIEW,0,0,1,0,
PLANE,Z,0,1,
CRSCIRCLE,1,50,50,0,50,100,0,12,
CRLINE,13,2,13,
PT,14,63,97,0,
CRDEL,13,13,1,
CRARC,13,2,13,14,18.3013,
CRDEL,1,12,1,
PTDEL,14,14,1,
SFPTCR,1,13,1,0,
CSANGLE,3,0,50,50,0,0,0,0,0,
```

```

SFGEN,11,1,1,1,1,0,0,30,
EGDEL,1,1,1,
EGROUP,1,SHELL3,0,0,0,0,0,0,0,0,
RCDEL,1,1,1,
RCON,1,1,1,6,0.2,0,0,0,0,0,
MA_SF,1,12,1,1,10,0,
NMERGE,1,132,1,0.0001,0,0,0,
NCOMPRESS,1,124,
ACTDMESH,SF,1,
ACTDMESH,PH,1,
DND,1,ALL,0,4,1,
DND,72,ALL,0,73,1,
DND,66,ALL,0,68,1,
DND,60,ALL,0,62,1,
DND,54,ALL,0,56,1,
DND,48,ALL,0,50,1,
DND,42,ALL,0,44,1,
DND,36,ALL,0,38,1,
DND,30,ALL,0,32,1,
DND,24,ALL,0,26,1,
DND,18,ALL,0,20,1,
DND,12,ALL,0,14,1,
PEL,1,100000,1,200,1,3,
SCALE,0,
C* R_CHECK,STATIC,
C* R_STATIC,

```

# Bibliography

- [1] J.H.Moore, C.C.Davis and M.A.Coplan, (1989), [Vacuum Technology] *Building Scientific Apparatus, 2nd ed.*, (75-118).
- [2] G.L. Weissler, (1979), [Survey], *Methods of Experimental Physics*, **14**, Vacuum Physics and Technology, (1-5).
- [3] V.O.Altomose, (1979), [Glass Vacuum Systems], *Methods of Experimental Physics*, **14**, Vacuum Physics and Technology, (313-343).
- [4] M.M.Michaelis, (1978), [A Glazed High Alumina Cement Vacuum chamber], *Vacuum*, **28**, (369).
- [5] K.F.Poole and M.M.Michaelis, (1980), [Hialvac and Teflon outgassing under ultra-high vacuum conditions], *Vacuum*, **30**, (415-417).
- [6] M. M. Michaelis and A Forbes, (1994), [Vacuum Vessels in Tension], *Vacuum*, **45**, (57-60).
- [7] J.R.J.Bennet, R.J.Elsey and R.W.Malton, (1992), [Convoluted vacuum tubes for long baseline interferometric gravitational wave detectors], *Vacuum*, **43**, (531-535).
- [8] J.R.J.Bennet and R.J.Elsey, (1992), [The design of the vacuum system for the joint German-British interferometric gravitational wave detector, GEO], *Vacuum*, **43**, (35-39).
- [9] J.R.J.Bennet, (1987), [The vacuum system for a British long baseline gravitational wave detector], *J. Vac.Sci.Technol.A*, **5**(4), (2363-2366).
- [10] A.Forbes, (1998), [Tensional Vacuum Vessels], *Photothermal Refraction and Focusing*, (190-219)
- [11] U.K. 1 031 415 June 1966

- [12] France 2326229 October 1975
- [13] U.K. 2026951 May 1979
- [14] C.T.F.Ross, (1990), [Novel Pressure Hull Designs], *Pressure Vessels Under External Pressure*, (197-206)
- [15] C.T.F.Ross, (1994), [The Silent Submarine], *The University of Portsmouth Inaugural Lectures*, <http://www.mech.port.ac.uk/CFTR/httoc.htm>, (1-25)
- [16] Anon, (1985), [Submarine Powered by Closed-Circuit Diesel], *Ocean Industry*, (63)
- [17] M.M.Michaelis, A.Forbes and E. McKenzie, (1995), [Alternative Vacuum Vessels]
- [18] C.T.F.Ross, (1990), [General Instability], *Pressure Vessels Under External Pressure*, (117-140)
- [19] R.D.Cook and W.C.Young, (1985), [Thin Shells of Revolution], *Advanced Mechanics of Materials*, (179-223)
- [20] D.J.Rose and M.Clark,Jr., (1961), [Plasma Stability], *Plasmas and Controlled Fusion*, (258-293)
- [21] F.F.Chen, (1974), [Introduction], *Introduction to Plasma Physics*, (1-16)
- [22] W.F.Riley, L.D.Sturges and D.H.Morris, (1995), [Combined Static Loading], *Statics and Mechanics of Materials*, (498-576)
- [23] R.J.Roark and W.C.Young, (1975), [Elastic Stability], *Formulas for Stress and Strain 5th ed.*, (531-563)
- [24] C.T.F.Ross, (1987), [Design of Dome Ends to Withstand Uniform External Pressure], *Journal of Ship Research*, (139-143)
- [25] C.T.F.Ross, (1990), [An overview of Pressure Vessels Under External Pressure], *Pressure Vessels Under External Pressure*, (1-10)
- [26] , E.Volterra and J.H.Gaines, (1971), [Bending of Plates], *Advanced Strength of Materials*, (429-505)
- [27] , R.D.Cook and W.C.Young, (1985), [Symmetric Bending of Circular Plates], *Advanced Mechanics of Materials*, (125-144)

- [28] C.T.F.Ross, (1990), [Shell Instability], *Pressure Vessels Under External Pressure*, (75-116)